Check for updates

Environmental Science Advances



Accepted Manuscript

This article can be cited before page numbers have been issued, to do this please use: Z. Huang, X. Huang, K. Liu, J. Fu and M. Liu, *Environ. Sci.: Adv.*, 2025, DOI: 10.1039/D5VA00262A.



This is an Accepted Manuscript, which has been through the Royal Society of Chemistry peer review process and has been accepted for publication.

Accepted Manuscripts are published online shortly after acceptance, before technical editing, formatting and proof reading. Using this free service, authors can make their results available to the community, in citable form, before we publish the edited article. We will replace this Accepted Manuscript with the edited and formatted Advance Article as soon as it is available.

You can find more information about Accepted Manuscripts in the <u>Information for Authors</u>.

Please note that technical editing may introduce minor changes to the text and/or graphics, which may alter content. The journal's standard <u>Terms & Conditions</u> and the <u>Ethical guidelines</u> still apply. In no event shall the Royal Society of Chemistry be held responsible for any errors or omissions in this Accepted Manuscript or any consequences arising from the use of any information it contains.



View Article Online DOI: 10.1039/D5VA00262A

Environmental Significance Statement:

Per- and polyfluoroalkyl substances (PFAS) are synthetic chemicals widely used in industrial and consumer products due to their thermal and chemical stability. However, their resistance to environmental degradation, bioaccumulative behavior, and links to serious health effects have raised global concern. Traditional removal methods, such as adsorption and filtration, are limited by their inability to destroy PFAS, risking secondary pollution. Fenton-based advanced oxidation processes offer a promising pathway toward PFAS mineralization under mild conditions. This review provides a comprehensive analysis of the mechanisms, effectiveness, and technological progress of Fenton-based PFAS degradation. By highlighting current limitations and future directions, it aims to guide the development of practical, scalable, and sustainable remediation strategies for PFAS-contaminated environments, contributing to global efforts in safeguarding ecological and human health.

Degradation of per- and polyfluoroalkyl substances (PFAS) by Fenton reactions

Zhicong Huang^a, Xi Huang^a, Kang Liu^a, Junwei Fu^a,*, and Min Liu^a,*

^a School of Physics, Central South University, Changsha 410083, People's Republic of

China; Email: fujunwei@csu.edu.cn; minliu@csu.edu.cn

Open Access Article. Published on 29 2025. Downloaded on 10.11.2025 10:02:00.

This article is licensed under a Creative Commons Attribution-NonCommercial 3.0 Unported Licence

Per- and polyfluoroalkyl substances (PFAS) are persistent organic pollutants with widespread environmental and health threats due to their chemical stability and bioaccumulative potential. The Fenton-based degradation of PFAS demonstrates several advantages, including mild reaction conditions, operational simplicity, and costeffectiveness, while simultaneously facing challenges such as inefficient cleavage of carbon-fluorine (C-F) bonds and low mineralization. This review comprehensively summarizes the degradation of PFAS using Fenton-based reactions, focusing on mechanisms, efficiencies, and technological advancements. Firstly, the reasons for PFAS prevalence in human society, their pathways into biological systems, the associated health risks, as well as their global distribution and contamination status are elucidated. Secondly, the current major PFAS degradation approaches are summarized, highlighting the principal advantages of Fenton-based degradation. Thirdly, a comprehensive overview of recent advancements in Fenton-based PFAS degradation technologies are reviewed, including chemical-Fenton, electro-Fenton, photo-Fenton, and photo-electro-Fenton processes. Finally, the future research directions are discussed, focusing on catalyst design optimization, structure-activity relationship, and feasibility assessment for large-scale applications. This review provides a critical foundation for advancing sustainable PFAS remediation technologies.

Keywords: PFAS degradation; Advanced oxidation processes; Fenton reaction; Degradation mechanisms; Large-scale application

View Article Online DOI: 10.1039/D5VA00262A

1. Introduction

Per- and polyfluoroalkyl substances (PFAS) comprise a class of over 6,500 distinct anthropogenic fluorinated organic compounds, 1,2 characterized by fully or partially fluorinated alkyl chains, terminated with polar acidic moieties such as carboxylates, sulfonates, or phosphonates.3 Based on the carbon-chain length, PFAS are generally classified into long-chain and short-chain types.⁴ Long-chain PFAS, such as perfluorononanoic acid (PFNA) and perfluoropentanoic acid (PP), with more than eight carbon atoms, exhibit distinct physicochemical properties compared to short-chain PFAS (such as perfluorobutanesulfonic acid (PFBS), perfluorohexanoic acid (PFHxA), and perfluorohexanesulfonic acid (PFHxS), with four to seven carbon atoms). These differences are especially evident in aqueous solubility and hydrophilicity, which can be quantified by solubility measurements and octanol-water partition coefficients. 5,6 For example, short-chain PFAS contain fewer fluorine atoms and lack the pronounced "molecular-brush" architecture of long-chain counterparts, 1.2 thus having stronger water solubility and affinity for aqueous phases.⁵ Beyond chain length, the inherent stability of PFAS stems from their abundant C-F bonds. The high electronegativity of F atoms induces strong electron localization, thereby giving the C-F bonds extremely high polarity and bond energy (~110 kcal/mol).8 The thermally and chemically robust C-F bonds endows PFAS with outstanding stability, unique lubricating and frictional characteristics, driving their extensive industrial applications since the 1940s, such as refrigerants, polymer-processing aids, pharmaceutical syntheses, adhesives, insecticides, and flame retardants.9,10

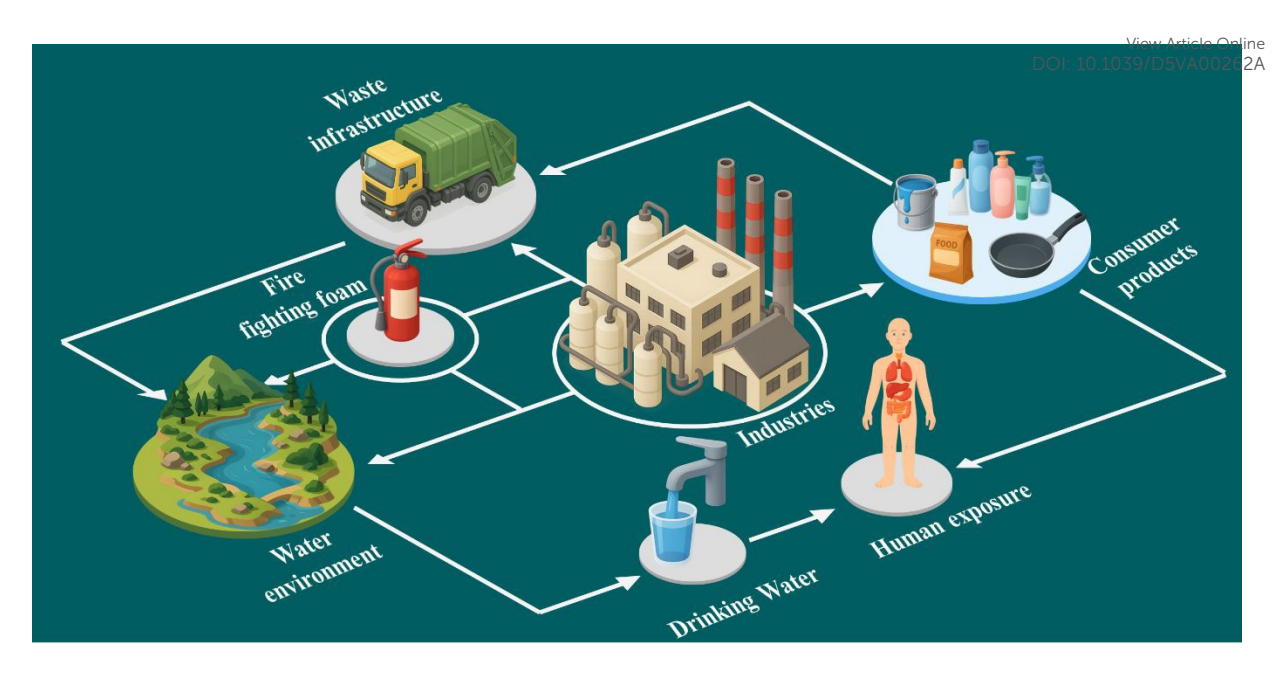


Figure 1. Migration process of PFAS in the environment.

PFAS were first detected in human serum in the 1960s,¹¹ which prompted studies on their environmental and biological risks. Their bioaccumulative potential is well established, with pronounced biomagnification in aquatic food webs.¹² Primary producers (e.g., phytoplankton) capture PFAS and introduce it into ecosystem. For aquatic vertebrates (e.g., cyprinus carpio, danio rerio), they directly absorb PFAS through gills, establishing trophic transfer pathways.¹³ In particular, the perfluoroalkyl phosphinic acids (PFPiAs) upregulate lipid transport genes (e.g., cd36, fabp1), leading to hepatic steatosis. The disruption of β -oxidation and phospholipid metabolism induces reactive oxygen species (ROS), activates NF- κ B, elevates pro-inflammatory cytokines (tnf- α , il-1 β , il-6), suppresses il-10,¹⁴⁻¹⁷ and triggers inflammation. The perfluorooctane sulfonates (PFOS) analogues bind transthyretin, disturbing thyroid homeostasis.¹⁸ In plants, PFAS are root-absorbed and transported to their above-ground parts. In wheat, fulvic and humic acids (HA) promote uptake of 6:2 Cl-PFAES via H⁺-

ATPase and Ca²⁺-dependent pathways.^{19,20} In arabidopsis, PFAS-induced ROS causes

lipid peroxidation and structural damage.²¹⁻²⁶ Structure-specific effects include PFOA-mediated cation disruption,²² PFOS-induced amino acid dysregulation,²³ and 8:2 FTSA conversion impacting lipid metabolism.²⁶ In mammals, PFAS induce neuro-, hepato-, and reproductive toxicity, and worsen gut inflammation.^{27,28} Dermal exposure models confirm systemic accumulation via CD36-mediated uptake, particularly in liver/kidneys.²⁹⁻³¹ Bioaccumulation is structure- and species-dependent, warranting further mechanistic research.

Due to the bioaccumulative potential and ecotoxicity of PFAS, their environmental contamination has become a pressing concern. Regulatory frameworks demonstrate increasing recognition of PFAS risks. In 2016, the U.S. Environmental Protection Agency (EPA) established health advisory levels at 0.070 μg/L for PFOS. Recent revisions have drastically reduced these thresholds to 0.004 ng/L for PFOA and 0.02 ng/L for PFOS.³² The EU Water Framework Directive proposes a cumulative limit of 0.1 μg/L for 20 prioritized PFAS compounds.³³ However, measured concentrations of PFAS in drinking water and groundwater worldwide often far exceed these thresholds (Figure 2).

Drinking water surveys reveal widespread contamination, with most urban supplies containing >100 ng/L PFAS globally.³⁴⁻⁴¹ South Korea exhibits the highest concentrations (644.6 ng/L) of the untreated drinking water (Figure 2a),³⁸ attributing to dense clustering of chemical plants, electronics manufacturers, and textile facilities discharging PFAS-laden effluents. Conversely, Kampala, the capital of Uganda, shows

minimal contamination (5.3 ng/L) (Figure 2a),⁴¹ potentially due to water sourcing from Wiew Article Online Murchison Bay where lake dilution mitigates PFAS levels.

The groundwater system is more severely polluted, with the concentrations of PFAS in it being 25 to 500 times higher than drinking water.⁴²⁻⁴⁹ Extreme contamination occurs near Swedish airports (51,000 ng/L) (Figure 2b),47 exceeding EU standards by 510 times, stemming from unregulated release of PFAS-containing firefighting foam over several decades. A recent investigation in Shandong Province of China—home to one of Asia's largest fluorochemical industrial parks-identified severe PFAS discharge into nearby streams. 50,51 Although the affected waterways are relatively small, the industrial park's emissions—totaling 8.4 t of HFPOs (hexafluoropropylene oxides)—represent 85% of all HFPOs discharge into rivers across China. 52 In contrast, North China Plain aguifers show relatively low PFAS levels (13.4 ng/L) (Figure 2b),42 correlating with limited industrial activity in the region. Recent reports indicate that PFAS concentrations in industrial wastewater treatment plants span a wide range, from 310 to 4920 ng/L in influents and from 246 to 27100 ng/L in effluents, reflecting variations over several orders of magnitude.53 The overall PFAS levels observed in these facilities are comparable to those recently reported in Korea for domestic wastewater (>1000 ng/L) and industrial wastewater (>5000 ng/L),54 as well as in fluorochemical wastewater treatment plants in France (25260 ng/L).55 These cases highlight that industrial wastewater discharge as the primary PFAS entry route into ecosystems. The extreme environmental persistence of PFAS facilitates progressive accumulation, posing severe ecological threats. Consequently, extensive researches

now focus on developing effective PFAS degradation technologies and remediation view Article Online strategies.

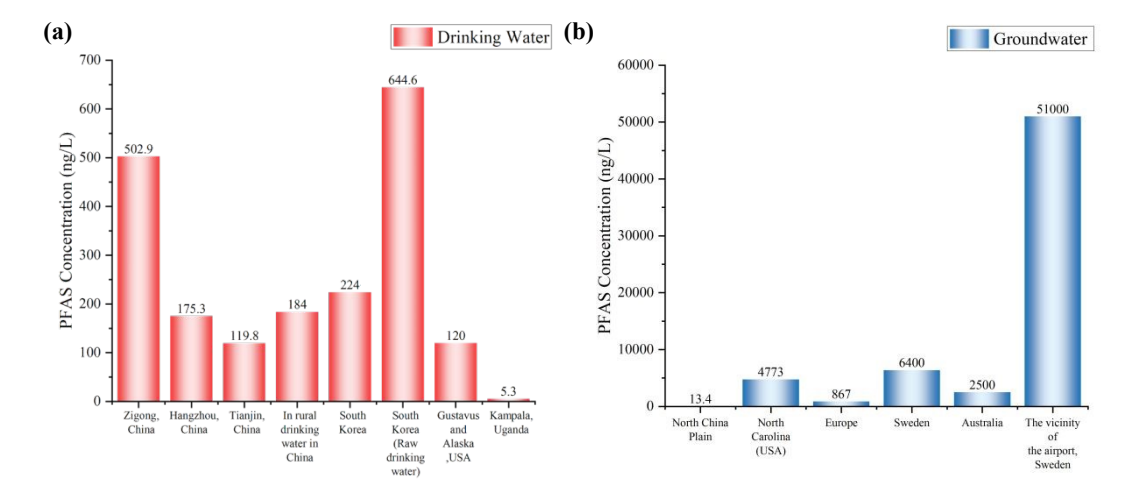


Figure 2. The concentration of PFAS in different water. (a) drinking water, and (b) groundwater.

2. Prevailing PFAS Degradation Strategies

A wide variety of purification methods for PFAS have been developed to date, including biodegradation approaches, 56,57 physical adsorption, 58,59 and chemical degradation (oxidation and reduction processes). 60-63 However, physical adsorption, being a non-destructive process, may generate secondary waste such as spent adsorbents, which pose a risk of re-releasing PFAS into the environment. In contrast, biodegradation and chemical degradation aim at the permanent removal of PFAS. Nevertheless, biodegradation is often incomplete, slow, and highly dependent on specific environmental conditions. 64 More importantly, it is difficult to break the extremely strong C–F bonds of PFAS molecules. Among the chemical degradation methods, advanced oxidation processes (AOPs), first introduced by Glaze in 1987, are

purification.71,72

characterized by the generation of highly reactive radical species as oxidants, and are regarded as promising technologies with strong potential for the complete mineralization of PFAS.65,66 Among AOPs, the Fenton reaction is one of the most classical and widely studied techniques. The Fenton reaction was first discovered in 1894 by the French scientist Henry. J. Fenton, who observed that tartaric acid could be deactivated and oxidized in a ferrous ion (Fe²⁺)/ hydrogen peroxide (H₂O₂) system at pH 2-3.67 The key advantages of the Fenton process include its high oxidative performance and operational simplicity under ambient temperature and atmospheric pressure. 68,69 Moreover, its toxicity is relatively low because H₂O₂ ultimately decomposes into environmentally benign species such as water (H2O) and oxygen (O₂).⁷⁰ Mechanistically, utilizing Fe²⁺ as a catalyst, it enables the continuous and stable decomposition of H₂O₂ to generate hydroxyl radicals (•OH) (shown in Eq (1) and Eq (2)). These highly reactive hydroxyl radicals subsequently attack organic pollutants present in water, initiating a cascade of oxidation reactions that ultimately mineralize the contaminants into carbon dioxide (CO₂) and H₂O, thereby achieving water

$$Fe^{2+} + H_2O_2 + H^+ \rightarrow Fe^{3+} + H_2O + \bullet OH$$
 (1)

$$Fe^{3+} + H_2O_2 \rightarrow Fe^{2+} + HO_2^{\bullet} + H^+$$
 (2)

For the complete mineralization of PFAS, the degradation pathway begins with the initial activation of the molecule to generate perfluoroalkyl radicals ($\cdot C_n F_{2n+1}$).

These radicals then react with •OH to form unstable perfluoroalcohol intermediates, which readily undergo elimination reactions to release hydrogen fluoride (HF). The resulting acyl fluoride intermediates are highly prone to hydrolysis, leading to the formation of shorter-chain perfluorocarboxylic acids. Through successive cycles of similar reactions, PFOA can eventually be mineralized into CO₂ and HF (Figure 3). The ability of the Fenton system to continuously supply hydroxyl radicals makes it a promising approach for driving the deep oxidative degradation and potential mineralization of PFAS.

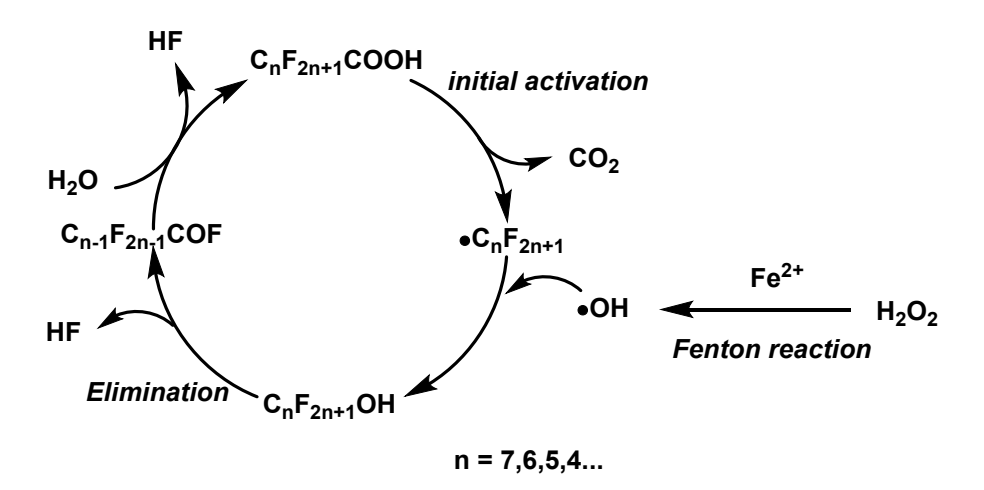


Figure 3. Reaction mechanism for degradation of PFOA via the Fenton process. Upon completion of each reaction cycle, the value of n decreases by one, initiating the subsequent cycle.

However, the Fenton reaction also exhibits certain limitations. When treating wastewater, its efficiency is influenced by factors such as pH and iron ion concentration of wastewater. Neither low nor high pH values enable effective treatment of organic pollutants. The optimal treatment efficiency is achieved within a pH range of 2.0–

4.0.76,77 Unfortunately, most organic wastewaters do not naturally fall within DH with range. The substantial amounts of chemical reagents are often required to adjust the pH prior to treatment, which increases the overall cost of wastewater remediation. Furthermore, while Equations (1) and (2) form the basis for the catalytic cycle of the Fenton reaction, the rate of reaction (1) is approximately 6,000 times faster than that of reaction (2),78 which severely hampers the regeneration of Fe²⁺ from Fe³⁺ and leads to the accumulation of Fe³⁺ in the system. When the pH values above 3, Fe³⁺ tends to precipitate as hydroxide complexes—commonly referred to as iron sludge.⁷⁹ This sludge is difficult to separate and recover, resulting in substantial loss of catalytic iron species, reduced process efficiency, and the risk of secondary environmental pollution. To overcome these limitations, various strategies have been developed to enhance the Fenton reaction. Depending on the enhancement method, these approaches can be categorized into chemical-Fenton, 80-87 electro-Fenton, 88-93 UV/visible/solar light-assisted Fenton (photo-Fenton), 94-101 and solar photo-electro-Fenton (SPEF) systems. 102-107 Moreover, these technologies can be integrated in a synergistic or coupled manner to minimize or even eliminate the limitations associated with individual processes.

Herein, we focus on the research progress in utilizing Fenton reaction systems for PFAS degradation (Figure 4). Through a systematic discussion of various Fenton systems, this review extensively elucidates degradation pathways, degradation efficiency, the redox potentials of different radical species, byproduct formation, and toxicity assessment. The primary objectives of this review are as follows: (1) to summarize the pathways and mechanisms of different Fenton reaction system; (2) to

summarize the degradation efficiencies of various radicals involved in PFAS removal properties and conditions; (3) to systematically compare factors influencing

PFAS degradation efficiency; (4) to summarize byproduct formation across different

Fenton reaction systems and critically analyze their associated toxicity; and (5) to

outline future research prospects. This review aims to establish a theoretical foundation

for PFAS removal in practical applications.

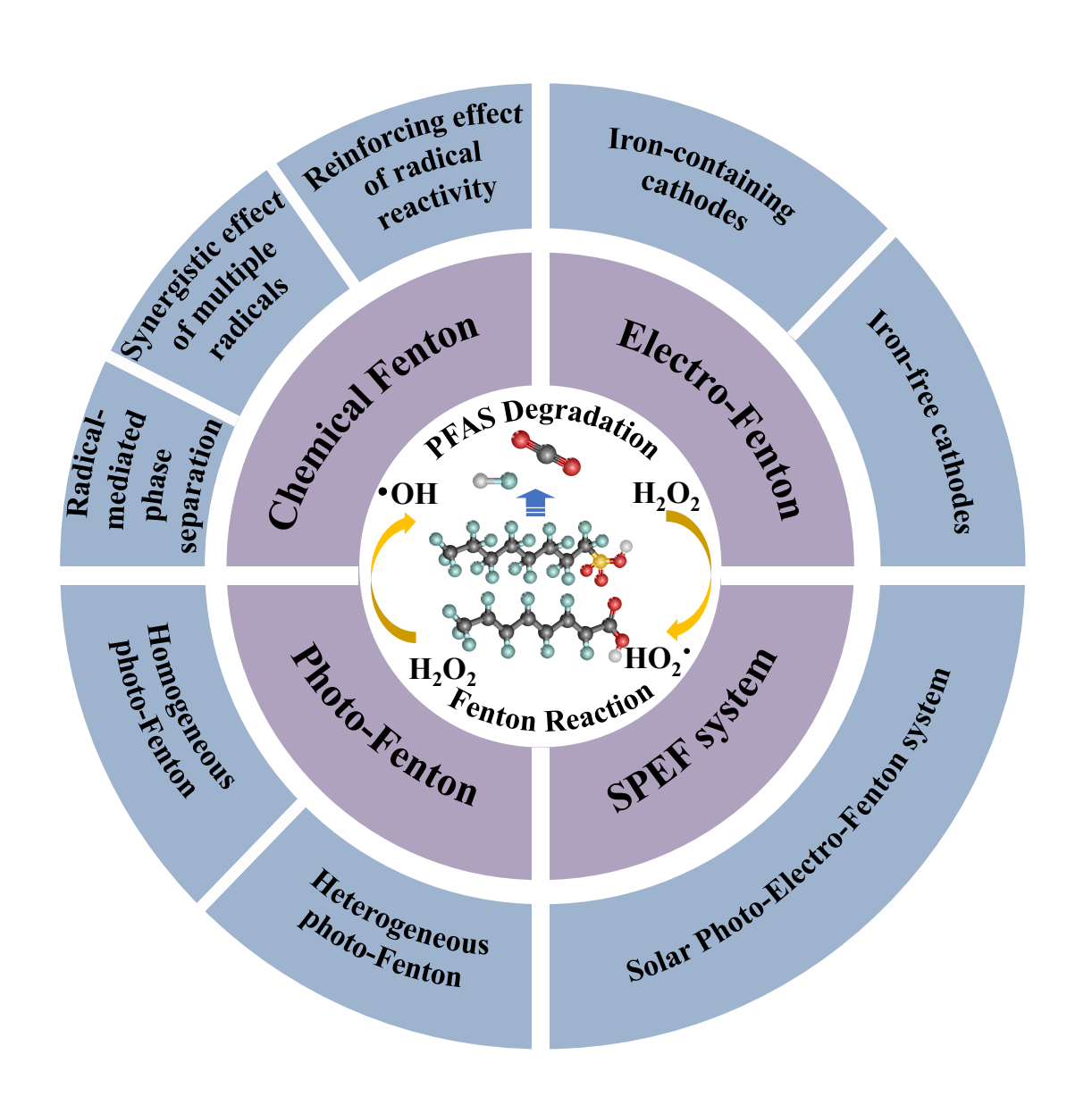


Figure 4. Summary diagram of the contents in this review.

View Article Online DOI: 10.1039/D5VA00262A

3. Degradation of PFAS via Fenton reactions

3.1 Chemical-Fenton reaction system

Although the classical chemical Fenton reaction provides a stable and efficient source of • OH, these radicals alone have proven inadequate for the effective degradation of PFAS. For instance, in the case of PFOA, studies have demonstrated that even under high concentrations of H₂O₂, the degradation efficiency is significantly low. Even with the addition of Fe²⁺ and H₂O₂, negligible degradation of PFOA and PFOS was observed, indicating the limited oxidative capacity of conventional •OH-based systems in attacking the highly stable C–F bonds. ^{108,109} In response, considerable efforts have been made to expand and modify chemical Fenton systems, employing diverse strategies to enhance the degradation efficiency of PFAS, such as synergistic effect of multiple radicals, reinforcing effect of radical reactivity, and radical-mediated phase separation (Figure 5).



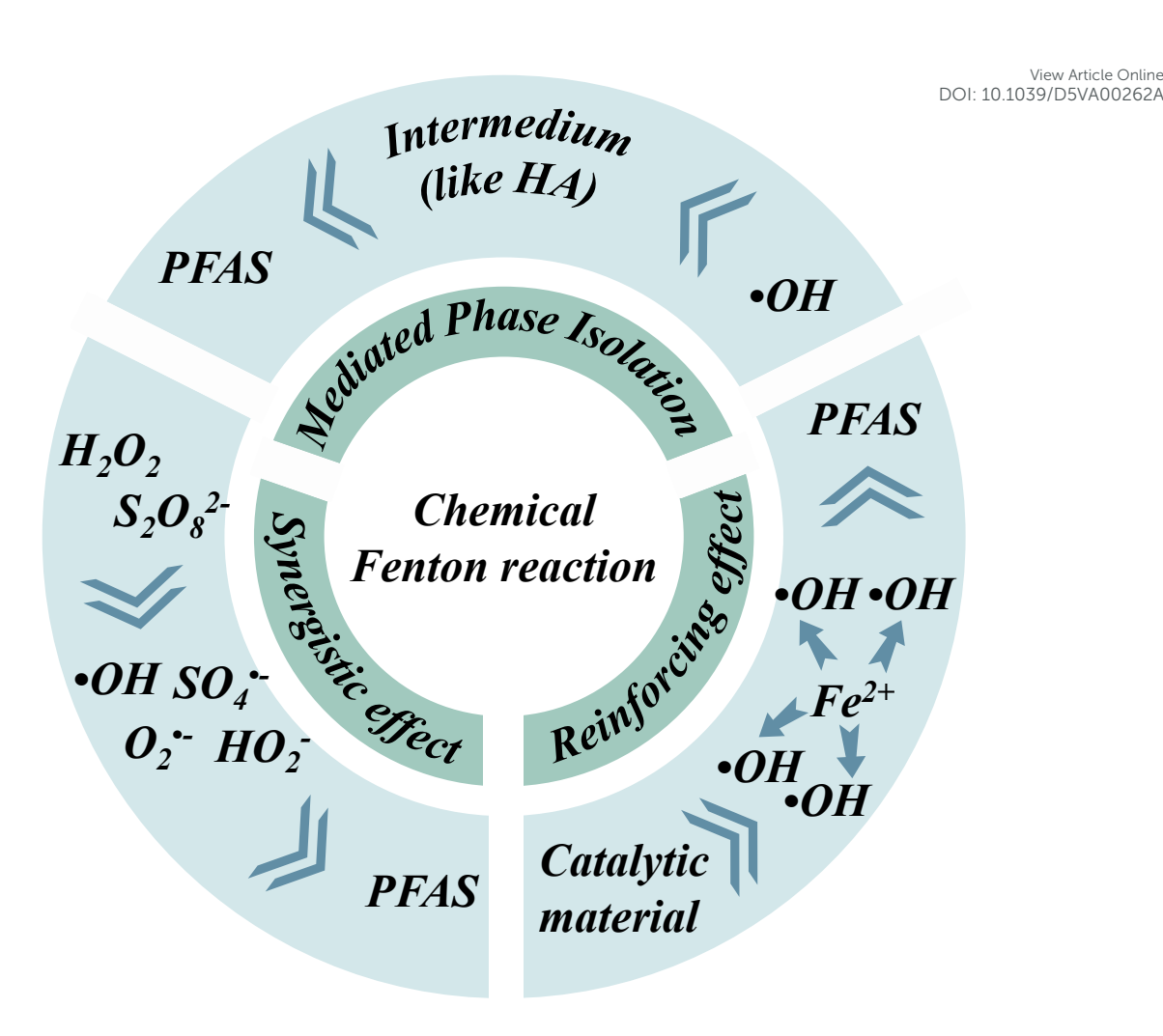


Figure 5. Progress in chemical Fenton reaction system toward PFAS remediation.

3.1.1 Synergistic effect of multiple radicals

To enhance the PFAS degradation ability of chemical Fenton reaction system, the potential of multi-radical synergistic degradation was evaluated, Lo et al. developed a chemical Fenton reaction system employing zero-valent iron (ZVI) to activate persulfate (PS) and •OH for the decomposition of perfluorooctanoic acid (PFOA).80 In this system, PS acts as a sulfate radicals (SO₄··) precursor, while ZVI serves as a catalyst to lower the activation energy required for the generation of SO₄. (shown in Eq (3) to Eq (6)). At the optimal temperature, the degradation rate of PFOA increased from 10% (using •OH alone) to 68% with the combined action of SO₄• and •OH (Figure 6a),

while the defluorination efficiency improved from 19% to 23% (Figure 6b) Within 2/D5VA00262A hours, indicating a significant synergistic effect between SO₄- and •OH radicals in promoting PFOA degradation. Notably, SO₄- has a higher redox potential of up to 2.6 V, exceeding that of •OH (2.3 V). Moreover, SO₄- demonstrate superior performance in initiating the degradation of PFOA by facilitating the formation of perfluoroalkyl radicals (Figure 6c).

$$Fe^{0} + \frac{1}{2}O_{2} + H_{2}O \rightarrow Fe^{2+} + 2OH^{-}$$
 (3)

$$Fe^0 + 2H_2O \rightarrow Fe^{2+} + 2OH^- + H_2$$
 (4)

$$S_2O_8^{2-} + \text{heat} \rightarrow 2SO_4^{\bullet-} \tag{5}$$

$$Fe^{2+} + S_2O_8^{2-} \rightarrow Fe^{3+}SO_4^{\bullet-} + SO_4^{2-}$$
 (6)

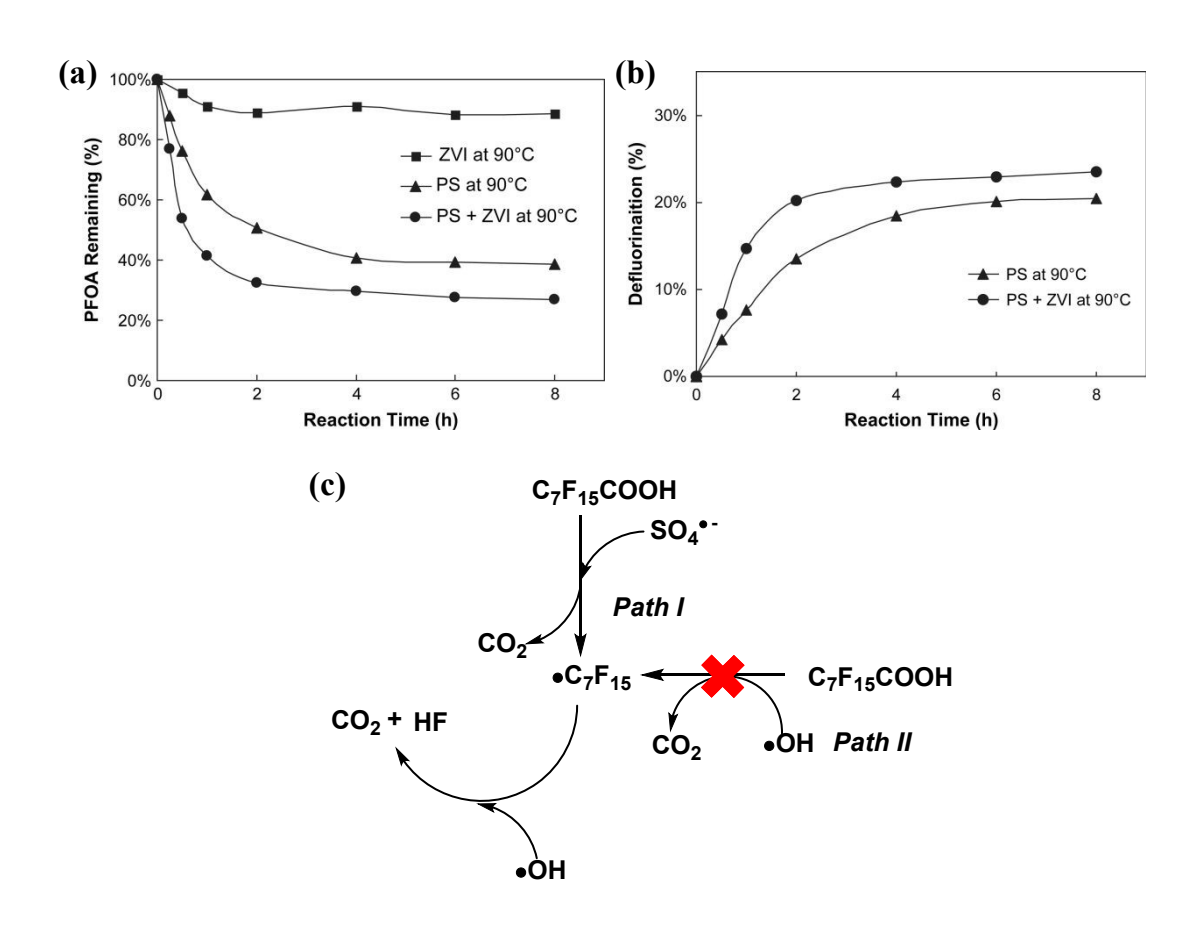


Figure 6. (a) Comparison the decomposition of PFOA in presence of persulfate (PS) at

90 °C with or without ZVI. (b) The defluorination of PFOA with persulfate at 00 10 Ct. 38 / D5 VA00262A

(c) The proposed synergistic mechanism of the •OH and SO₄ for PFAS degradation.

In order to further expand the reactive species involved in multi-radical coupling. Watts et al. developed a •OH/superoxide (O2•-)/ hydroperoxide anion (HO2•)-based multi-radical system, enabling a stable and efficient chemical Fenton process for the degradation of PFOA.81 Through catalyzed hydrogen peroxide (H₂O₂) propagation (CHP) reactions, H₂O₂ can be continuously decomposed to generate O₂ and HO₂ (shown in Eq (7) to Eq (9)). The O_2^{\bullet} contributes to maintaining the continuity of the Fenton process by reducing Fe³⁺ to Fe²⁺, while HO₂• is generally regarded as a strong nucleophile, capable of attacking electron-deficient carbon atoms in PFOA, particularly those adjacent to the carboxyl group (e.g., the α-carbon). This process facilitate C-F bond cleavage and thus promote both degradation and defluorination (Figure 7a). 110 The concentrations of H₂O₂ affect the types and concentrations of free radicals. The synergistic effect of multiple radicals (•OH, O2•, and HO2•) was supported by the optimal degradation efficiency exceeding 80% (Figure 7b). One mol of PFOA molecules contains 15 mol F atoms, at a 1 M H₂O₂ concentration, the ratio of F⁻ ions to PFOA molecules is approximately 15, indicating complete defluorination mineralization performance (Figure 7c).

$$\bullet OH + H_2O_2 \rightarrow HO_2^{\bullet} + H_2O$$
 (7)

$$HO_2^{\bullet} \leftrightarrow O_2^{\bullet-} + H^+(pK_a = 4.8)$$
 (8)

$$HO_2^{\bullet} + Fe^{2+} \rightarrow Fe^{3+} + HO_2^{-}$$

View Article Online DOI 98.1039/D5VA00262A

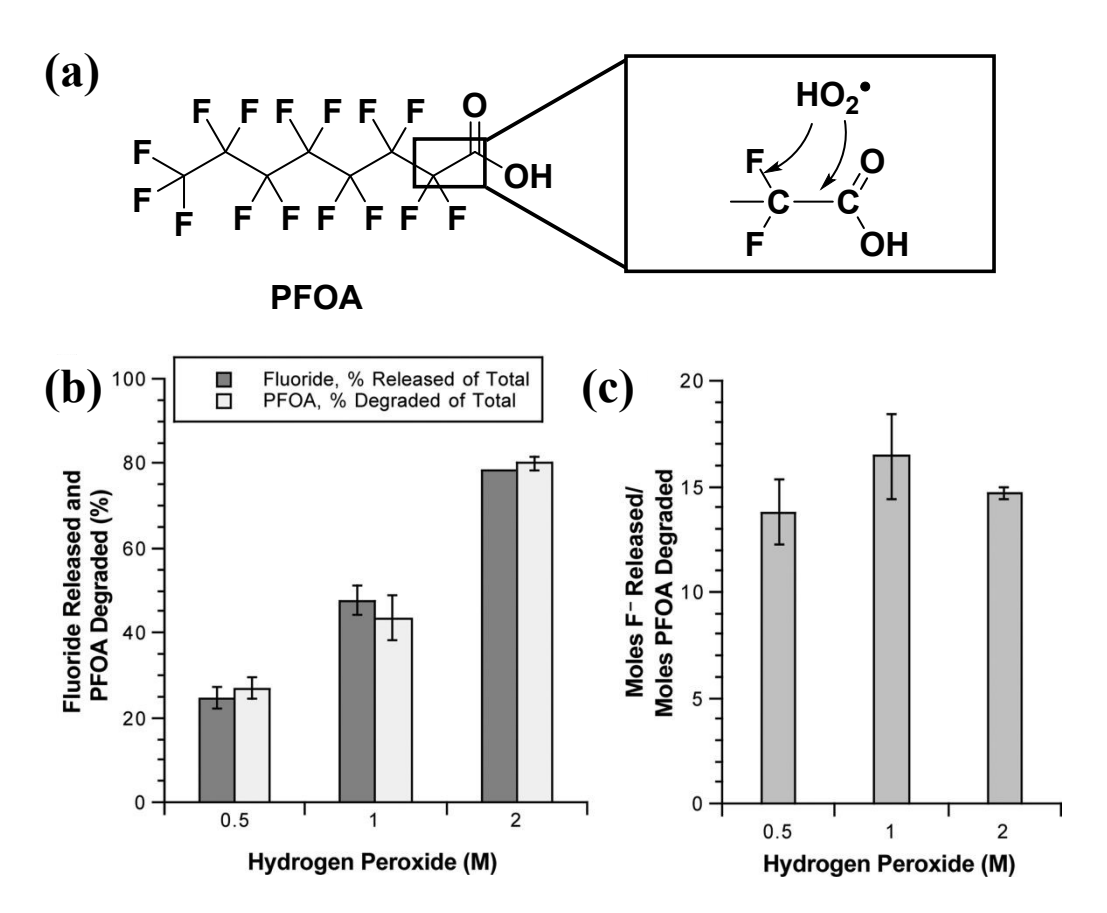


Figure 7. (a) A schematic diagram of HO₂* radical attacking electron-deficient carbon atoms in PFOA. (b) The defluorination and degradation efficiency of PFOA under the different concentrations of hydrogen peroxide. (c) The ratio of moles of fluoride released to moles of PFOA degraded under different concentrations of hydrogen peroxide.⁸¹

In addition, the combination of SO_4 , $\bullet OH$, and O_2 radicals has also proven effective. Choi et al. developed an iron-modified diatomite (MD) catalyst capable of efficiently generating SO_4 , $\bullet OH$, and O_2 , thereby promoting PFOA degradation through synergistic radical interactions.⁸² The key advantage of the MD catalyst lies in

Open Access Article. Published on 29 2025. Downloaded on 10.11.2025 10:02:00.

BY-NC This article is licensed under a Creative Commons Attribution-NonCommercial 3.0 Unported Licence.

its naturally abundant and low-cost material, as a stable and easily separable support for iron loading. At the same time, its high surface area is conducive to the generation of free radicals and the adsorption of pollutants. This system utilizes the catalytic ability of Fe²⁺ to activate H₂O₂ and PS, and can continuously and stably generate •OH, O₂• and $SO_4^{\bullet-}$ (shown in Eq(1), Eq(10) and Eq(11)). In conventional dual-radical systems such as •OH/ SO₄·-, the cleavage of highly inert C-F bonds in PFOA remains limited. However, the introduction of O₂ induces an additional reductive and nucleophilic pathway targeting electron-deficient α -carbon atoms adjacent to the carboxyl group, thereby enhancing C–F bond cleavage (Figure 8a). Moreover, the combination of SO₄*-(a strong oxidant 2.6 V) and O₂. (a moderate reductant -0.33 V) provides a more diverse redox environment for Fe²⁺/Fe³⁺ that improves the overall degradation efficiency. As experiment demonstrated, MD was capable of catalyzing both the Fenton reaction with H₂O₂ and the CHP reaction, achieving a moderate PFOA degradation efficiency of 60% (Figure 8b). When PS was further introduced into the reaction system, the synergistic effect of SO₄., •OH, and O₂. radicals enhanced the degradation efficiency to 69% (Figure 8c), highlighting the effectiveness of multi-radical cooperation.

$$HO_2^- + S_2O_8^{2-} \rightarrow SO_4^{\bullet-} + SO_4^{2-} + H^+ + O_2^{\bullet-}$$
 (10)

$$S_2O_8^{2-} + 2H_2O_2 \rightarrow 2SO_4^{2-} + 2O_2^{\bullet-} + 4H^+$$
 (11)

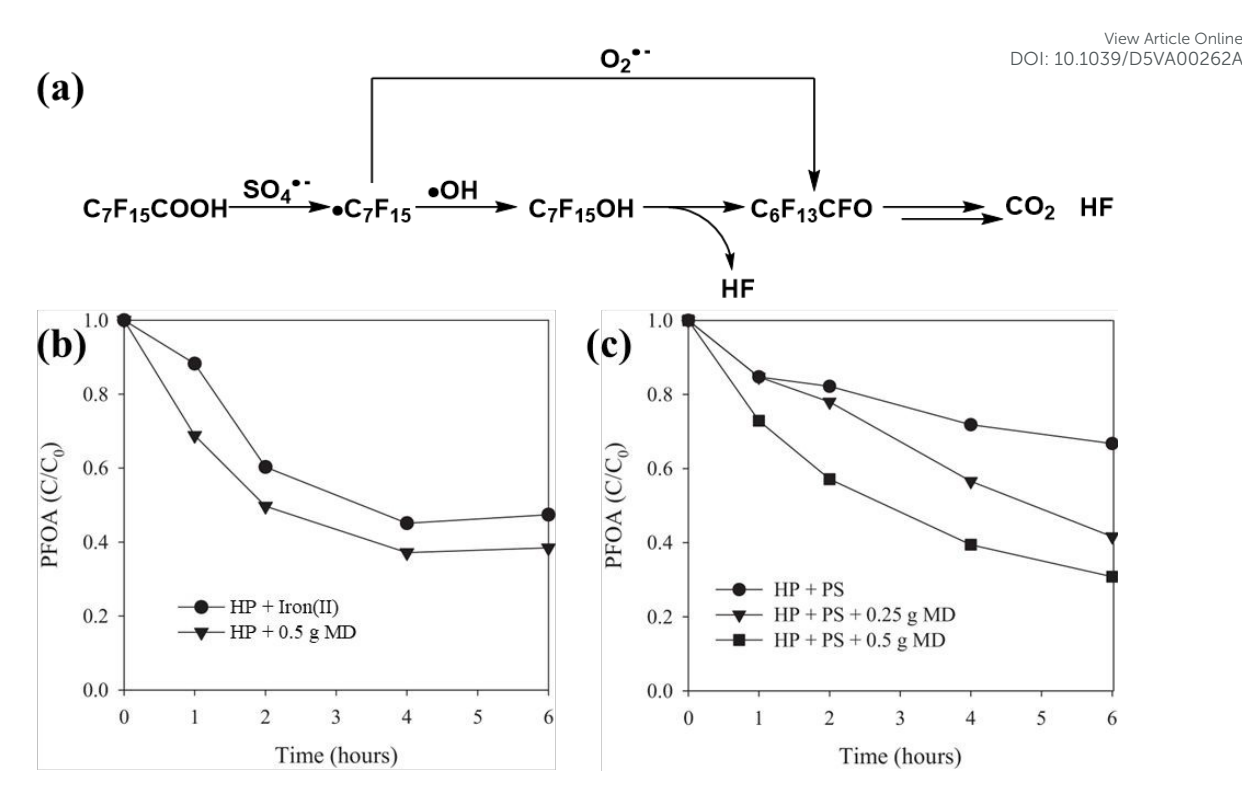


Figure 8. (a) The PFOA degradation mechanism of •OH, O₂• and SO₄• radicals. (b) Decomposition of PFOA by catalyzed hydrogen peroxide propagation (CHP) reactions in the presence of dissolved Fe ions and in the presence of MD containing Fe species. (c) Decomposition of PFOA by different HP-activated PS systems. PP: hydrogen peroxide, H₂O₂; PS: persulfate, S₂O₈²-.

In summary, the development of multi-radical synergistic degradation strategies within Fenton-based systems has shown significant promise for improving PFAS treatment efficiency. The combined action of various reactive species—such as •OH, SO₄·-, O₂·-, and HO₂·-—can substantially enhance the degradation process. This improvement is primarily attributed to: (1) the stronger oxidative potential of SO₄·-, which can overcome the limitations of •OH in initiating the activation of PFAS molecules; (2) the presence of a multi-radical environment that increases the probability

Open Access Article. Published on 29 2025. Downloaded on 10.11.2025 10:02:00.

BY-NG This article is licensed under a Creative Commons Attribution-NonCommercial 3.0 Unported Licence.

and efficiency of radical attacks on PFAS compared to systems dominated by a single radical species. However, multi-radical Fenton systems also face several limitations.

The complexity of the reaction environment, which makes it difficult to clearly elucidate the underlying mechanisms and pathways of radical synergy. In addition, the overall degradation efficiency remains insufficient to meet the demands of rapid and effective PFAS removal. Therefore, efforts are being made to develop strategies aimed at further enhancing the radical reactivity.

3.1.2 Reinforcing effect of radical reactivity

To enhance the activity of reactive radicals, researchers have focused on material structural design with high specific surface areas, whose unique architectures provide several key advantages: (1) increased number of exposed Fe active sites, particularly on surfaces and within micropores; (2) limited diffusion pathways of PFAS molecules, enhancing the contact between contaminants and catalytic sites; and (3) confined microenvironments promoted the local accumulation and prolonged lifetime of reactive radicals.

Wang et al. fabricated a composite material by anchoring Pb-doped BiFeO₃ (Pb-BFO) nanoparticles onto reduced graphene oxide (rGO) nanosheets,⁸³ forming a layered architecture. The Pb-BFO nanoparticles were firmly immobilized on the rGO surface, which effectively inhibited nanoparticle agglomeration and preserved high surface reactivity. Moreover, the formation of nanoscale interlayer gaps between rGO sheets facilitated rapid electron transfer, thereby enabling the localized enrichment of •OH

within the confined interlayer space and the oxidative interaction between •OH and PFONA00262A
PFAS molecules (Figure 9a and 9b). Additionally, Pb doping improved the intrinsic charge transport properties of BFO, while the oxygen-containing functional groups
(e.g., carboxyl and hydroxyl groups) of rGO were capable of activating H₂O₂ to produce
•OH radicals, collectively contributing to the improved catalytic efficiency of the composite system (Figure 9c). This approach achieved over 95% degradation efficiency of PFOA within 5 minutes, with nearly half of the PFOA undergoing complete mineralization (Figure 9d). These results underscore the feasibility of employing porous materials to promote chemical Fenton-based degradation of PFAS.

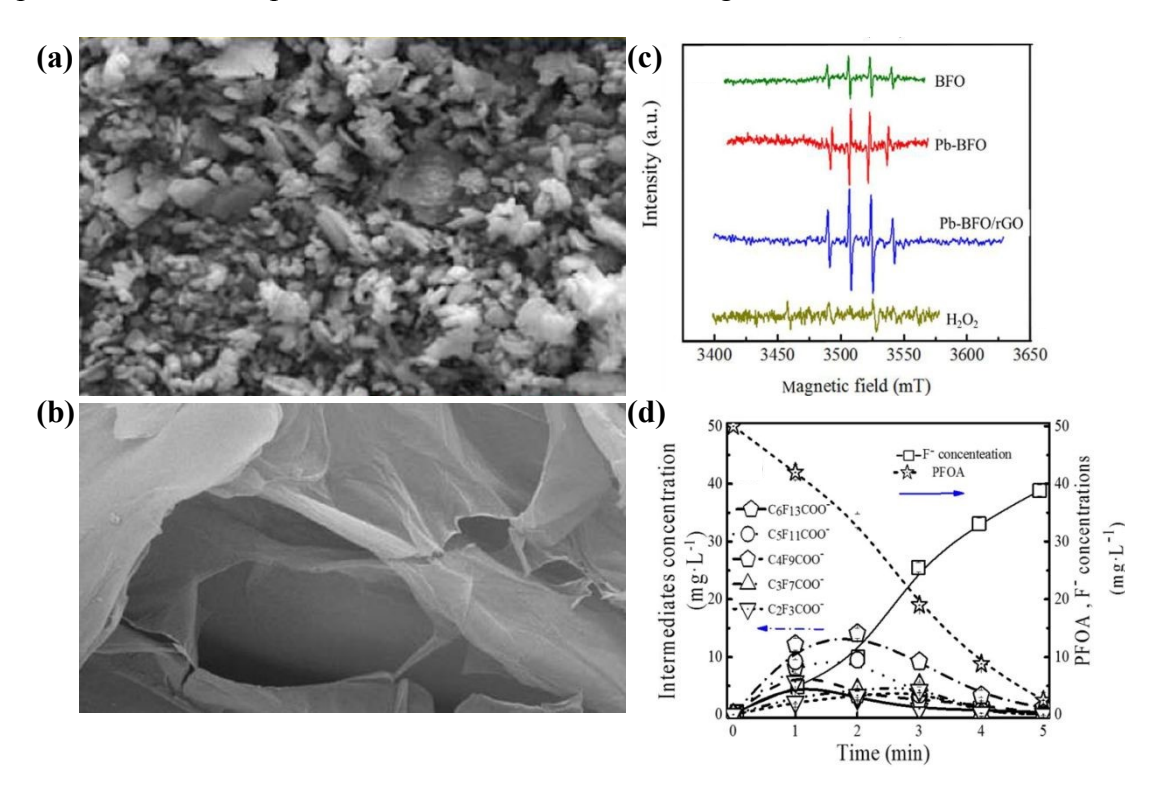


Figure 9. SEM images of Pb-BFO/rGO (a) and GO (b) composite. (c) The EPR spectra of different catalyst suspensions. (d) Evolution of the F concentration and degradation byproducts as a function of degradation time with Pb-BFO/rGO system.⁸³

For the purpose of further understanding the influence of material structure on the $^{\text{View Article Online}}_{\text{LO}}$

efficiency of chemical Fenton degradation of PFAS, Shi et al. extended the structure of conventional two-dimensional reduced graphene oxide (rGO) into a three-dimensional graphene-based framework (OG),⁸⁴ in which the abundant C–O–C bridging structures were found to significantly enhance the Fenton reaction by promoting the generation efficiency of •OH (Figure 10a).Notably, the OG material was derived from recycled biomass waste, aligning with the principles of green chemistry and offering promising advantages in terms of environmental sustainability and economic viability. Density functional theory (DFT) calculations indicated that the C–O–C bridging structure of OG was key to electron transport. Electrons from the C–F bonds in PFOA could transfer to the OG surface via these bridges (Figure 10b), with the F atom's HOMO contribution increasing significantly from 0.95% to 15.46% (Figure 10c). Moreover, the spatial confinement effect of OG reduced the activation energy for H₂O₂ decomposition (1.10 eV for OG vs. 1.60 eV for 2D graphene).

This article is licensed under a Creative Commons Attribution-NonCommercial 3.0 Unported Licence

Open Access Article. Published on 29 2025. Downloaded on 10.11.2025 10:02:00.

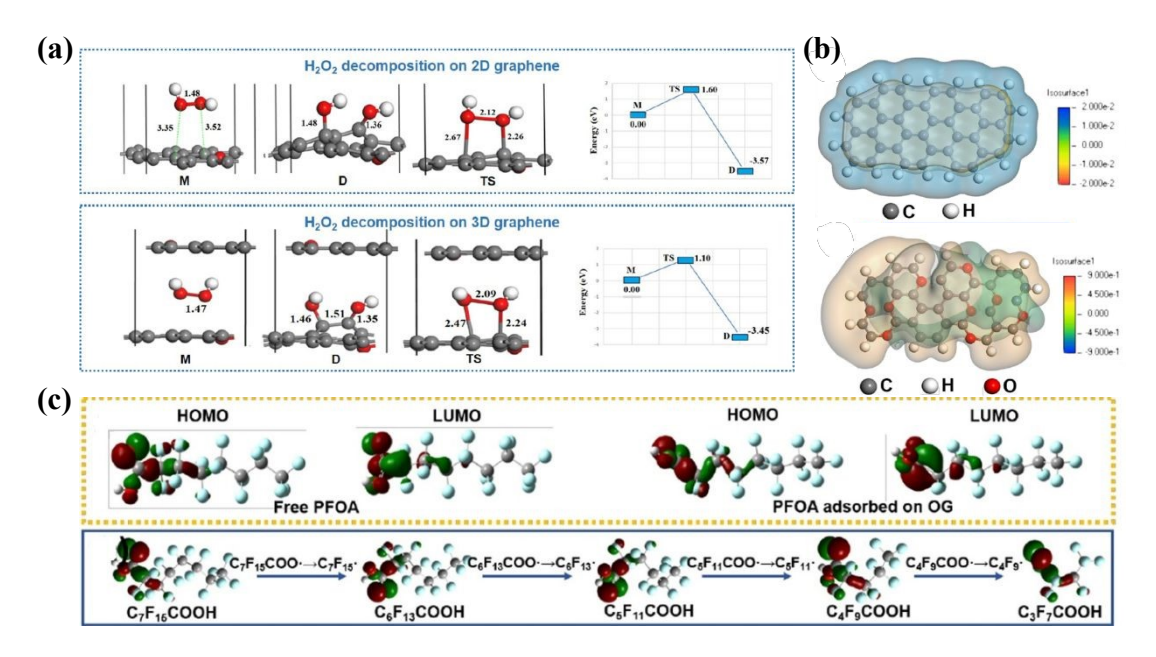


Figure 10. (a) Energy profiles of H₂O₂ decomposition on 2D and 3D graphene. (b)

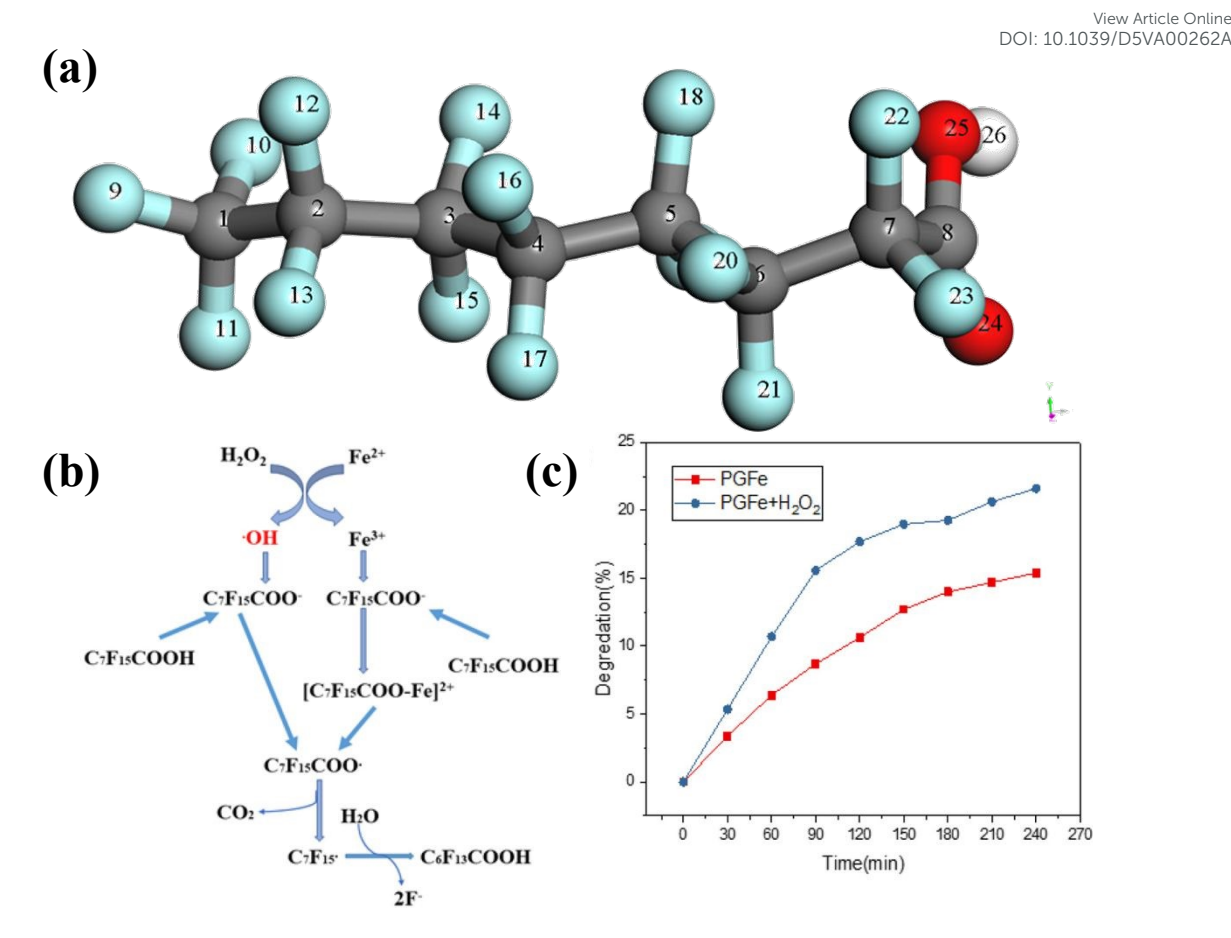
Open Access Article. Published on 29 2025. Downloaded on 10.11.2025 10:02:00.

BY-NG This article is licensed under a Creative Commons Attribution-NonCommercial 3.0 Unported Licence

Comparison of the electrostatic potential distributions of porous graphene and modified graphene. (c) HOMO and LUMO energies of free PFOA, PFOA adsorbed on OG and PFOA intermediates during degradation.⁸⁴

Similar to the above strategy, Zhuang et al. synthesized a Fe/S co-doped carbon aerogel (PGFe),⁸⁵ in which sulfur doping played a crucial role in facilitating covalent bonding between iron and carbon, thereby enhancing the electronic conductivity of the material and accelerating the Fenton reaction by creating a more stable environment for • OH generation. Additionally, the incorporation of polyvinyl alcohol during the carbonization process promoted the formation of a highly porous structure, effectively increasing the specific surface area and exposing a greater number of active sites. Charge and electrophilicity analyses identified C7, C8, terminal F23, and electron-rich O24 atoms in the PFAS molecule as the most susceptible to •OH attack (Figure 11a), providing a theoretical basis for predicting bond cleavage pathways (Figure 11b). This study provides a solid theoretical foundation for understanding the PFOA degradation process. The PFAS degradation efficiency via PGFe modified chemical Fenton-based reactions improved from 15% to 22% (Figure 11c).





This article is licensed under a Creative Commons Attribution-NonCommercial 3.0 Unported Licence

Open Access Article. Published on 29 2025. Downloaded on 10.11.2025 10:02:00.

Figure 11. (a) Structure of PFOA denoted by sequence number: 1-8 carbon, 9-23 fluorine, 24-25 oxygen and 26 hydrogen. (b) Schematic diagram of degradation process of PFOA in PGFe/H₂O₂ Fenton system. (c) PFOA degradation rate in PGFe and PGFe/H₂O₂ system.85

To further investigate the relationship between material porosity and the degradation rate of PFAS, Zhang et al. developed a layered iron oxychloride (FeOCl) catalyst.86 By confining reactive species within a sub-nanometer spatial domain, the hydration coordination number of O₂ radicals generated from the Fenton reaction was modulated, reducing the average coordination number from 3.3 to 1.89 (Figure 12a and 12b). The decreased coordination number concentrated the negative charge on O_2^{\bullet} ,

strengthening its interaction with PFAS molecules. To further enhance spatial effect, the FeOCl was immobilized onto ceramic membranes, the active channels were confined within a 20 nm scale (Figure 12c). As a result, the apparent reaction rate constant (k_{obs}) reached 1.2 min⁻¹ (Figure 12d), which was 86 times higher than that of a traditional batch-mode system (0.014 min⁻¹). This study quantitatively demonstrated the performance enhancement of PFAS degradation reactions achieved by confinement effect of high specific surface area materials, and provides a feasible approach for future investigations into the structure–activity relationship for PFAS degradation.

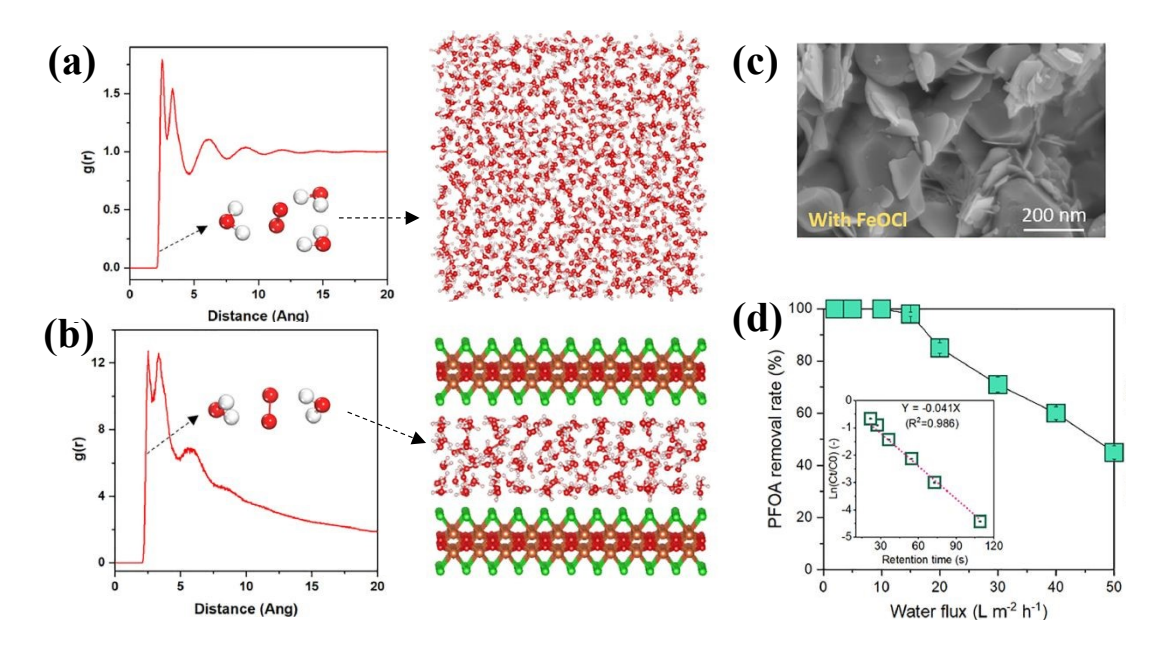


Figure 12. (a) The RDF as a function of distance from free O_2^{\leftarrow} radicals and snapshot of the free O_2^{\leftarrow} radicals in aqueous phase. (b) The RDF as a function of distance from confined O_2^{\leftarrow} radicals and snapshot of the O_2^{\leftarrow} radicals confined inside the FeOCl structure. (c) Cross-sectional SEM images of the FeOCl-incorporated ceramic membrane. (d) Fast degradation of PFOA through heterogeneous Fenton reaction inside FeOCl membrane.⁸⁶

Although structural design of materials can effectively enhance the interaction between reactive radicals and PFAS, numerous unresolved issues remain—such as how the sensitivity of spatial confinement to material dimensions influences radical reactivity, and whether atomic-level features within the catalyst structure affect the confinement effect. Additionally, the deep defluorination remains a challenge, especially for the degradation by-products of short chains.

3.1.3 Radical-mediated phase separation

To address the deep defluorination of PFAS and the accumulation of short-chain byproducts, Santos employed the abundant • OH generated in the Fenton reaction system to oxidatively modify humic acid (HA) for phase separation of aqueous PFAS and their short-chain byproducts. FT The HA molecules contain various functional groups, such as carboxyl and phenolic hydroxyl groups, which may be oxidized or rearranged during the reaction, resulting in the formation of new chemical bonds and larger structural assemblies. Through the oxidative transformation and restructuring of functional groups on HA, the interaction between HA and PFOA was enhanced, ultimately facilitating the transfer of PFOA from the aqueous phase to the solid phase via a co-precipitation and phase separation mechanism (Figure 13a).

As the structure of HA evolves, it may form larger polymeric or network-like aggregates. These aggregates can physically entrap PFOA molecules adsorbed on their surfaces, effectively encapsulating them within the HA matrix (Figure 13b). This encapsulation hinders the re-release of PFOA into the aqueous phase, thereby

facilitating its removal from water. However, this process does not involve the chemical PDSVA00262A degradation of PFOA; rather, the molecule merely transfers from the aqueous phase to the solid phase. Consequently, the development of effective strategies for the removal of PFAS immobilized in solid phases has emerged as a critical focus area. Materials such as graphene, metal-organic frameworks (MOFs), and covalent organic frameworks (COFs) are being explored as advanced platforms capable of adsorbing PFAS and enabling their subsequent solid-phase separation under catalytic or advanced oxidation conditions.¹¹¹

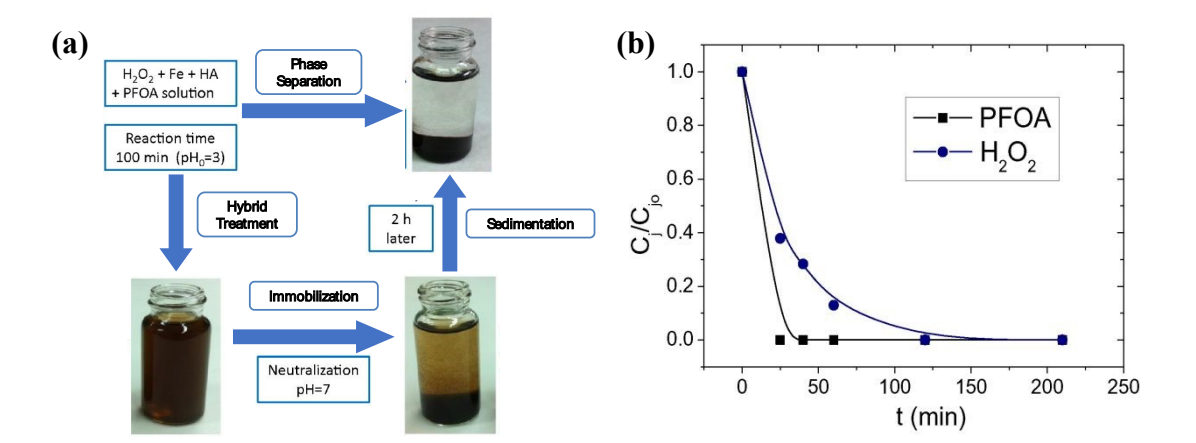


Figure 13. (a) Illustration of HA-coupled Fenton reaction driving multiphase conversion of PFOA. (b) Residual PFOA and oxidant in hybrid treatment of PFOA solution with Fenton like reagent and humic acid.⁸⁷

Substantial progress has been made in understanding the application of chemical-Fenton reactions for PFAS treatment. The chemical-Fenton system offers several advantages, including relatively simple experimental conditions, high selectivity, the synergistic action among multiple reactive radicals, and high achieving efficient PFAS degradation through material structure designs. However, several limitations remain. (1)

The requirement for high concentrations of H_2O_2 (≥ 1 M) not only leads to excessive reagent consumption but also poses significant safety concerns. (2) The system generally exhibits limited capacity to sustain the Fe^{2+}/Fe^{3+} redox cycle, raising challenges for maintaining long-term Fenton reactivity. (3) Like conventional Fenton systems, chemical Fenton processes have not overcome the inherent pH constraint, typically requiring pre-acidification of the aqueous environment, which further restricts their practical applications.

3.2 Electro-Fenton reaction system

The electro-Fenton (EF) process differs from the conventional chemical-Fenton reaction in mechanism. Efficient PFAS mineralization typically requires the initial activation of PFAS molecules into perfluoroalkyl radicals. In the chemical Fenton process, the generation of •OH alone is often insufficient; therefore, additional more potent oxidation species are needed to achieve effective degradation. In contrast, electro-Fenton systems utilize electrocatalysis—one of the most powerful redox techniques—to directly oxidize PFAS and form perfluoroalkyl radicals, thereby promoting further •OH generation and overall degradation efficiency. Moreover, the electro-Fenton process offers two additional advantages for PFAS remediation: (1) insitu generation of H₂O₂ via the oxygen reduction reaction (ORR), reducing reliance on external H₂O₂ dosing; and (2) improved Fe²⁺/Fe³⁺ redox cycling under optimized electrochemical conditions, minimizing the formation of iron sludge (Figure 14).

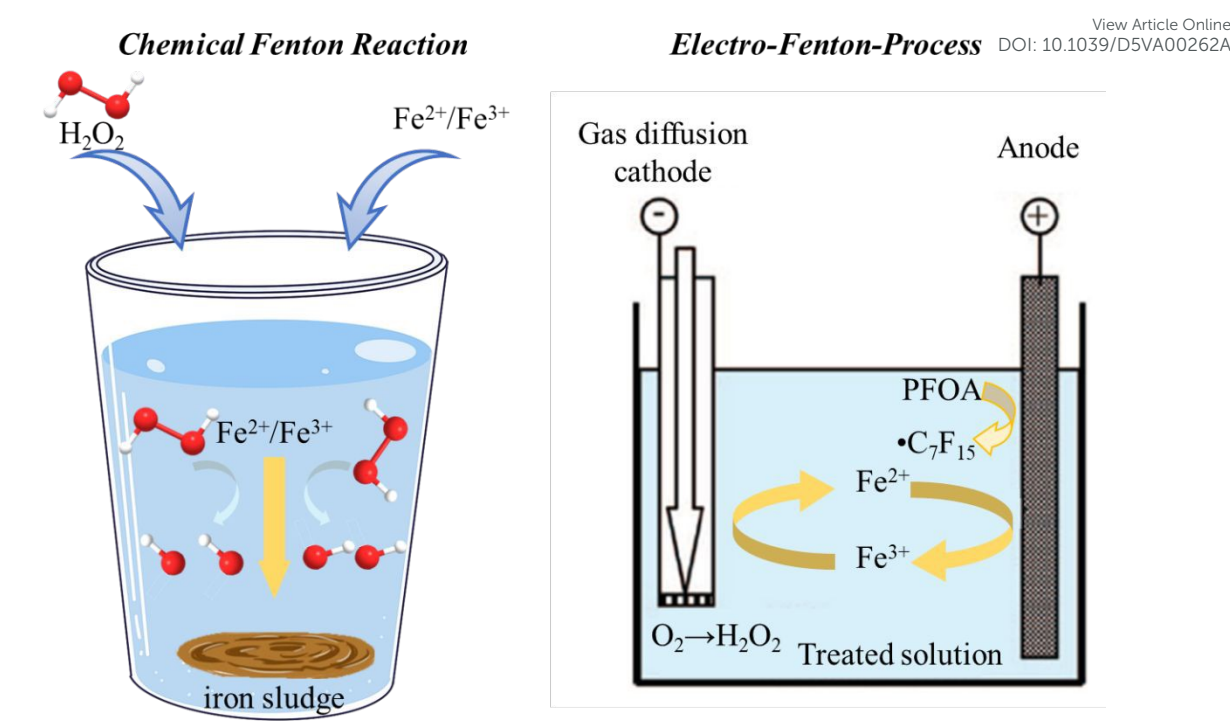


Figure 14. Comparison between chemical-Fenton reaction and electro-Fenton process.

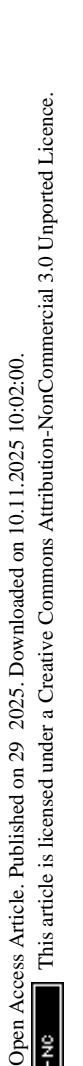
The electro-Fenton reaction represents a synergistic integration of chemical-Fenton and electrochemical method. The anodes used in electro-Fenton systems are commonly boron-doped diamond (BDD) or Magnéli phase titanium suboxides (Ti₄O₇), similar to those in conventional electrochemical oxidation processes. These non-active anode materials are favored due to the following characteristics: (1) high chemical stability and inertness, conferring long operational lifespans;112,113 (2) wide potential windows and high oxygen evolution potentials (>2.7 V vs. NHE), conducive to the cleavage of C-F bonds;114,115 and (3) excellent corrosion resistance, enabling compatibility with strong acidic or basic environments. 116

The anode materials used in electro-Fenton systems are relatively fixed, ongoing research focuses on developing efficient cathode materials to enhance ORR

performance for H_2O_2 generation. In this review, the electro-Fenton systems are categorized based on the cathode materials: iron-containing cathodes and iron-free cathodes.

3.2.1 Iron-containing cathodes

To evaluate the feasibility of a synergistic electro-catalytic system integrating cathodic electro-Fenton and anodic oxidation for effective PFOA removal, Zhao et al. synthesized a Fe-Mn co-doped carbon aerogel material (Fe10MnC). In this system, PFOA was initially activated at the anode, while the cathode facilitated the electro-Fenton reaction to efficiently generate • OH radicals (Figure 15a). Through the strategic combination of these processes, an effective approach for the synergistic degradation of PFAS was developed.88 BDD was employed as the anode material, capable of generating •OH (H₂O oxidation) with high efficiency. These radicals, alongside direct anodic oxidation, contributed to the cleavage of C-F bonds in PFOA (Figure 15b). Meanwhile, Fe10MnC acted as the cathode, enabling the in-situ electrogeneration of H₂O₂ by ORR reaction, which was subsequently activated to produce •OH under the catalytic effect of Fe and Mn (Figure 15c). Surface valence analysis revealed that Mn improved the selectivity for the two-electron ORR for H₂O₂ production (Figure 15d). This system achieved a 97% PFOA removal rate within 4 hours of electrolysis, without hydrogen peroxide added and no iron sludge produced.



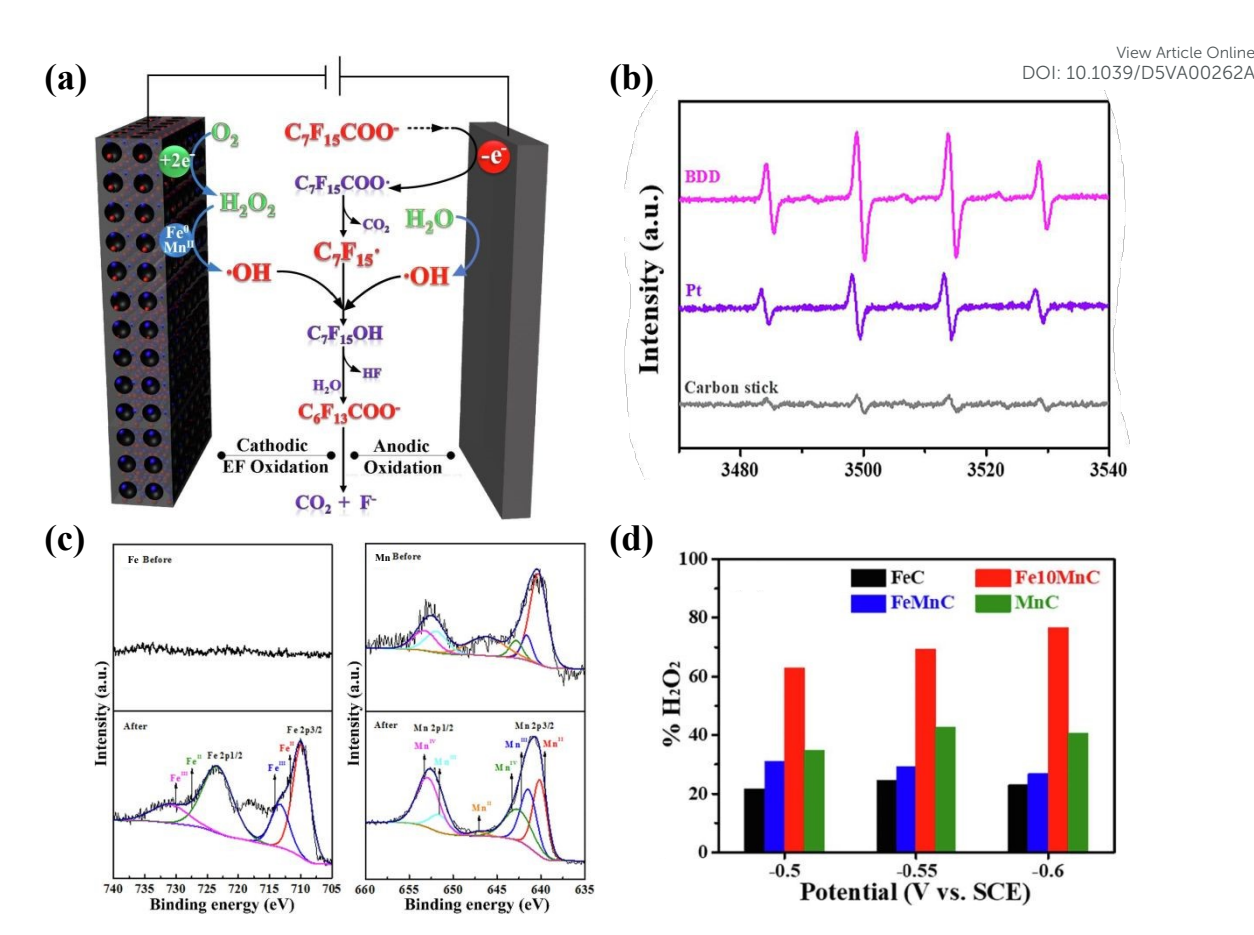


Figure 15. (a) Catalytic mechanism of electro-Fenton oxidation for efficiently removing PFOA with Fe10MnC as the cathode and BDD as the anode. (b) EPR spectra of DMPO•OH adducts with different anodes. (c) Fe and Mn XPS spectra of Fe10MnC before and after PFOA degradation. (d) Productivity for H₂O₂ of different cathodes.⁸⁸

For the purpose of further expanding the range of reactive radicals in electro-Fenton processes, Cai et al. developed an iron–nickel co-doped carbon aerogel (Fe_xNiC), which enabled the coupling of SO₄. and •OH radicals for effective PFOA degradation (Figure 16a). Unlike previous studies, a graphite electrode was employed as the anode, which minimized anodic oxidation of PFOA and thus better highlighted the superior performance of the cathodic material in the degradation process. By adjusting the Fe/Ni ratio, the generation rates of SO₄. and •OH radicals can be

modulated (Figure 16b). While iron is essential for Fenton chemistry, it tends 10^{1} favor 10^{1} favor

In real wastewater treatment scenarios (Figure 16d), for raw effluent from a fluorochemical plant in Sichuan (PFOA = 8.69 mg/L), electro-Fenton treatment achieved promising performance after biochemical treatment, with 81% degradation and 52% defluorination within 4 h (Effluent II). Even for raw wastewater without biochemical pretreatment, comparable results were obtained under the same conditions, with 75% degradation and 58% defluorination after 4 h (Effluent I), clearly demonstrating the application potential of this method. In terms of chemical oxygen demand (COD) reduction, the process was likewise effective: for Effluent II, COD decreased from 47.7 mg/L to 26.4 mg/L, while for Effluent I, COD was reduced from 1060 mg/L to 540 mg/L, meeting the Chinese Surface Water Quality Standard (GB3838-2002). Notably, the energy consumption for the treatment of Effluents I and II was approximately 0.39 and 0.018 kWh g⁻¹, respectively, further underscoring the

This article is licensed under a Creative Commons Attribution-NonCommercial 3.0 Unported Licence

Open Access Article. Published on 29 2025. Downloaded on 10.11.2025 10:02:00.

View Article Online DOI: 10.1039/D5VA00262A

viability of this approach for industrial applications.

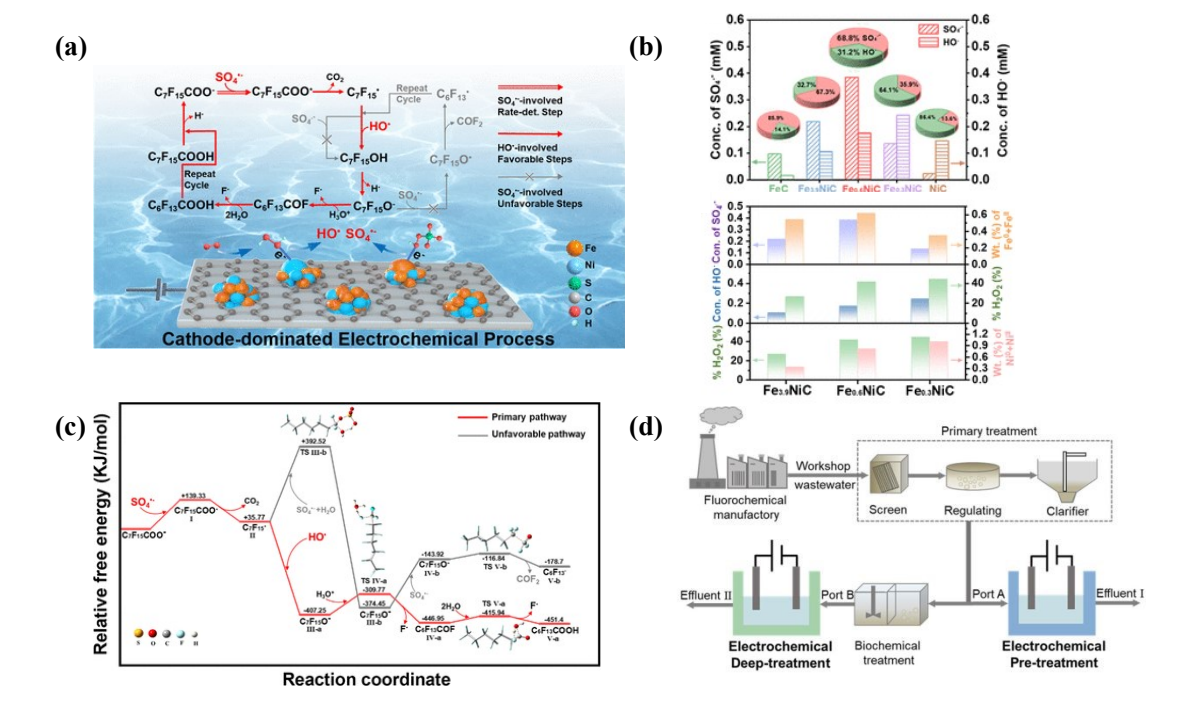


Figure 16. (a) Schematic of PFOA degradation in cathode-dominated electro-Fenton process. (b) The quantitative and accumulate concentration of SO₄*- and •OH in different cathodes. (c) Profile of the potential energy surfaces for the PFOA degradation dominated by SO₄*- and •OH. (d) Flowchart of fluorochemical manufactory wastewater treatment.⁸⁹

In order to highlight the positive contribution of cathodic electro-Fenton reactions for effective degradation of PFOA, Han et al. synthesized a bifunctional single-atom catalyst with a Co-CN₂ configuration supported on an Fe₂O₃ substrate (Co-CN₂-Fe₂O₃) (Figure 17a).⁹⁰ The critical role of the cathode in enhancing the generation of reactive oxygen species and improving overall system performance were investigated. A platinum anode was used to eliminate contributions from anodic oxidation, enabling a focused assessment of cathodic degradation. In this system, the Co-CN₂ single-atom

layer facilitated the two-electron ORR for efficient H_2O_2 generation (Figure 17b and View Article Online layer facilitated the two-electron ORR for efficient H_2O_2 generation (Figure 17b and View Article Online layer facilitated the two-electron ORR for efficient H_2O_2 generation (Figure 17b and View Article Online layer facilitated the two-electron ORR for efficient H_2O_2 generation (Figure 17b and View Article Online layer facilitated the two-electron ORR for efficient H_2O_2 generation (Figure 17b and View Article Online layer facilitated the two-electron ORR for efficient H_2O_3 generation (Figure 17b and View Article Online layer facilitated the two-electron ORR for efficient H_2O_3 generation (Figure 17b and View Article Online layer facilitated the two-electron ORR for efficient H_2O_3 generation (Figure 17b and View Article Online layer facilitated the two-electron ORR for efficient H_2O_3 generation (Figure 17b and View Article Online layer facilitated the two-electron ORR for efficient H_3O_3 generation (Figure 17b and View Article Online layer facilitated the two-electron ORR for efficient H_3O_3 generation (Figure 17b and View Article Online layer facilitated the two-electron ORR facilitated the

17c). The low-coordination Co sites in the Co-CN₂ structure weakened O₂ adsorption and prevented O–O bond cleavage, thereby improving H₂O₂ selectivity. The Fe₂O₃ substrate functioned as the Fenton catalyst to activate the in-situ generated H₂O₂ into •OH. This system achieved 96% PFOA degradation (Figure 17d) and defluorination (Figure 17e) within 120 minutes, representing near-complete mineralization. Long-term stability tests confirmed >95% degradation and defluorination over 10 cycles (Figure 17f), while avoiding the formation of iron sludge commonly associated with traditional Fenton systems.

This article is licensed under a Creative Commons Attribution-NonCommercial 3.0 Unported Licence.

Open Access Article. Published on 29 2025. Downloaded on 10.11.2025 10:02:00.

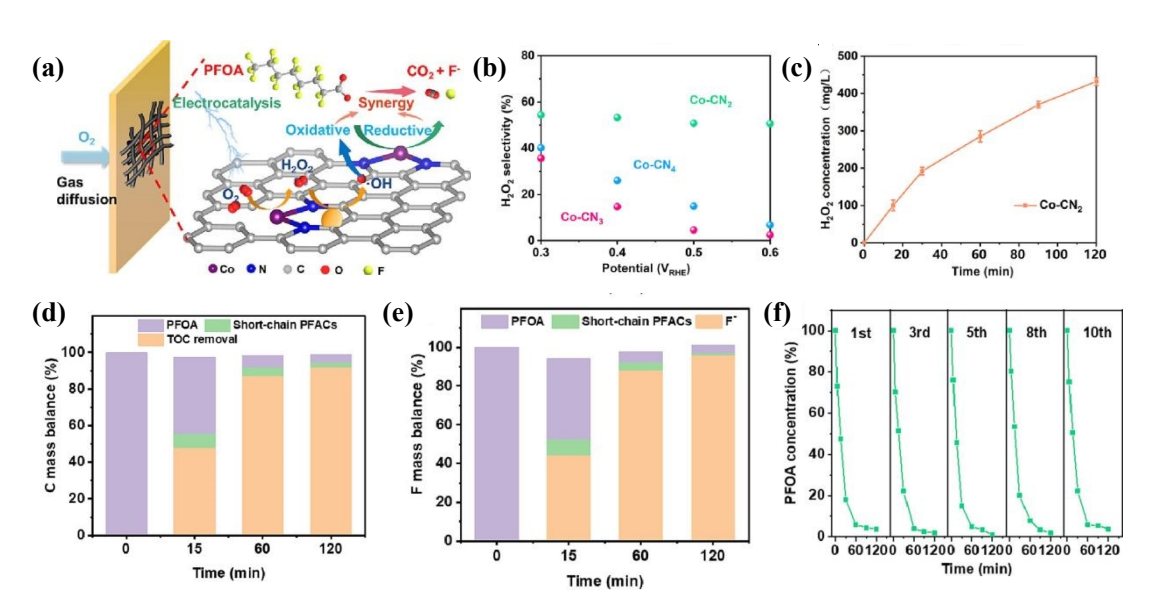


Figure 17. (a) Schematic of PFOA degradation in Co-CN₂-Fe₂O₃ cathode electro-Fenton process. (b) The calculated H₂O₂ selectivity as a function of the applied potentials. (c) Concentrations of H₂O₂ produced with Co-CN₂ as a function of electrolysis time. (d) C and (e) F mass balance during PFOA degradation over Co-CN₂-Fe₂O₃. (f) The recyclability of Co-CN₂-Fe₂O₃ for electro-Fenton PFOA degradation.⁹⁰

Open Access Article. Published on 29 2025. Downloaded on 10.11.2025 10:02:00.

This article is licensed under a Creative Commons Attribution-NonCommercial 3.0 Unported Licence

degradation in the electro-Fenton reaction, Yu et al. conducted a systematic investigation on a Fe/N co-doped graphene electrode (Fe/N-GE@GF) (Figure 18a).91 A synergistic electrochemical process at the cathode was proposed, and key factors influencing the efficiency of the electro-Fenton reaction were scientifically explored. The co-doping of Fe and N introduced significant lattice distortion and structural defects in the graphene framework, resulting in increased surface area and abundant microporosity (Figure 18b). These features exposed more active sites for PFAS degradation. Moreover, N-containing precursors such as pyridine promoted uniform Fe dispersion and the formation of a robust three-dimensional porous structure. The presence of N also enabled PFAS molecules to interact with the electrode material, facilitating their enrichment near the reactive zones. Through precise spatial overlap of radical generation sites and PFAS accumulation regions (Figure 18c), a "Focused Active Reaction Region" that significantly improved degradation efficiency was established. This system achieved 95% PFOA degradation, 90% total organic carbon (TOC) removal, and 80% defluorination within 3 hours. Notably, the Fe/N-GE@GF electrode was capable of generating •OH in neutral conditions by leveraging singlet oxygen (1O₂) as a supplementary oxidant (Figure 18d), thereby overcoming the classical Fenton system's dependence on pH environment. Under neutral conditions (pH = 7), the PFOA degradation efficiency of Fe/N-GE@GF was nearly identical to that observed under acidic conditions (pH = 3), reaching 92.7% compared to 92.8%. In contrast, a marked decrease in degradation efficiency was observed under alkaline

conditions (pH = 10), though a considerable efficiency of 58.8% was still achieved (Figure 18e).

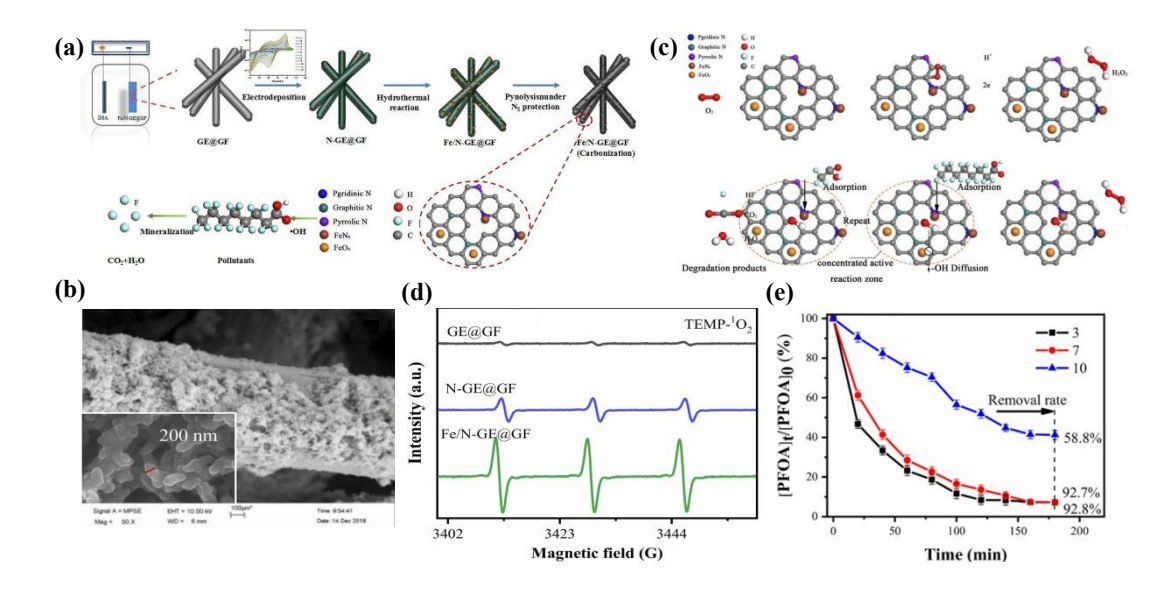


Figure 18. (a) Schematic diagram of Fe/N-GE@GF preparation and degradation experiments. (b) SEM images of N-GE@GF. (c) Possible catalytic mechanism of Fe/N-GE@GF for PFOA degradation. (d) DMPO-¹O₂ by GE@GF, N-GE@GF and Fe/N-GE@GF cathode in electrocatalytic process. (e) PFOA adsorption performance of Fe/N-GE@GF at different pH.⁹¹

3.2.2 Iron-free cathodes

While iron-containing cathodic materials have attracted considerable attention, certain unique structural features of iron-free cathodes also exhibit interactions relevant to PFAS degradation. Wang et al. developed an iron-free biomass-derived nitrogen and sulfur self-doped porous carbon electrode (NSGC) for electro-Fenton degradation of hexafluoropropylene oxide dimer acid (GenX) (Figure 19a), a widely used substitute for the banned PFOA.⁹² Previous studies have demonstrated that fluorine–fluorine

Open Access Article. Published on 29 2025. Downloaded on 10.11.2025 10:02:00.

This article is licensed under a Creative Commons Attribution-NonCommercial 3.0 Unported Licence

(F···F) interactions between perfluorinated polymers and the perfluoroalkyl chains of PFOA play a critical role in enhancing adsorption from aqueous solutions (Figure 19b).¹¹⁸ The incorporated perfluoropolyether into the NSGC framework exhibited hydrophobic and fluorophilic, and significantly enhanced performance for GenX removal, that is consistent with the DFT calculation results, where the adsorption energy of Gen-X on F-NSGC was significantly enhanced from -35.93 kJ/mol to -46.91 kJ/mol in the presence of F–F interactions (Figure 19c). In the electro-Fenton system, F-NSGC achieved an electro-adsorption efficiency of 59% for GenX within 60 minutes, followed by a degradation efficiency of 96% and a defluorination efficiency of 63% after 180 minutes (Figure 19d). These results indicate both excellent degradation capacity and promising mineralization potential. The presence of competing anions exhibited negligible impact, with removal efficiencies exceeding 95% in all tested scenarios (Figure 19e). When applied to real water samples—including lake water, secondary effluent from a municipal wastewater treatment plant, and tap water—the system consistently achieved over 90% GenX removal within 180 minutes (Figure 19f). To further explore the application potential of this method, the reaction setup was adapted to continuous-flow reactors. Under a flow rate of 5 mL/min with a circulation time of 180 min, the GenX removal efficiency of up to 94% was achieved. However, excessively low flow rates reduced the contact between GenX and the catalytic material, thereby limiting the overall degradation efficiency.

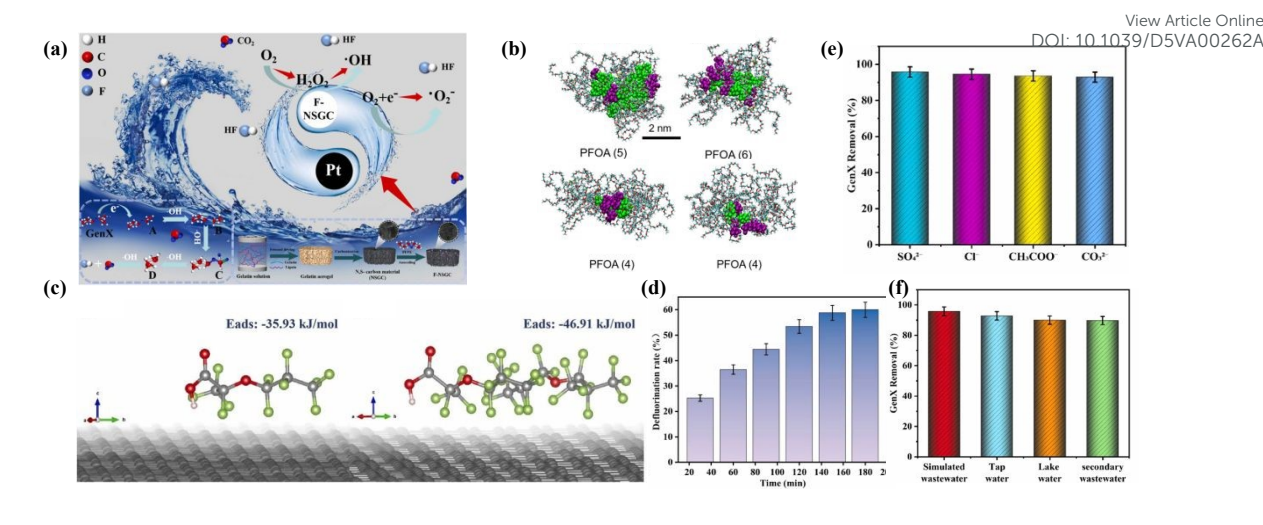


Figure 19. (a) Degradation mechanism of GenX by F-NSGC in electro-Fenton system. (b) Snapshots of molecular dynamics simulations of association of PFOA molecules with the self-assembled block copolymers ¹¹⁸. (c) DFT simulations to calculate the adsorption energy of GenX by NSGC (left) and F-NSGC (right). (d) F- concentration after degradation. (e) Influence of different anions on GenX removal. (f) Influence of different water on GenX removal.

With the aim of broadening the applicability of combined electro-oxidation and electro-Fenton systems for PFAS treatment, Luu et al. conducted a comprehensive evaluation of the Fenton-assisted electrochemical advanced oxidation process for the removal of 29 representative PFAS compounds, including both long- and short-chain species, as well as linear and branched isomers.⁹³ Ti/BDD and Ti/IrO₂ were used as anode materials for comparison, with Pt serving as the cathode. Fe₃O₄ nanoparticles were directly introduced into the reaction system as catalysts to enhance Fenton reactions. The researchers systematically optimized operational parameters such as pH, Fe₃O₄ concentration, current density, electrolysis duration, and electrolyte

Open Access Article. Published on 29 2025. Downloaded on 10.11.2025 10:02:00.

This article is licensed under a Creative Commons Attribution-NonCommercial 3.0 Unported Licence

concentration. Under optimized conditions, removal efficiencies ranging from 86% 139 D5 VA00262A 100% were achieved within 120 minutes, with a low energy consumption of just 9.0 kWh/m³ (Figure 20a and 20b). Following the attainment of high PFAS removal efficiencies, the study further investigated intermediate products and degradation pathways. Using mass spectrometry and kinetic modeling, the plausible mineralization mechanisms were proposed (Figure 20c). These mechanistic insights provide valuable references for treating other recalcitrant organic pollutants using electro-Fenton-based approaches.

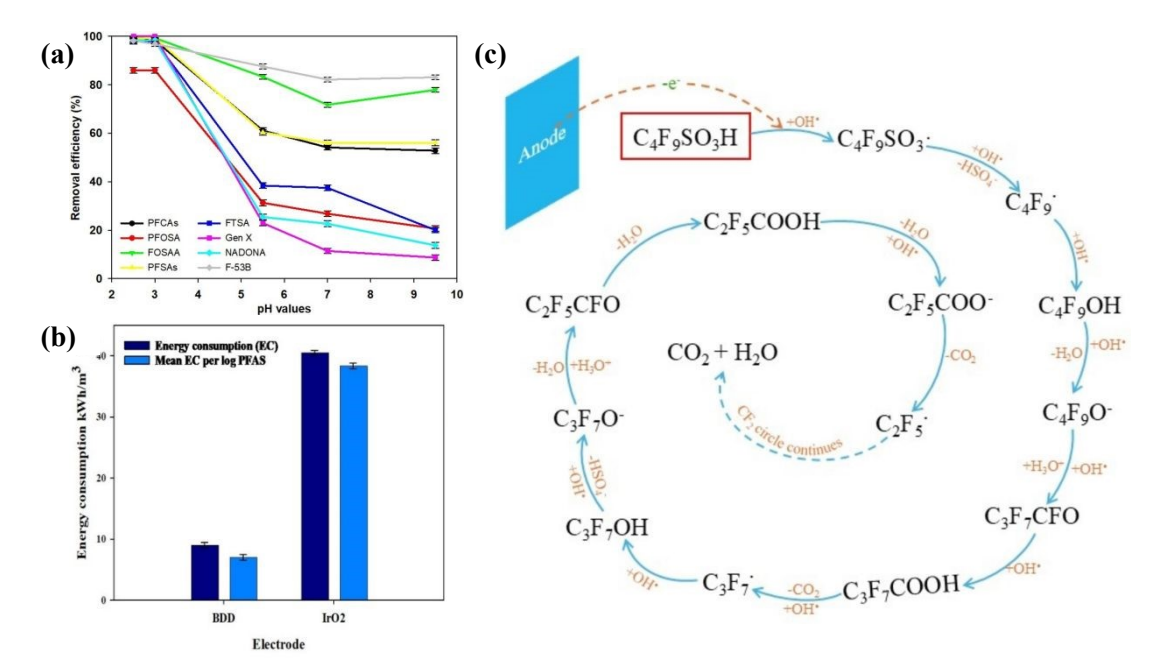


Figure 20. (a) PFAS removal efficiency via the Fenton-assisted electrochemical oxidation process. (b) Energy consumption via the Fenton-assisted electrochemical oxidation process. (c) Intermediate compounds and degradation pathway of PFBS.⁹³

Electro-Fenton reactions have demonstrated the capability for rapid PFAS degradation, accompanied by significant improvements in defluorination efficiency.

Notably, by expanding the sources of oxygen, the electro-Fenton process has overcome the pH limitations inherent to traditional chemical Fenton systems, enabling the in situ generation of • OH under neutral conditions without the need for external H₂O₂ addition, while also substantially reducing the formation of iron sludge. However, several challenges remain. One of the primary limitations is the high energy consumption associated with the electro-Fenton process, which has increasingly drawn attention focused on techno-economic assessments. Reducing energy demand thus represents a critical direction for future development. Additionally, improvements in the durability and stability of electrode materials are necessary to achieve more favorable life-cycle performance. At present, most research remains at a preliminary or

laboratory scale, and there is a pressing need for comprehensive evaluation data on the

3.3 Photo-Fenton reaction system

treatment of large-scale contaminated water systems.

Compared to electro-Fenton systems, which rely on externally applied electric power to drive electron transfer processes, photo-Fenton reactions are generally considered to be a greener and more environmentally friendly class of AOPs (Figure 21).^{119,120} In a photo-Fenton system, UV or visible light irradiation facilitates the photoreduction of ferric complexes to Fe²⁺, thereby accelerating the decomposition of H₂O₂. Specifically, under mildly acidic conditions (pH 2.8–3.5), Fe³⁺ forms light-responsive ferric hydroxo complexes, such as [Fe(OH)]²⁺,^{68,121} which can undergo ligand-to-metal charge transfer (LMCT) excitation, regenerating Fe²⁺ and promoting

further •OH production.¹²² Recent studies have also shown that Fe³⁺ can form complexes with PFAS anions, and these complexes may exhibit enhanced photoresponse under irradiation, facilitating PFAS degradation.

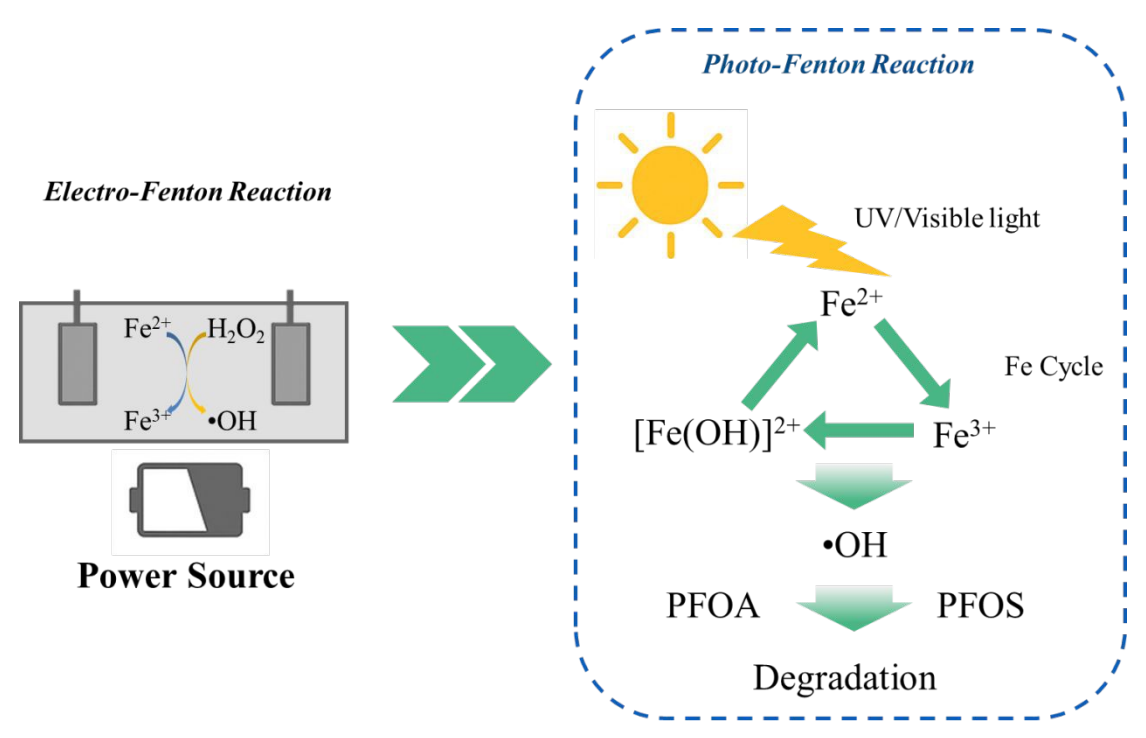


Figure 21. Comparison between electro-Fenton and photo-Fenton for the degradation of PFAS.

Although solar light is more widely available and cost-effective, the efficient control and utilization of photonic energy remain a key research challenge in photo-Fenton systems. These systems are typically classified into homogeneous and heterogeneous processes, depending on the physical state of the catalyst. In homogeneous photo-Fenton systems, both the catalyst and reactants are dissolved in aqueous media, providing high dispersibility and intimate contact with contaminants. However, the generally poor light absorption capacity of homogeneous species limits their degradation efficiency, making this a focus for further optimization. In contrast,

Open Access Article. Published on 29 2025. Downloaded on 10.11.2025 10:02:00.

This article is licensed under a Creative Commons Attribution-NonCommercial 3.0 Unported Licence.

heterogeneous photo-Fenton systems exhibit greater capability for absorbing and converting light into chemical energy. Photoinduced holes generated on solid catalyst surfaces can effectively participate in PFAS degradation. Nonetheless, rational design of the catalyst surface and optimization of PFAS mass transfer to reactive sites remain essential considerations for performance improvement.

3.3.1 Homogeneous photo-Fenton systems

Homogeneous photo-Fenton reactions were developed earlier than their heterogeneous counterparts due to no complex catalyst design or synthesis steps required. 124 The fundamental mechanism of PFAS degradation in homogeneous photo-Fenton systems has been relatively well elucidated. However, limited solubility and recovery challenges of homogeneous catalysts have constrained the application for PFAS degradation.

To verify the feasibility of PFAS degradation via the photo-Fenton process, Tang et al. developed a homogeneous ultraviolet-assisted photo-Fenton system with ferric and ferrous sulfate dissolved in PFOA solution (Figure 22a).⁹⁴ The influence of reagent stoichiometry (i.e., concentrations of Fe²⁺ and H₂O₂) and solution pH on PFOA degradation efficiency were systematically investigated. An optimal Fe²⁺ concentration of 2.0 mM was identified: at this level, more •OH radicals were generated to enhance both PFOA degradation and defluorination (Figure 22b). However, excessive Fe²⁺ could also act as a scavenger for •OH, thereby reducing the availability of reactive species for PFAS oxidation. Solution pH was found to play a critical role (Figure 22c).

At pH < 2.0, H_2O_2 is readily protonated to form $H_3O_2^+$, decreasing its reactivity with Fe²⁺. At pH > 4.0, Fe³⁺ tends to hydrolyze rapidly, forming Fe(OH)₃ precipitates, which hinder both light penetration and complexation with PFOA. Accordingly, the optimal pH range for homogeneous photo-Fenton reactions was determined to be between 2.8 and 3.5.

In addition to the •OH, the interaction between Fe³⁺ and PFOA contributed to the enhancement of the degradation process. A two-stage degradation mechanism was proposed (Figure 22d). In the initial stage, •OH is present in sufficient concentrations to directly activate PFOA anions, forming •C₇F₁₅ radicals. These radicals further react with •OH to generate C₇F₁₅OH, which undergoes hydrolysis and HF elimination to yield short-chain PFAS intermediates, CO₂, and HF. In the second stage, once •OH is depleted, Fe³⁺ forms a [C₇F₁₅COO–Fe]²⁺ complex with PFOA, which, under UV irradiation, is photo-reduced to Fe²⁺ and a carboxyl radical (C₇F₁₅COO•), initiating another degradation cycle with the limited •OH available.

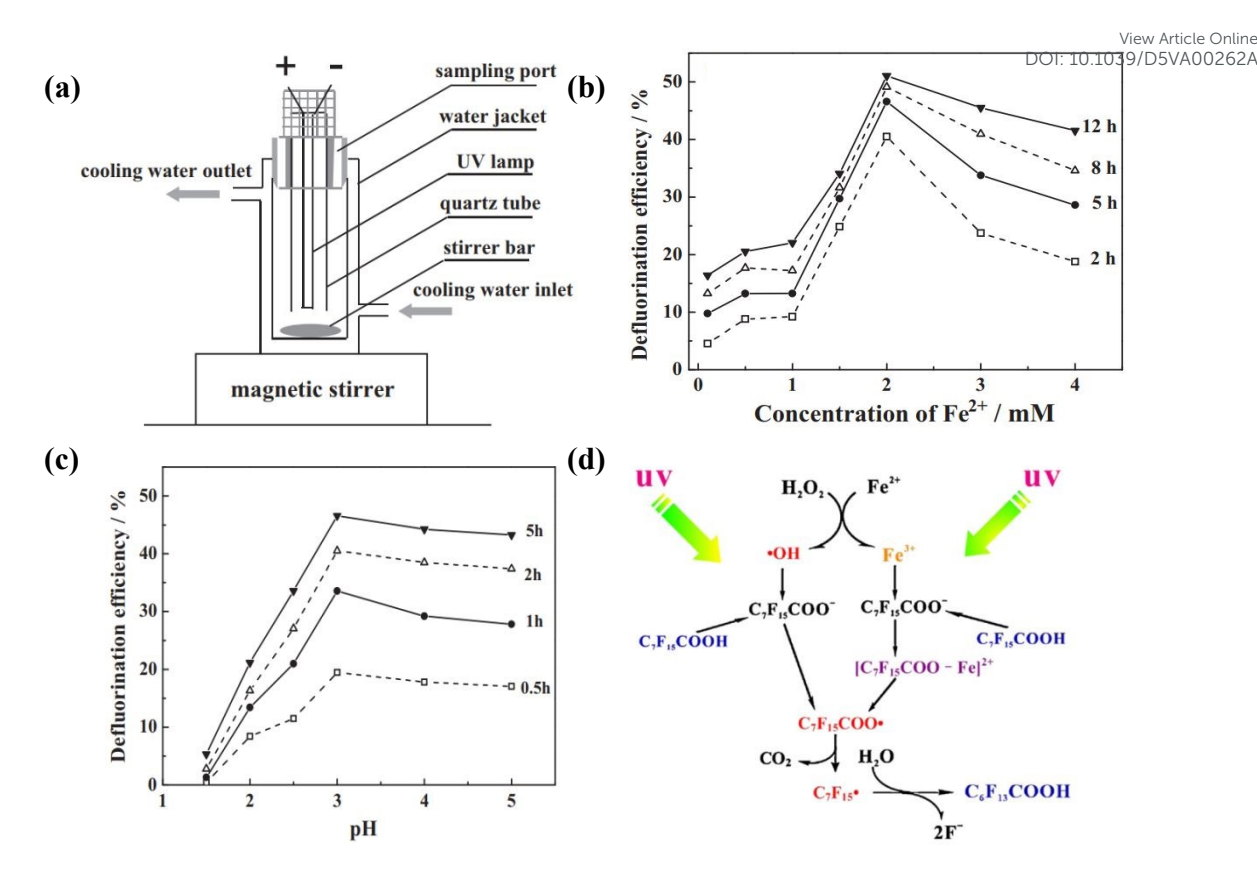


Figure 22. (a) The diagram of the experimental set-up for homogeneous photo-Fenton degradation of PFOA. (b) Effects of initial Fe²⁺ concentration on the defluorination efficiency of PFOA. (c) Effects of H₂O₂ concentration on the defluorination efficiency of PFOA. (d) A two-stage mechanism for the degradation of PFOA in the homogeneous photo-Fenton process.⁹⁴

In order to further broaden the spectral utilization of the photo-Fenton process, Alvarez et al. extended the conventional UV-based photo-Fenton system by introducing visible light as an alternative irradiation source. The potential of utilizing visible light to effectively drive the photo-Fenton degradation of PFOA was proved. Visible light, as one of the most green and renewable energy sources, offers significant advantages for photo-Fenton degradation of PFOA. It greatly reduces the energy consumption of

Open Access Article. Published on 29 2025. Downloaded on 10.11.2025 10:02:00.

This article is licensed under a Creative Commons Attribution-NonCommercial 3.0 Unported Licence

the reaction, enhances operational safety, and lowers equipment requirements. Therefore, visible light is considered an ideal energy input for such advanced oxidation processes. Electron paramagnetic resonance (EPR) spectroscopy confirmed that •OH was the primary reactive species (Figure 23a and 23b). However, the process required prolonged treatment—28 days—to achieve 98% PFOA degradation (Figure 23c), with only 13% defluorination, highlighting limitations in efficiency, particularly for the degradation of short-chain PFAS. A plausible mechanism for PFAS degradation via the photo-Fenton process was also proposed, which is generally consistent with those suggested in previous studies. In this mechanism, •OH not only directly attack PFOA but may also target the [C₇F₁₅COO–Fe]²⁺ complex. Fe³⁺ is believed to further reduce the activation energy barrier for •OH-mediated PFOA degradation. Additionally, a more detailed pathway for the formation of intermediates was presented, indicating broader recognition of this mechanism. (Figure 23d).



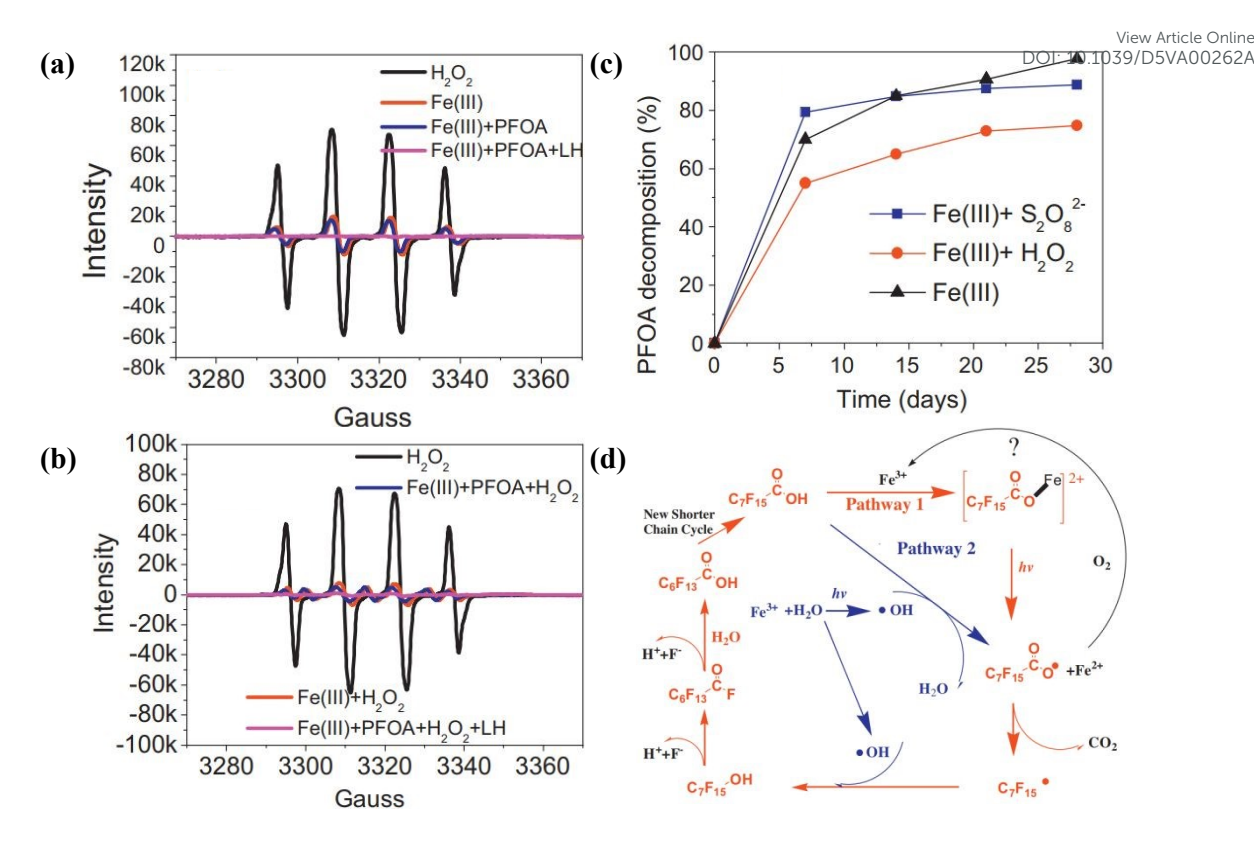


Figure 23. (a) EPR spectra of radicals generated in different experimental groups. (b) EPR spectra of radicals generated in Fe(III) – H₂O₂ (2 mM) system; EPR samples were taken after 10 min UV irradiation. (c) Comparison of PFOA degradation by different reaction systems. (d) Proposed PFOA degradation pathway in the presence of Fe(III) and sunlight.⁹⁵

To further enhance the degradation efficiency of the homogeneous photo-Fenton reaction and to gain a more comprehensive understanding of its underlying mechanism, Zhang et al. developed a hybrid system combining Fe⁰/granular activated carbon (Fe⁰/GAC) microelectrolysis with a vacuum UV-Fenton (VUV-Fenton) process for PFOA mineralization.⁹⁶ In this system, Fe⁰/GAC was first mixed with PFOA to generate numerous microscale galvanic cells that continuously supplied electrons and Fe²⁺ ions, facilitating the initial breakdown of the PFOA structure through enhanced electron

transfer (Figure 24a). Following a pre-activation step, the photo-Fenton reaction was conducted under UV irradiation at 254 nm (Figure 24b), resulting in a defluorination efficiency of 47%, which represents a notable improvement compared to the 39% achieved using the VUV-Fenton system alone (Figure 24c). High-performance liquid chromatography tandem mass spectrometry (HPLC/MS/MS) was employed to identify and quantify degradation intermediates. The detected short-chain perfluorocarboxylic acids (PFCAs)—including PFHpA (C7), PFHeA (C6), PFPeA (C5), PFBA (C4), PFPrA (C3), and TFA (C2)—further confirmed the proposed degradation mechanism of PFOA under photo-Fenton conditions.

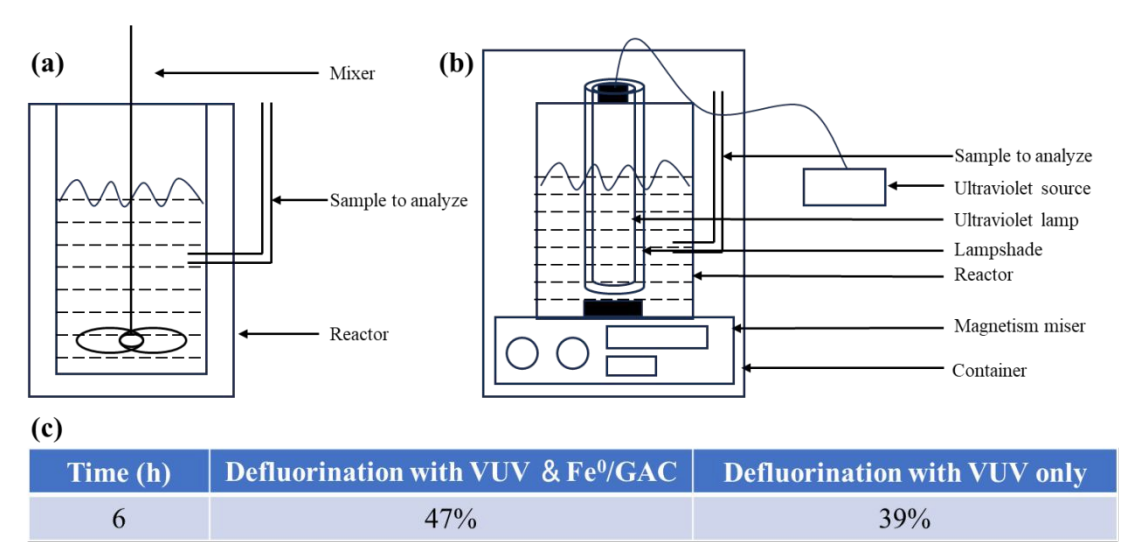


Figure 24. (a) Schematic representation of reactor iron carbon micro-electrolysis and (b) VUV-Fenton. (c) Photochemical defluorination ratio under VUV and Fe⁰/GAC micro-electrolysis and VUV-Fenton systems.

3.3.2 Heterogeneous photo-Fenton systems

Compared to homogeneous photo-Fenton reactions, heterogeneous photo-Fenton systems typically utilize iron-containing catalysts, which can reduce the need for

additional anions and facilitate catalyst recovery through the magnetic properties of solid-phase iron. Based on this concept, Urtiaga et al. employed a TiO2/reduced graphene oxide composite catalyst (95% TiO₂/5% rGO) for the photo-Fenton degradation of PFOA.97 After 12 hours of UV-visible irradiation using a mercury lamp, the PFOA degradation efficiency of TiO₂-rGO reached 93 ±7 %, representing a substantial improvement compared with TiO_2 photocatalysis (24 ± 11% removal) and direct photolysis (58 \pm 9%) (Figure 25a). It was reasonably hypothesized that rGO effectively captured photogenerated electrons from TiO₂, thereby suppressing electron– hole recombination (Figure 25e). This process promoted PFOA degradation through direct oxidation by photogenerated holes or via reactive radical pathways. The progressive decomposition mechanism was further supported by the identification of short-chain perfluorocarboxylic acids (Figure 25b) and the release of fluoride ions (Figure 25c), which closely matched the reduction in total organic carbon (Figure 25d), in line with a stepwise degradation pathway mediated by photogenerated hydroxyl radicals. These findings strongly verified the critical role of •OH radicals and the stepwise degradation mechanism in PFOA removal by TiO₂-rGO. Moreover, kinetic studies revealed a clear correlation between degradation efficiency and molecular structure, as the apparent first-order rate constants for UV-visible degradation of PFOA and its intermediate perfluorocarboxylic acids increased with decreasing carbon chain length (Figure 25b). In summary, the development of a heterogeneous photo-Fenton system based on TiO₂-rGO provides a feasible strategy for PFAS degradation and offers detailed mechanistic insights, thereby laying a solid scientific foundation for

View Article Online DOI: 10.1039/D5VA00262A

future research.

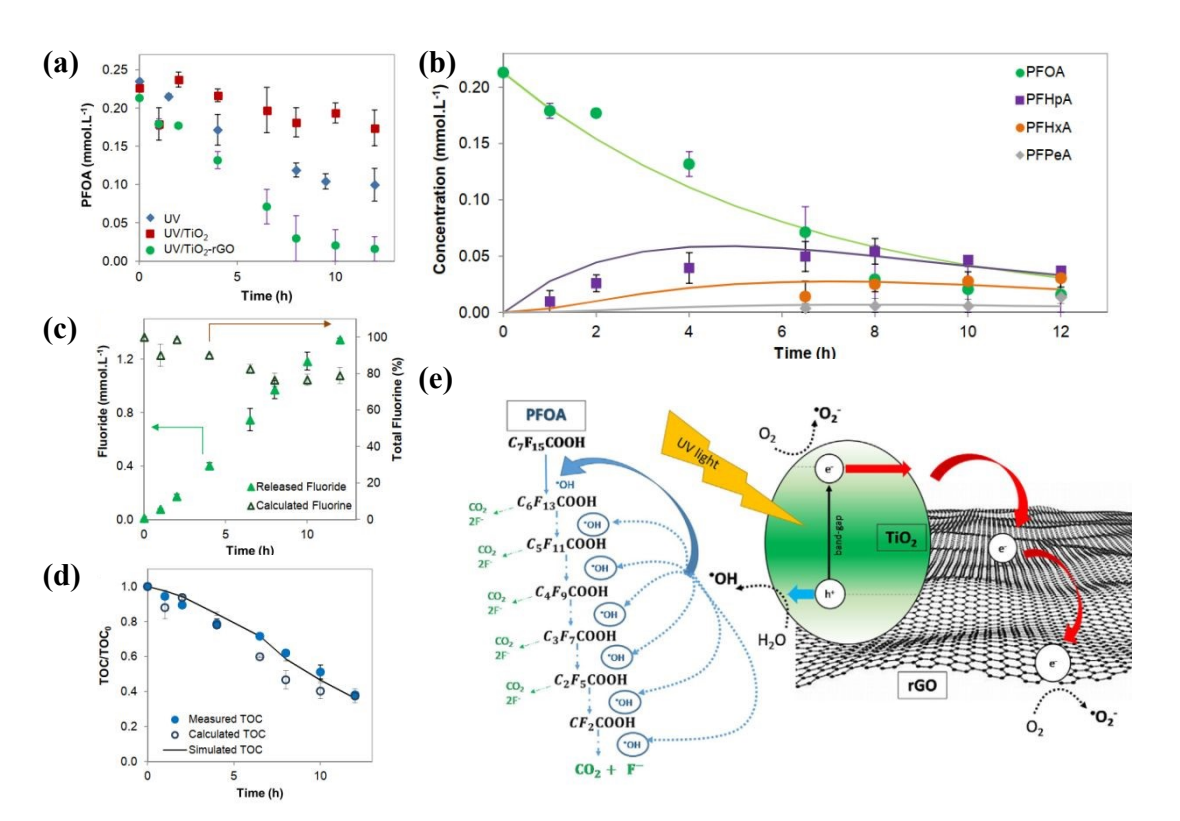


Figure 25. (a) Evolution of PFOA concentration with irradiation time by photolysis and photocatalysis using TiO₂ and TiO₂-rGO. (b) Evolution of PFOA, PFHpA, PFHxA and PFPeA, and their simulated concentrations using the pseudo-first order estimated kinetic parameters. (c) Fluoride in solution and calculated total fluorine. (d) Measured TOC/TOC⁰, calculated TOC/TOC⁰ from the analyzed PFAS, and simulated TOC/TOC⁰ using the simulated PFAS concentrations. (e) Photocatalytic pathways of PFOA decomposition using the TiO₂-rGO catalyst. 97

In order to achieve a more uniform distribution of iron on the catalyst surface and to elucidate the mechanism of heterogeneous photo-Fenton degradation of PFAS, Wang et al. synthesized a cellulose-based membrane ($Co_3O_4@Fe_3O_4$) by coating Co_3O_4 nanoparticles onto rod-like MOF-derived Fe_3O_4 and incorporating the composite into a

Open Access Article. Published on 29 2025. Downloaded on 10.11.2025 10:02:00.

This article is licensed under a Creative Commons Attribution-NonCommercial 3.0 Unported Licence.

cellulose solution (Figure 26a). This membrane was then applied in a visible-lightdriven photo-Fenton system,98 where efficient energy conversion and a rich reactive radical environment enabled effective PFOA degradation. The degradation mechanism relied on the synergistic interplay among photogenerated electrons, holes (h⁺), and various reactive species rather than a single dominant species. The photogenerated h⁺ directly attacked the carboxylic group (—COOH) of PFOA, initiating decarboxylation and forming C_7F_{15} • radicals. The electrons (e⁻) reduced dissolved oxygen to O_2 •, which contributed to further degradation, and also regenerated Fe²⁺ from Fe³⁺, maintaining •OH production (Figure 26b). The Co₃O₄@Fe₃O₄ membrane demonstrated outstanding performance, achieving 95% PFOA degradation, maintaining 80% efficiency after five cycles (Figure 26c), and exhibiting minimal metal leaching (Fe: 0.05 ppm; Co: 0.49 ppm). These results were attributed to the material's architecture: regenerated cellulose formed a 3D porous network under alkaline/urea/thiourea conditions, which helped disperse the Co₃O₄@Fe₃O₄ nanoparticles and prevent aggregation (Figure 26d). This study provides valuable experimental and theoretical insights into the rational design of heterogeneous photo-Fenton catalysts.

View Article Online DOI: 10.1039/D5VA00262A Co₃O₄ NHE Fumaric acid Fe-MOFs -0.33 eV Cellulose solution H₂O/OH 2.40 eV Co₃O₄@Fe₃O₄/cellulose Co₃O₄@Fe₃O₄ (c) HF CO₂+HF 100 PFOA removal (%) 91.6 85.3 79.7 80.4 40 20

Figure 26. (a) Schematic illustration of the steps to prepare Co₃O₄@Fe₃O₄/cellulose blend membranes. (b) Type-II heterojunction reaction mechanism. (c) Reusability of blend membrane. (d) Proposed degradation pathway of PFOA in the H₂O₂/membrane/visible light system.⁹⁸

2

3 Cycles 4

To elucidate the synergistic mechanism between PFAS adsorption and photoactivity, Zhang et al. developed ZIF-67@C₃N₄ and MIL-100(Fe)@C₃N₄ composites with high specific surface areas and adsorption capacity for photo-Fenton degradation of PFOA (Figure 27a and 27b).⁹⁹ Experimental results revealed that ZIF-67@C₃N₄ and MIL-100(Fe)@C₃N₄ achieved PFOA removal efficiencies of 79.2% and 60.5% (Figure 27c and 27d), respectively—substantially higher than unmodified C₃N₄. Quenching experiments indicated that photogenerated holes (h⁺) played the primary

Open Access Article. Published on 29 2025. Downloaded on 10.11.2025 10:02:00.

This article is licensed under a Creative Commons Attribution-NonCommercial 3.0 Unported Licence.

role in photo-Fenton PFOA degradation, mainly by directly attacking PFOA molecules described adsorbed on the catalyst surface and oxidizing water to produce • OH (Figure 27e).

Beyond the photon-induced pathways, PFOA adsorption and charge separation mechanisms also contributed to the high degradation efficiency, such as. The catalyst's ability to accumulate PFOA near photoactive C₃N₄ sites, the enhanced visible-light absorption and charge separation induced by heterojunctions.

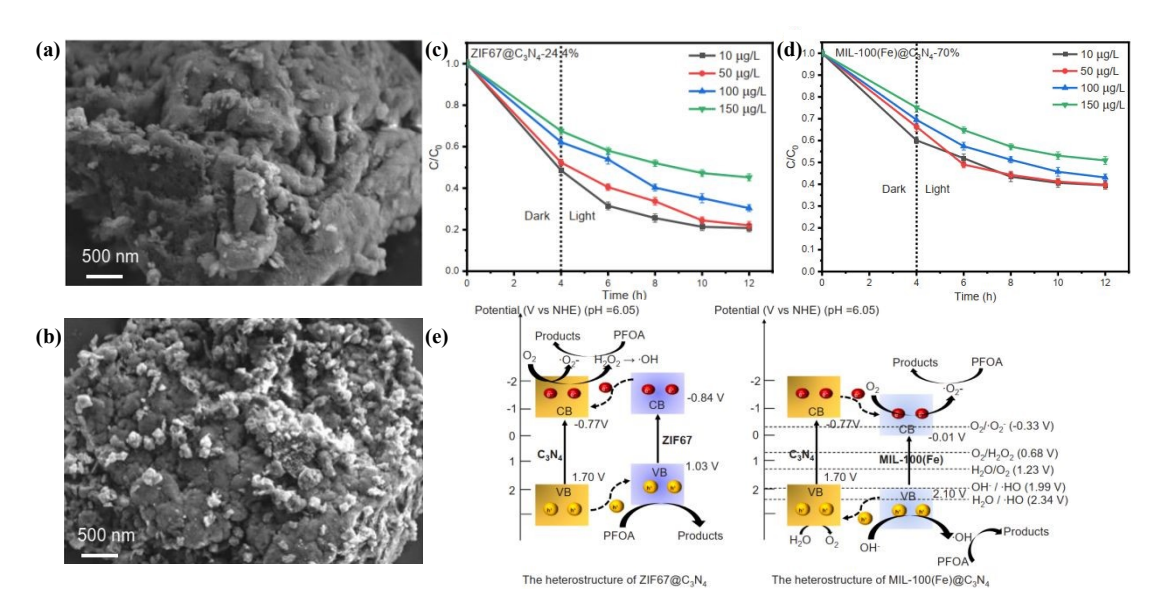


Figure 27. SEM images of C₃N₄ (a) and MIL-100(Fe)@ C₃N₄ (b). Photodegradation of PFOA with the presence of ZIF67@C₃N₄-24.4% (c)and MIL-100(Fe)@C₃N₄-24.4% (d) with different initial concentrations of PFOA. (e) The heterostructure of ZIF67@C₃N₄ and MIL-100(Fe)@C₃N₄.99

Integrating the heterogeneous photo-Fenton reaction and material structure design for enhancing the radical reactivity, Chen et al. developed Fe(III)-saturated porous montmorillonite (Fe-MMT) as a heterogeneous catalyst to enhance the photo-Fenton reaction. The pore structure microenvironment facilitates effective collisions

Open Access Article. Published on 29 2025. Downloaded on 10.11.2025 10:02:00.

This article is licensed under a Creative Commons Attribution-NonCommercial 3.0 Unported Licence.

between • OH and PFOA, thereby establishing an alternative strategy for PFOA ON 1000 PFOA ON 100 degradation. In a system containing 1 g/L Fe-MMT and 24 µM PFOA, approximately 90% of the initial PFOA was degraded within 48 hours. The enhanced degradation was attributed to the generation of reactive oxygen species and LMCT mechanism involving Fe species in the interlayer of MMT. Fe³⁺ coordinated with the carboxylate group (– COO⁻) of PFOA to form a PFOA–Fe²⁺ complex (Figure 28a). Upon UV irradiation, electrons were transferred from the PFOA ligand to the Fe³⁺ center, producing •C₇F₁₅COO radicals and Fe²⁺. This LMCT process significantly lowered the activation free energy for PFOA oxidation from 163 to 59.3 kJ/mol (Figure 28b). Further experiments demonstrated that the UV/Fe-MMT system maintained high PFOA removal efficiency even in the presence of natural organic matter and inorganic ions, indicating strong anti-interference capability (Figure 28c and 28d) and potential for practical applications in diverse wastewater treatment scenarios. Moreover, the Fe-MMT catalyst could be regenerated and reused, offering an economic advantage for industrial-scale PFOA remediation (Figure 28e).

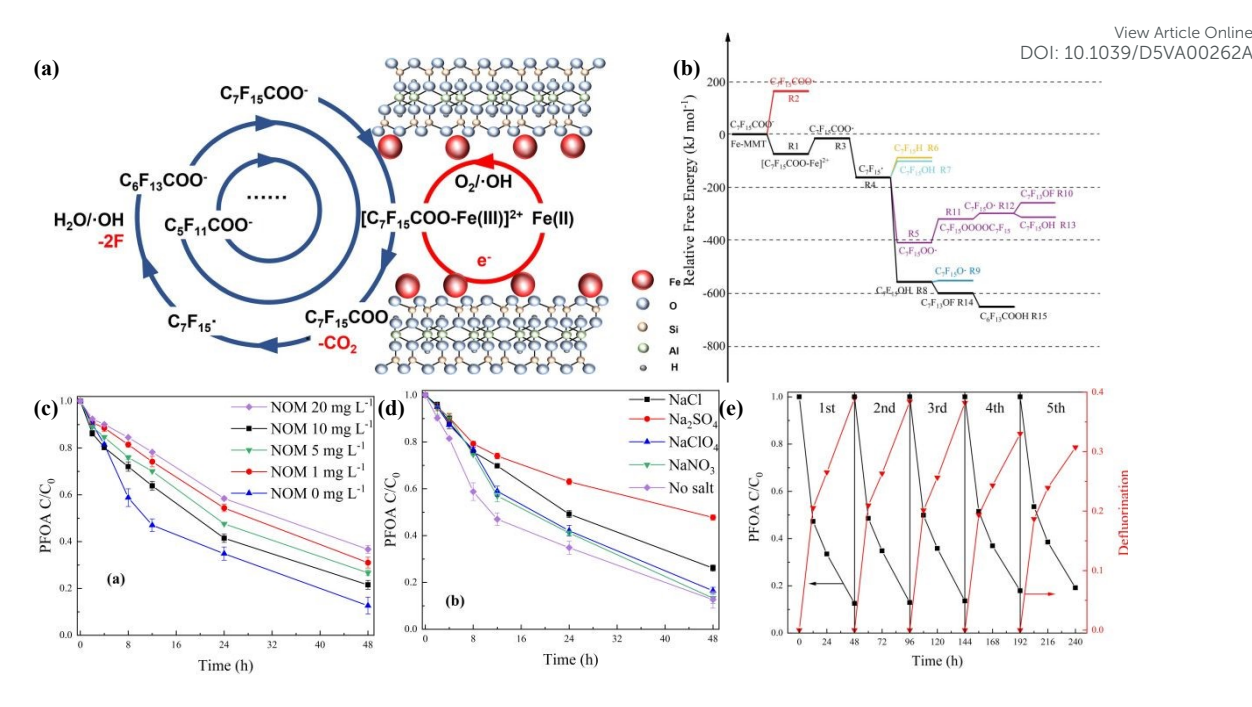


Figure 28. (a) Proposed reaction mechanism for the photo-decomposition of UV/Fe-MMT Fenton system. (b) Scheme of the potential energy surface for the degradation of PFOA in the presence of Fe-MMT. Effect of NOM (c) and inorganic ions (d) on PFOA degradation in UV/Fe-MMT Fenton system. (e) PFOA degradation (black) and defluorination (red) in consecutive batch runs of UV/Fe-MMT Fenton system. (100)

Besides experimental validation of scientific hypotheses, theoretical modeling also plays a crucial role in guiding experimental design. Zúniga-Benítez et al. systematically optimized the key parameters (ferrous ion concentration and hydrogen peroxide concentration) for the ultraviolet photo-Fenton (UV/photo-Fenton) degradation of PFOA using response surface methodology (Figure 29a and 29b). Under optimal conditions (Fe²⁺ = 0.1675 g/L, H_2O_2 = 14.0 g/L, pH 3.0), a 99% removal efficiency was achieved within 60 minutes (Figure 29c). Interestingly, the presence of natural water matrices (e.g., TOC = 2.895 mg/L, nitrate) enhanced degradation

efficiency. In untreated surface water, the degradation rate was approximately 30% faster than in deionized water. When UV irradiation was replaced with natural sunlight ($\lambda > 290$ nm), the system still achieved a 95% removal rate within 60 minutes under optimized conditions (Figure 29d), suggesting that solar photo-Fenton processes offer a low-energy alternative particularly suited for sun-rich regions.

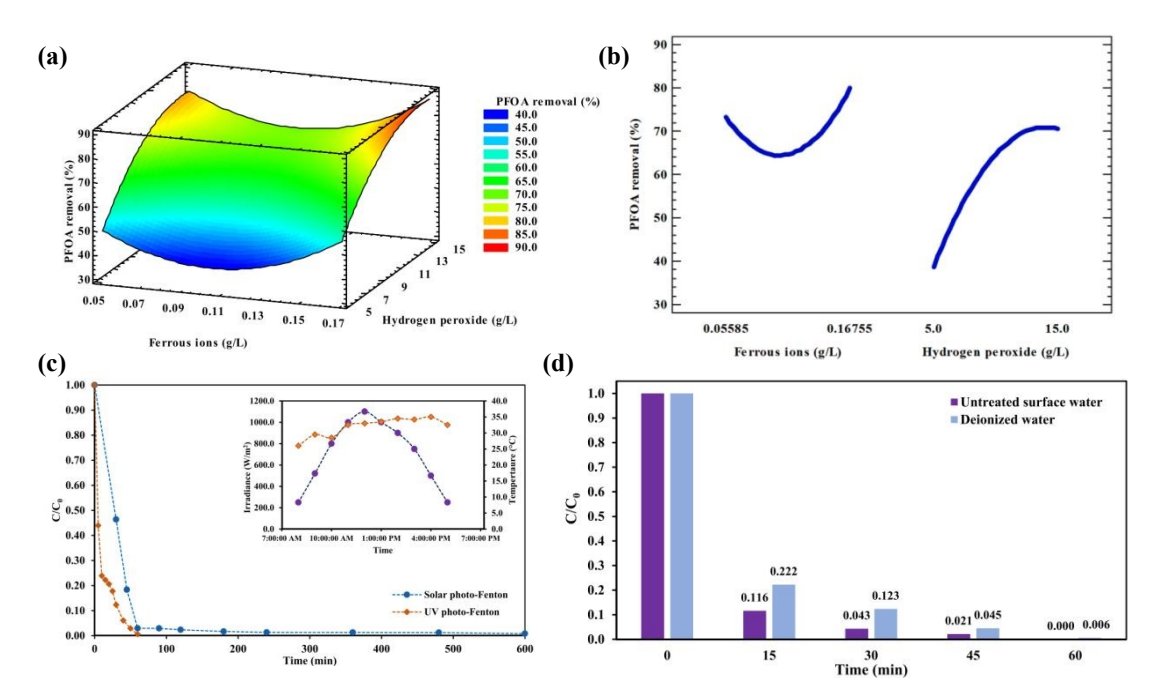


Figure 29. (a) Response surface for PFOA removal using photo-Fenton system. (b) Main effects plot for PFOA removal using photo-Fenton system. (c) PFOA removal under optimized conditions using photo-Fenton and direct solar radiation. (d) Effect of the water matrix in the PFOA removal using photo-Fenton system. ¹⁰¹

Homogeneous photo-Fenton reactions offer important mechanistic insights into the degradation pathways of PFAS, while heterogeneous photo-Fenton systems further reveal the structure-activity relationships between material architecture and degradation performance. One of the most significant advantages of photo-Fenton processes is their

use of renewable light energy, aligning closely with the principles of green and processes sustainable chemistry. However, compared to electro-Fenton systems that enable in situ H_2O_2 generation, the requirement for external H_2O_2 addition in photo-Fenton reactions remains a notable limitation. Furthermore, current research is predominantly focused on UV light-driven systems, which, although effective, often entail higher energy consumption. Although visible light has also been demonstrated to activate photo-Fenton processes for PFAS degradation, the technological maturity of such systems still requires further advancement. Additionally, the scope of photo-Fenton treatment must be broadened to a wider range of PFAS species, particularly those with more complex molecular structures and diverse chemical bond types, which demand more robust and efficient degradation strategies.

3.4 Solar Photo-Electro-Fenton (SPEF) system

SPEF systems represent a promising and emerging advancement in the development of Fenton-based processes. By integrating the benefits of photo-assisted and electrochemical Fenton mechanisms, SPEF systems build upon traditional chemical Fenton reactions to offer a greener and more energy-efficient approach for pollutant degradation. In particular, 2e⁻-ORR generates in situ H₂O₂, reducing the need for external Fenton reagents. Simultaneously, photoinduced electron-hole transfer further enhances oxidative efficiency while minimizing energy input. ¹²⁵ One of the major challenges in SPEF technology lies in the system design, ¹²⁶ which must accommodate the simultaneous requirements of both photo-Fenton and electro-Fenton

Open Access Article. Published on 29 2025. Downloaded on 10.11.2025 10:02:00.

PY-NC

This article is licensed under a Creative Commons Attribution-NonCommercial 3.0 Unported Licence

processes, posing considerable demands on catalyst architecture and operational compatibility.

As an initial attempt to apply photo-electro-Fenton reactions for PFAS degradation, Yu et al. developed a magnetic Fe₃O₄@SiO₂-BiOBr (FSB) composite, which was integrated into a dielectric barrier discharge (DBD) reactor and employed as a heterogeneous Fenton-like photocatalyst for PFOA degradation.¹⁰² The system effectively established a photo-electro-Fenton framework. Compared to DBD alone, the DBD-FSB system enhanced PFOA removal from 74% to 93% and TOC removal from 29% to 63% within 60 minutes (Figure 30a and 30b). The energy efficiency also increased significantly from 46.4 mg kW⁻¹·h⁻¹ to 72.5 mg kW⁻¹·h⁻¹. This performance was attributed to multiple reactive species pathways: (i) generation of •OH, H₂O₂, and O₃ by DBD plasma; and (ii) light-induced Fenton-like reactions on FSB. Multiple PFOA degradation pathways were proposed (Figure 30c), including: (1) hole-driven decarboxylation and radical formation on FSB; (2) direct oxidation in the plasma discharge; and (3) hydroxyl radical attack at the α -CF₂ site, triggering defluorination. The synergistic design improved both degradation efficiency and mechanistic understanding.

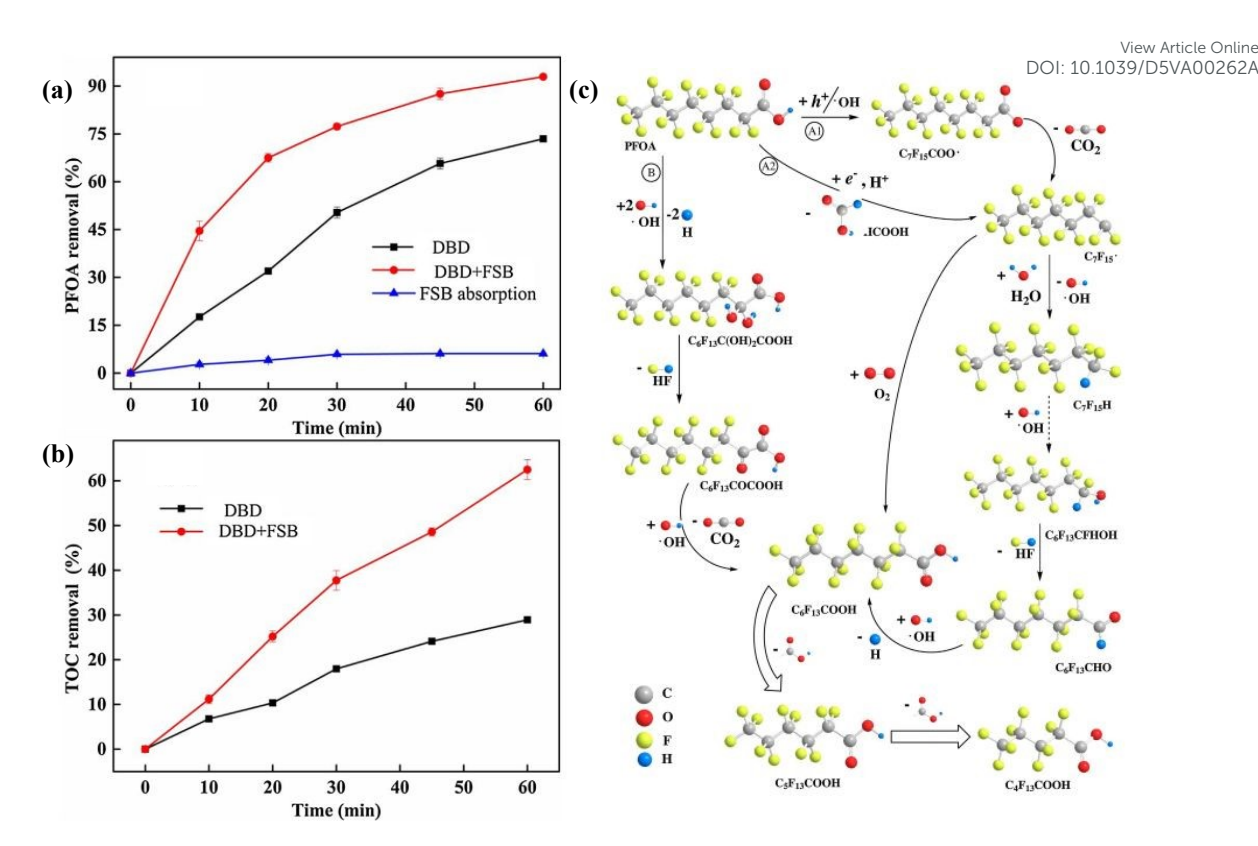


Figure 30. (a) PFOA removals in different treatment processes. (b) TOC removals in different treatment processes. (c) Proposed mineralization mechanism of PFOA in the DBD-FSB system. ¹⁰²

Subsequently, to further refine the photo-electro-Fenton system and expand the variety of reactive radical species, Lin et al. successfully fabricated a graphene oxide—titanium dioxide (GO-TiO₂) photoelectrode.¹⁰³ The efficient energy input of a photoelectrochemical (PEC) system and the synergistic effects of multiple reactive radicals, significantly enhanced the Fenton reaction efficiency and PFOS remediation (Figure 31a). The process involved electron transfer, hydroxyl radical generation, and superoxide anion radicals. The degradation pathway was investigated through identification of 25 intermediate products, including perfluoroalkyl sulfonates (PFSAs) (Figure 31b and 31c), perfluoroaldehydes (PFALs), and hydrofluorocarbons (HFCs).

Two primary mineralization routes were proposed (Figure 31d): one via Stepwise conversion to shorter-chain PFSAs, and another involving initial transformation to PFOA-like structures followed by PFOA degradation. PFALs and HFCs were confirmed as oxidation byproducts of perfluoroalkyl radicals (Figure 31d). The study also showed that shorter-chain PFAS displayed lower degradation rates, indicating stronger resistance and competitive inhibition in PFAS mixtures.

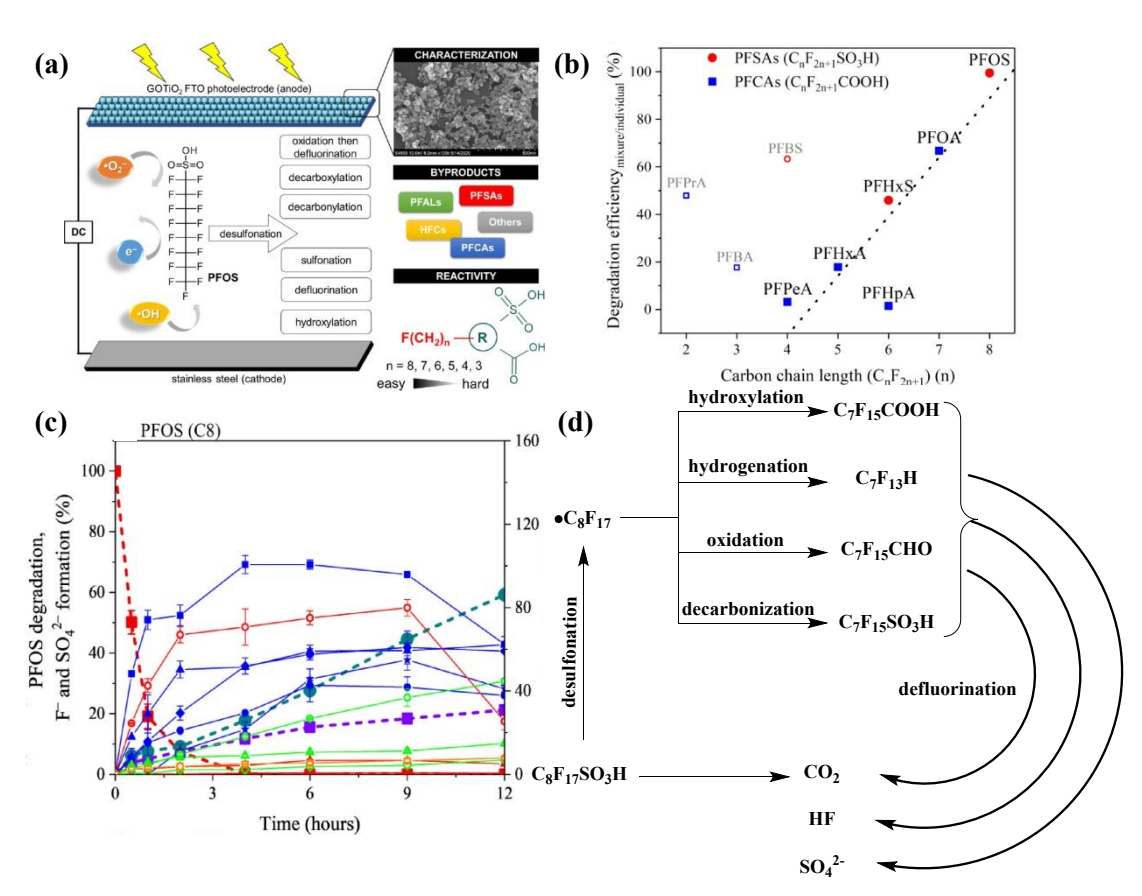


Figure 31. (a) Schematic of PFOS degradation in photoelectrochemical system. (b) The relationship between the carbon chain length and degradation efficiency ratio $(\eta_{\text{mixture}}/\eta_{\text{individual}})$ of PFAS. (c) Formation of the transformation byproducts, F⁻ and SO₄²⁻ from PFOS degradation in PEC systems. (d) Proposed degradation pathway of PFOS in the PEC system.

Open Access Article. Published on 29 2025. Downloaded on 10.11.2025 10:02:00.

(cc) EY-NO This article is licensed under a Creative Commons Attribution-NonCommercial 3.0 Unported Licence.

(Figure 32f).

The photo-electro-Fenton system was then further advanced into SPEF system by utilizing a more sustainable and readily available light source—sunlight. Following the design principles of SPEF, Wang et al. introduced a dual-function MOF/carbon nanofiber (MOF/CNF) composite membrane (Figure 32a) for efficient solar photoelectro-Fenton degradation of PFOA.¹⁰⁴ The bifunctional cathode was fabricated by solvothermal growth of Fe/Co bimetallic MOFs onto electrospinning PAN-derived CNFs, exhibiting both photo- and electrocatalytic activity. EPR analysis confirmed enhanced • OH generation under solar irradiation. The system achieved 99% PFOA removal within 120 minutes (Figure 32b). XPS analysis revealed valence changes of Fe and Co, and a corresponding mineralization mechanism was proposed (Figure 32c). In 2022, the same group advanced this design by integrating a glucose fuel cell (GFC) with the SPEF system to create a sustainable biomass-powered platform for PFOA degradation (Figure 32d). 105 Oxygen-deficient CoFe alloy nanoparticles were anchored onto CNFs (CoFe-OVs@CNF), enabling dual-function cathodes (Figure 32e). The toxicity evolution of degradation intermediates was evaluated, confirming the system's potential to degrade PFOA and other persistent pollutants while mitigating toxic risks



This article is licensed under a Creative Commons Attribution-NonCommercial 3.0 Unported Licence

Open Access Article. Published on 29 2025. Downloaded on 10.11.2025 10:02:00.

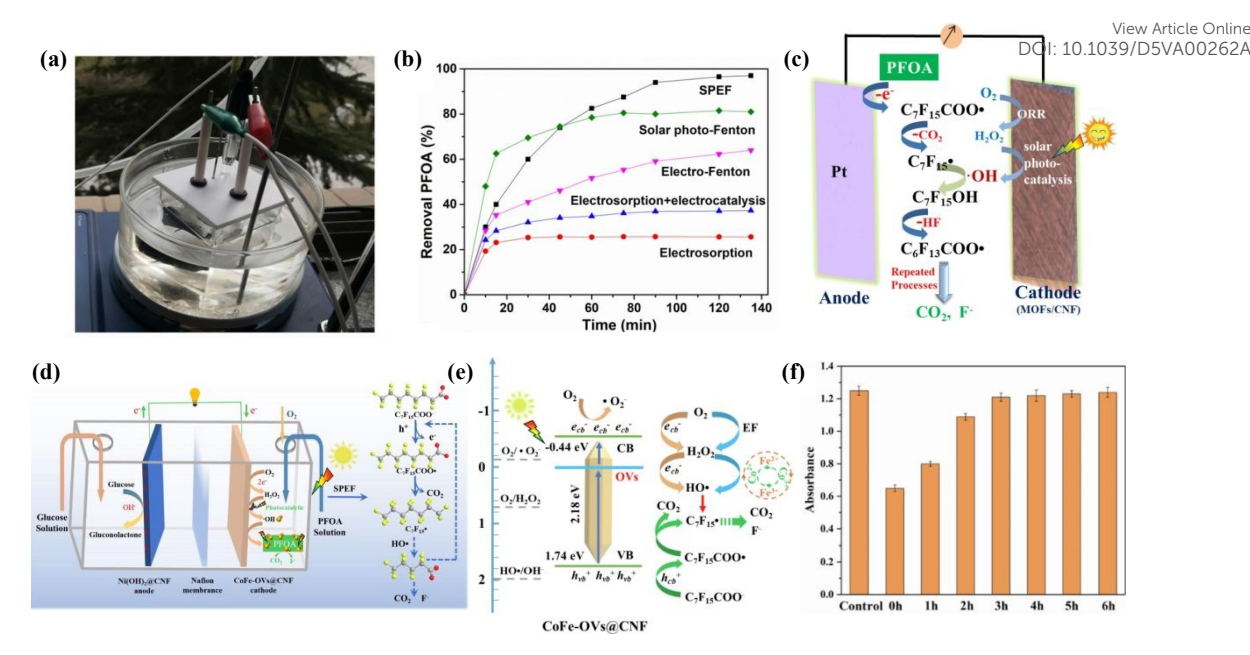


Figure 32. (a) SPEF degradation of PFOA under the natural solar light in outdoors conditions. (b) Removal of PFOA by SPEF, electro-Fenton, electrocatalysis and electrosorption, and electrosorption was conducted under N₂. (c) Mechanism of PFOA mineralization by the MOFs/CNF constructed SPEF system. ¹⁰⁴ (d) Glucose fuel cell driven SPEF process for the degradation of PFOA. (e) Proposed mechanism of solar-photocatalytic coupled Electro-Fenton process for PFOA degradation in GFC-SPEF system. (f) MTT assay for the cell viability of L-02 cells incubated with various degradation time (0–6 h) of PFOA. ¹⁰⁵

To further expand the application scope of the SPEF system for PFAS degradation, Hou et al. developed a Cu-based peroxidase-mimicking colorimetric sensor integrated with an SPEF system for PFOA detection and removal (Figure 33a). The flexible, freestanding CNF-Cu/C membrane was synthesized via solvothermal processing, secondary seeding, and in situ thermal reduction (Figure 33b). Derived from MOF/PAN precursors, the resulting 3D carbon network exhibited excellent conductivity,

dispersion, and cycling stability (Figure 33d). The CNF-Cu/C membrane showed strong peroxidase-like activity and enabled rapid PFOA detection via inhibition of TMB chromogenic reactions (Figure 33c), with a detection limit of 0.133 μM. Under optimized conditions, the Cu-SPEF system achieved 98% PFOA removal within 180 minutes. This work illustrates a successful integration of SPEF degradation and real-time detection, with significant practical potential.

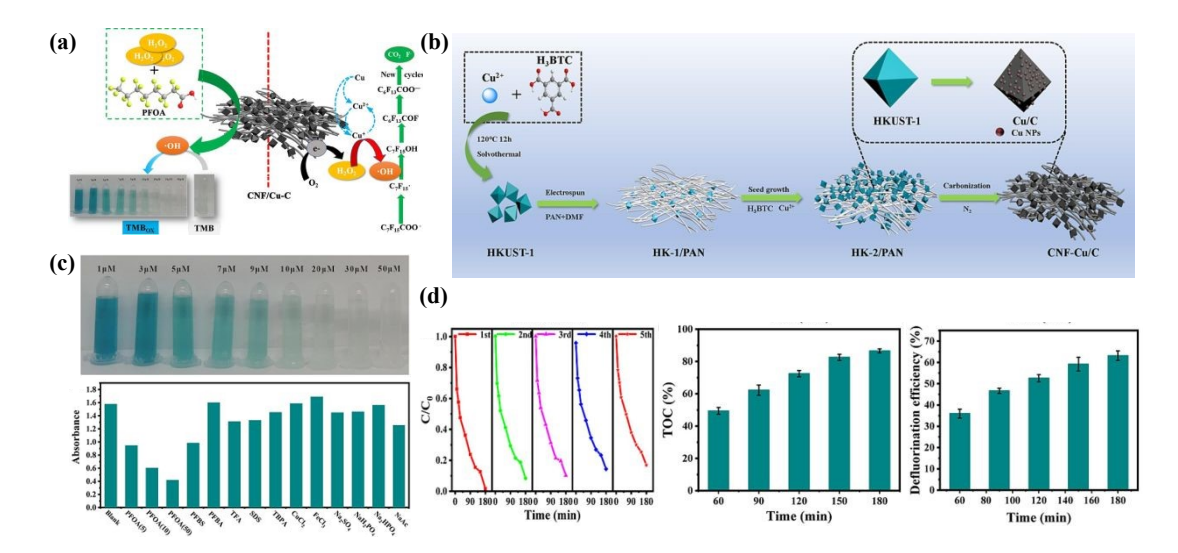


Figure 33. (a) Schematic illustration of PFOA degradation via MOFs-derived Cu/Carbon membrane. (b) Schematic diagram demonstration of the preparation of CNF-Cu/C. (c) Corresponding photographs for the colorimetric detection of PFOA (top) and selectivity of PFOA with other interfering substance (bottom). (d) Degradation rates at different conditions: reusability tests of CNF-Cu/C-800 in SPEF (left), TOC removal efficiency (mid), and defluorination efficiency (right). 106

In order to further elucidate the relationship between the structural characteristics of catalytic materials and PFAS degradation efficiency in SPEF systems, Hou et al. designed two-dimensional layered MOF-based CoFe nanosheets as

photoelectrocatalysts.¹⁰⁷ The material featured abundant unsaturated coordination stress, which facilitated rapid mass and charge transport (Figure 34a). Notably, low-temperature synthesis introduced oxygen vacancies (OVs) that modulated orbital interactions between Fe d-bands and O LUMO states, enhancing PFOA adsorption and reactivity (Figure 34b and 34c). These OVs reduced the bandgap and improved charge separation, significantly boosting photoelectrocatalytic performance (Figure 34d). The catalyst achieved effective degradation even in complex ionic matrices and real water samples (Figure 34e), advancing the practical applicability of SPEF systems and deepening mechanistic understanding at the molecular interface.

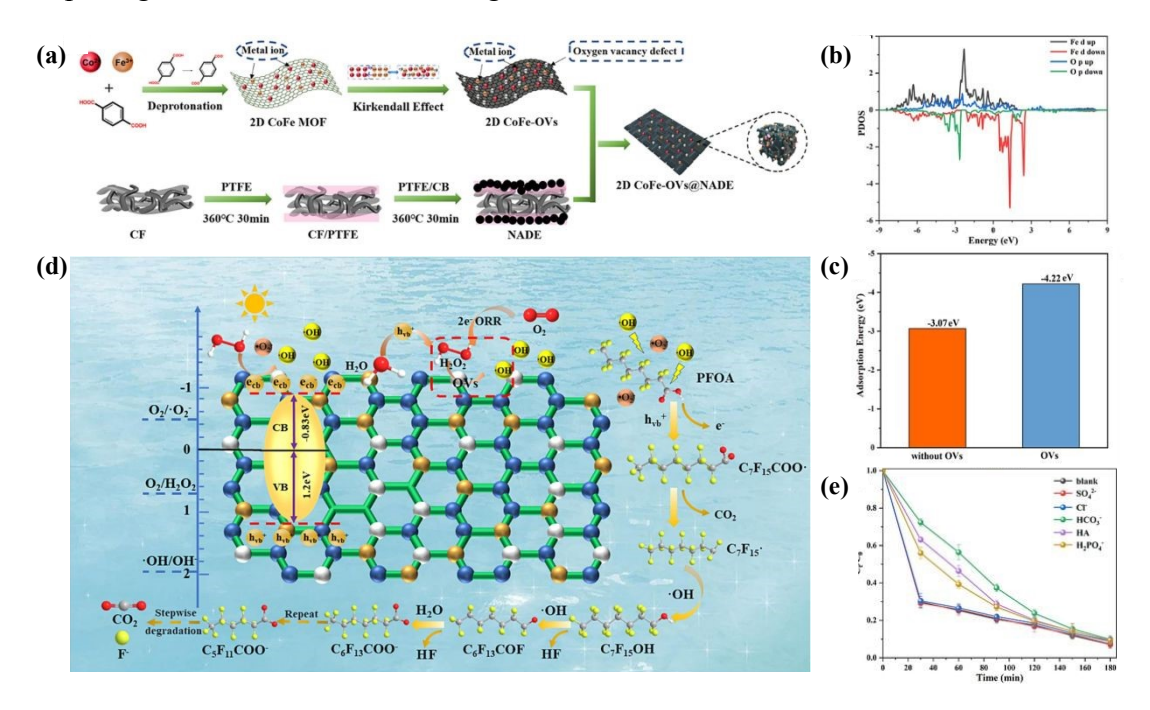


Figure 34. (a) The preparation process of 2D CoFe-OVs@NADE cathode and the construction process of SPEF system. (b) The density of states in 2D CoFe-OVs. (c) The adsorption energy between PFOA and two materials. (d) Mechanism of solar-photocatalytic coupled EF process for PFOA degradation in SPEF system. (e) The effect of coexisting substances in the SPEF system.¹⁰⁷

View Article Online DOI: 10.1039/D5VA00262A

The solar photo-electro-Fenton (SPEF) system integrates the advantages of both photo-Fenton and electro-Fenton processes by utilizing solar energy as a sustainable light source to generate photogenerated holes for PFAS activation, while simultaneously enabling the *in-situ* generation of H₂O₂ and maintaining a stable Fe²⁺/Fe³⁺ redox cycle inherent to electro-Fenton systems. This allows for efficient and environmentally friendly PFAS degradation without the need for external H₂O₂ addition. Moreover, SPEF systems can be coupled with colorimetric reactions to develop highly sensitive, real-time detection platforms for PFAS, highlighting their significant potential for future applications. However, the development of SPEF faces considerable challenges. Due to the complexity of the integrated system, there are stringent requirements for the structural design of materials used within the reaction framework. Achieving optimal performance demands materials that can simultaneously fulfill the distinct requirements of both photo-Fenton and electro-Fenton processes, which remains one of the most critical barriers to the broader application of SPEF technologies.

Table 1. Recent studies on degradation of PFAS by Fenton reaction.

Ca	talysts	Target PFAS	[PFAS] ₀	Experimental Conditions	Degradation	Defluorination	Oxidant reactive species	Ref.
	ZVI	PFOA	100 mg/L	ZVI (3.6 mM); PS (5.0 mM); 90 °C; microwave irradiation	68%	23%	SO₄•·; •OH	80
Chemical -Fenton reaction	Fe(III)	PFOA	100 μg/L	Fe(III) (0.5 mM); H ₂ O ₂ (1.0 M); pH=3.5; 20 °C	89%	\	•OH, O_2 •-, and HO_2 •	81
	MD	PFOA	10 mg/L	HP (0.5 M); PS (0.3 M); MD (0.5 g in 60 mL solution);	69%	\	SO ₄ •-, •OH,	82

				FexNiC as cathodes, graphite sheet			SO ₄ •-	
	FexNiC	PFOA	50 mg/L	as anode; O ₂ (100 mL/min);	81%	\	and	89
				KHSO ₅ (40 mM); pH=3.0; I=25 mA			•OH	
	Co CN			Co-CN ₂ -Fe ₂ O ₃ as cathodes, Pt as				
	Co-CN ₂ -	PFOA	10 mg/L	anode; O ₂ (10 mL/min); Na ₂ SO ₄	96%	96%	•OH	90
	Fe ₂ O ₃			(0.05 M); pH=2; V=-0.06V				
	Fa/N GE@GE	PFOA 2	20 mg/L	Fe/N-GE@GF as cathodes, DSA as	95%	80%	•OH	91
	Fe/N-GE@GF			anode; Na ₂ SO ₄ (0.05 M); pH=7		8070		91
	ENGGG	GenX	20 ma/I	F-NSGC as cathodes, Pt as anode;	96%	63%	•OH	92
	F-NSGC Fe(II)	, and the second	X 20 mg/L	Na ₂ SO ₄ (0.05 M); pH=3	95%	0370	•011	92
Photo-			8 mg/L	Fe(II) (2.0 mM); H ₂ O ₂ (30.0 mM);		53%	•OH	94
Fenton		TTOA	o mg/L	pH=3.0;UV lamp (9W)	95/0	<i>33</i> / 0	·O11	7 1
reaction	Fe(III)	PFOA	20 mg/L	Fe(III) (1 mM); H ₂ O ₂ (2.0 mM);	98%	13%	•OH	95

				UV light (4 W)				
	Fe ⁰ /GAC	PFOA	50 mg/L	Fe ⁰ (7.5 g/L); GAC (12.5 g/L);	\	47%	•OH	96
				H ₂ O ₂ (22.8 mM); pH=3; VUV light				
	TiO ₂ –rGO	PFOA	10 mg/L	TiO ₂ -rGO (0.1 g/L); pH=3.8;	93%	98%	•OH	97
		11011	10 1119/12	Hg lamp		7070	and O ₂ •-	<i>31</i>
				Co ₃ O ₄ @Fe ₃ O ₄ /cellulose as	95%		•OH	
	Co ₃ O ₄ @Fe ₃ O ₄	PFOA	20 mg/L	membrane; H ₂ O ₂ (30 mM); pH=3;		\	and O_2^{\bullet}	98
				Xenon lamp (300 W)			and O_2	
	Fe-MMT	PFOA	10 mg/L	Fe-MMT (1.0 g/L); HClO ₄ (0.1 M);	90%	\	•OH	100
	1.C-IVIIVI I	TTOA 10	TO HIG/L	pH=3; Hg lamp (36 W)		\	and O ₂ •-	100
Solar	DBD/FSB	PFOA	20 mg/L	FSB (100 mg/L); pH=4.28;	93%	32%	•OH	102
Photo-	DDD/13D ITOA	20 mg/L	22 kV peak voltage	73/0	32/0	-011	102	
Electro-	GO-TiO ₂	PFOS	250 μg/L	NaClO ₄ (50 mM); pH=5.64;	99%	20%	•OH	103

Fenton				j=20 mA/cm2			and O ₂ •-	
system	MOF/CNF	PFOA	20 mg/L	Na ₂ SO ₄ (50 mM); pH=3; V=-0.6 V	99%	59%	•OH	104
	CoFe-	PEG 4	20 /1	Na ₂ SO ₄ (50 mM); pH=3; O ₂ purge;	050/	700/	•OH	105
	OVs@CNF	PFOA	20 mg/L	Xenon lamp (300 W)	95%	70%	and O ₂ •-	105
							•OH,	
	CNF Cu/C	C PFOA 20 m	20 mg/L	Na ₂ SO ₄ (50 mM); pH=3; O ₂ purge;	98%	63%	O ₂ •-,	106
	CNF-Cu/C			Xenon lamp (300 W)	7070	0370	and	
							HO_2	
	CoFe-	PFOA	20 mg/L	Na ₂ SO ₄ (0.5 M); pH=3; O ₂ purge;	93%	67%	•OH	107
	OVs@NADE		TTOA	20 Hig/L	Xenon lamp (300 W)	73/0	0770	and O ₂ •-

View Article Online DOI: 10.1039/D5VA00262A

4. Summary and outlook

The degradation of PFAS is inherently challenging due to the high bond dissociation energy of C–F bonds, which requires not only large quantities of •OH but also effective activation of PFAS molecules to form reactive ${}^{\bullet}\text{C}_n\text{F}_{2n+1}$ intermediates. Fenton reactions, owing to their ability to stably generate ${}^{\bullet}\text{OH}$, naturally emerged as a leading strategy. However, ${}^{\bullet}\text{OH}$ alone is often insufficient to initiate PFAS activation. To overcome this limitation, multiple innovative approaches have been proposed.

Recent advances in Fenton-based strategies for PFAS degradation have been systematically summarized (Table 1), providing a more intuitive comparison of the relationships among reaction systems, operating conditions, and degradation efficiencies. Distinct reaction systems rely on different oxidative reactive species, which in turn lead to significant variations in PFAS degradation behaviors. In traditional Fenton systems, various radical precursors have been introduced to promote synergistic radical generation for enhanced PFAS degradation. Alternatively, spatial confinement strategies have been employed to restrict PFAS and •OH interactions to confined catalytic environments, thereby increasing the local radical concentration and reactivity. Additionally, several physical techniques—including electro-Fenton, photo-Fenton, and SPEF—have been developed to facilitate PFAS activation through direct oxidation or electron-hole transfer, thereby enhancing coupling with • OH and subsequent defluorination steps. These hybrid methods not only circumvent the limitations of chemical Fenton systems, such as excessive H₂O₂ requirements, poor catalyst stability, and strict pH conditions, but also open up new possibilities for the

sustainable treatment of PFAS. However, these advancements come with new challenges—particularly in the rational design of catalytic systems that can meet multiple performance criteria.

Considerable research efforts are still required to fully understand and optimize Fenton-based PFAS degradation. Continued exploration of Fenton-derived AOPs is essential to broaden the scope of PFAS treatment and to proactively address the challenges posed by emerging PFAS variants in future environmental scenarios. Among these developments, multi-strategy coupled Fenton systems, such as the recently proposed SPEF process, are regarded as some of the most promising approaches. By integrating multiple mechanisms, these systems can overcome the limitations inherent to individual methods. However, such integration also significantly increases the complexity of system design and material engineering. Based on the content of this review, the following research gaps and perspectives are proposed:

- (1) Most existing studies have focused on the degradation of PFOA and PFOS, which are typically present at the highest concentrations in contaminated water. However, the PFAS concentrations (~10-50 mg/L) used in laboratory-scale experiments are far higher than those typically found in natural waters. Therefore, future research should focus on low-concentration PFAS degradation under environmentally relevant conditions to better meet real-world treatment demands.
- (2) Current Fenton-based degradation systems have been primarily developed for PFOA, whereas studies on other PFAS species with diverse functional groups or backbone structures remain limited. Expanding the applicability of Fenton reactions to

View Article Online

a broader range of PFAS is therefore an important direction for future research. Moreover, the influences of PFAS functional groups, backbone architectures, and spatial conformations on the degradation efficiency, degradation pathways, and byproduct formation in Fenton-based systems require further systematic investigation.

- (3) Although novel Fenton-based systems have shown impressive performance, achieving over 95% PFAS degradation within a few hours, the formation of diverse transformation products—including short-chain intermediates, functional group modifications, and possible backbone alterations—remains a major concern. The limited identification of these byproducts and the lack of comprehensive toxicological assessment raise the risk of secondary pollution. Addressing this challenge calls for integrated, multidisciplinary frameworks that link degradation efficiency with systematic analyses of byproduct formation, toxicity, and environmental fate. Future research should therefore move beyond removal rates toward holistic evaluations that ensure both treatment effectiveness and long-term environmental and biological safety.
- (4) The development of increasingly sophisticated multi-method coupled Fenton systems presents considerable challenges for catalyst design and material selection. Future work should aim to elucidate the structure-activity relationships between catalyst composition and PFAS degradation performance. Establishing general design principles will enable the development of more effective catalytic materials specifically tailored for PFAS treatment.
- (5) Despite widespread attention to Fenton-based AOPs for PFAS degradation, their performance in complex environmental waters has not been systematically evaluated.

View Article Online

Moreover, current Fenton systems typically operate at relatively small treatment volumes. Large-scale water treatment applications require comprehensive studies of process scalability and techno-economic performance. In this context, life cycle assessment (LCA) and techno-economic analysis (TEA) should be considered in future evaluations of PFAS treatment technologies.

Author contributions

Zhicong Huang: Conceptualization; Data curation; Visualization; Validation; Writing – original draft; Writing – review & editing. Xi Huang: Investigation. Kang Liu: Supervision. Junwei Fu: Conceptualization; Funding acquisition; Project administration; Resources; Supervision; Writing – review & editing. Min Liu: Supervision.

Conflicts of interest

The authors declare that they have no known competing financial interests or personal relationships that could have appeared to influence the work reported in this paper.

Acknowledgements

The authors gratefully thank the National Natural Science Foundation of China (Grant No. 22579190, 52372253), Central South University Innovation-Driven Research Programme (Grant No. 2023CXQD042), and the Natural Science Foundation

View Article Online DOI: 10.1039/D5VA00262A

of Hunan Province for Excellent Youth Scholars (Grant No. 2024JJ4051).

References

- 1.H. Li, A. L. Junker, J. Wen, L. Ahrens, M. Sillanpää, J. Tian, F. Cui, L. Vergeynst and Z. Wei, A recent overview of per- and polyfluoroalkyl substances (PFAS) removal by functional framework materials, *Chem. Eng. J.*, 2023, **452**, 139202.
- 2.Y. Li, Z. Niu and Y. Zhang, Occurrence of legacy and emerging polyand perfluoroalkyl substances in water: A case study in Tianjin (China), *Chemosphere*, 2022, **287**, 132409.
- 3.K. Kannan, Perfluoroalkyl and polyfluoroalkyl substances: current and future perspectives, *Environ. Chem.*, 2011, **8**, 333.
- 4.N. Chowdhury, S. Prabakar and H. Choi, Dependency of the photocatalytic and photochemical decomposition of per- and polyfluoroalkyl substances (PFAS) on their chain lengths, functional groups, and structural properties, *Water Sci Technol*, 2021, **84**, 3738-3754.
- 5.F. Li, J. Duan, S. Tian, H. Ji, Y. Zhu, Z. Wei and D. Zhao, Short-chain per- and polyfluoroalkyl substances in aquatic systems: Occurrence, impacts and treatment, *Chem. Eng. J.*, 2020, **380**, 122506.
- 6.J. John, F. Coulon and P. V. Chellam, Detection and treatment strategies of per- and polyfluoroalkyl substances (PFAS): Fate of PFAS through DPSIR framework analysis, *J. Water Process Eng.*, 2022, **45**, 102463.
- 7.S. Garg, J. Wang, P. Kumar, V. Mishra, H. Arafat, R. S. Sharma and L. F. Dumée,

Remediation of water from per-/poly-fluoroalkyl substances (PFAS) – Challenges and perspectives, *J. Environ. Chem. Eng.*, 2021, **9**, 105784.

- 8.J. P. Giesy and K. Kannan., Peer Reviewed: Perfluorochemical Surfactants in the Environment, *Environ. Sci. Technol.*, 2002, **36**, 146A-152A.
- 9.B. D. Key, R. D. Howell and C. S. Criddle, Fluorinated Organics in the Biosphere, *Environ. Sci. Technol.*, 1997, **31**, 2445-2454.
- 10.M. Kotthoff, J. Muller, H. Jurling, M. Schlummer and D. Fiedler, Perfluoroalkyl and polyfluoroalkyl substances in consumer products, *Environ. Sci. Pollut. Res. Int.*, 2015, **22**, 14546-14559.
- 11.D. R. Taves, Evidence that there are Two Forms of Fluoride in Human Serum, *Nature*, 1968, **217**, 1050-1051.
- 12.C. G. Pan, S. K. Xiao, K. F. Yu, Q. Wu and Y. H. Wang, Legacy and alternative per- and polyfluoroalkyl substances in a subtropical marine food web from the Beibu Gulf, South China: Fate, trophic transfer and health risk assessment, *J. Hazard. Mater.*, 2021, **403**, 123618.
- 13.X. Liang, J. Zhou, X. Yang, W. Jiao, T. Wang and L. Zhu, Disclosing the bioaccumulation and biomagnification behaviors of emerging per/polyfluoroalkyl substances in aquatic food web based on field investigation and model simulation, *J.*

This article is licensed under a Creative Commons Attribution-NonCommercial 3.0 Unported Licence

Open Access Article. Published on 29 2025. Downloaded on 10.11.2025 10:02:00.

Haz 14.S chlo spec 15.A Tox

Hazard. Mater., 2023, 445, 130566.

View Article Online
DOI: 10.1039/D5VA00262A

ms of novel

- 14.S. Yi, P. Chen, L. Yang and L. Zhu, Probing the hepatotoxicity mechanisms of novel chlorinated polyfluoroalkyl sulfonates to zebrafish larvae: Implication of structural specificity, *Environ. Int.*, 2019, **133**, 105262.
- 15.A. Hagenaars, D. Knapen, I. J. Meyer, K. van der Ven, P. Hoff and W. De Coen, Toxicity evaluation of perfluorooctane sulfonate (PFOS) in the liver of common carp (Cyprinus carpio), *Aquat. Toxicol.*, 2008, **88**, 155-163.
- 16.K. Li, P. Gao, P. Xiang, X. Zhang, X. Cui and L. Q. Ma, Molecular mechanisms of PFOA-induced toxicity in animals and humans: Implications for health risks, *Environ*. *Int.*, 2017, **99**, 43-54.
- 17.M. Liu, S. Yi, H. Yu, T. Zhang, F. Dong and L. Zhu, Underlying Mechanisms for the Sex- and Chemical-Specific Hepatotoxicity of Perfluoroalkyl Phosphinic Acids in Common Carp (Cyprinus carpio), *Environ. Sci. Technol.*, 2023, 57, 14515-14525.
- 18.S. Yi, J. Wang, R. Wang, M. Liu, W. Zhong, L. Zhu and G. Jiang, Structure-Related Thyroid Disrupting Effect of Perfluorooctanesulfonate-like Substances in Zebrafish Larvae, *Environ. Sci. Technol.*, 2024, **58**, 182-193.
- 19.J. Guo, J. Zhou, S. Liu, L. Shen, X. Liang, T. Wang and L. Zhu, Underlying Mechanisms for Low-Molecular-Weight Dissolved Organic Matter to Promote Translocation and Transformation of Chlorinated Polyfluoroalkyl Ether Sulfonate in Wheat, *Environ. Sci. Technol.*, 2022, **56**, 15617-15626.
- 20.S. Liu, J. Zhou, J. Guo, M. Xue, L. Shen, S. Bai, X. Liang, T. Wang and L. Zhu, Impact Mechanisms of Humic Acid on the Transmembrane Transport of Per- and Polyfluoroalkyl Substances in Wheat at the Subcellular Level: The Important Role of Slow-Type Anion Channels, *Environ. Sci. Technol.*, 2023, **57**, 8739-8749.
- 21.X. Yang, C. Ye, Y. Liu and F. J. Zhao, Accumulation and phytotoxicity of perfluorooctanoic acid in the model plant species Arabidopsis thaliana, *Environ Pollut*, 2015, **206**, 560-566.
- 22.L. Fan, J. Tang, D. Zhang, M. Ma, Y. Wang and Y. Han, Investigations on the phytotoxicity of perfluorooctanoic acid in Arabidopsis thaliana, *Environ. Sci. Pollut. Res. Int.*, 2020, **27**, 1131-1143.
- 23.Q. Guo, Z. He, X. Liu, B. Liu and Y. Zhang, High-throughput non-targeted metabolomics study of the effects of perfluorooctane sulfonate (PFOS) on the metabolic characteristics of A. thaliana leaves, *Sci. Total Environ.*, 2020, **710**, 135542.
- 24.P. Li, X. Oyang, X. Xie, Z. Li, H. Yang, J. Xi, Y. Guo, X. Tian, B. Liu, J. Li and Z. Xiao, Phytotoxicity induced by perfluorooctanoic acid and perfluorooctane sulfonate via metabolomics, *J. Hazard. Mater.*, 2020, **389**, 121852.
- 25.P. Li, J. Sun, X. Xie, Z. Li, B. Huang, G. Zhang, J. Li and Z. Xiao, Stress response and tolerance to perfluorooctane sulfonate (PFOS) in lettuce (Lactuca sativa), *J. Hazard. Mater.*, 2021, **404**, 124213.
- 26.F. Chi, S. Zhao, L. Yang, X. Yang, X. Zhao, R. Zhao, L. Zhu and J. Zhan, Unveiling behaviors of 8:2 fluorotelomer sulfonic acid (8:2 FTSA) in Arabidopsis thaliana: Bioaccumulation, biotransformation and molecular mechanisms of phytotoxicity, *Sci. Total Environ.*, 2024, **927**, 172165.
- 27.S. E. Fenton, A. Ducatman, A. Boobis, J. C. DeWitt, C. Lau, C. Ng, J. S. Smith and

- S. M. Roberts, Per- and Polyfluoroalkyl Substance Toxicity and Human Health Review Syldsvanded Current State of Knowledge and Strategies for Informing Future Research, *Environ*. *Toxicol. Chem.*, 2021, **40**, 606-630.
- 28.Y. Zhu, X. Yang, X. Song, Y. Jia, Y. Zhang and L. Zhu, Insights into the Enhanced Bioavailability of Per- and Polyfluoroalkyl Substances in Food Caused by Chronic Inflammatory Bowel Disease, *Environ. Sci. Technol.*, 2024, **58**, 11912-11922.
- 29.Q. Chen, S. Yi, Y. Sun, Y. Zhu, K. Ma and L. Zhu, Contribution of Continued Dermal Exposure of PFAS-Containing Sunscreens to Internal Exposure: Extrapolation from In Vitro and In Vivo Tests to Physiologically Based Toxicokinetic Models, *Environ. Sci. Technol.*, 2024, **58**, 15005-15016.
- 30.J. F. C. Glatz and J. Luiken, Dynamic role of the transmembrane glycoprotein CD36 (SR-B2) in cellular fatty acid uptake and utilization, *J. Lipid Res.*, 2018, **59**, 1084-1093. 31.Y. Jia, Y. Zhu, R. Wang, Q. Ye, D. Xu, W. Zhang, Y. Zhang, G. Shan and L. Zhu, Novel insights into the mediating roles of cluster of differentiation 36 in transmembrane transport and tissue partition of per- and polyfluoroalkyl substances in mice, *J. Hazard. Mater.*, 2023, **442**, 130129.
- 32.U. S. E. P. Agency., Interim Updated PFOA and PFOS Health Advisories, Available online: https://www.epa.gov/sdwa/drinking-water-health-advisories-pfoa-and-pfos (accessed on 15 June 2022)).
- 33.Eurofins., PFAS in the Revised Drinking Water Directive (DWD), Available online: https://www.eurofins.se/tjaenster/miljoeoch-vatten/nyheter-miljo/pfas-in-the-revised-drinking-water-directive-dwd/ (accessed on 26 May 2023).).
- 34.L. Liu, Y. Qu, J. Huang and R. Weber, Per- and polyfluoroalkyl substances (PFASs) in Chinese drinking water: risk assessment and geographical distribution, *Environ. Sci. Eur.*, 2021, **33**, 6-17.
- 35.K. Y. Tan, G. H. Lu, H. T. Piao, S. Chen, X. C. Jiao, N. Gai, E. Yamazaki, N. Yamashita, J. Pan and Y. L. Yang, Current Contamination Status of Perfluoroalkyl Substances in Tapwater from 17 Cities in the Eastern China and Their Correlations with Surface Waters, *Bull Environ Contam Toxicol*, 2017, **99**, 224-231.
- 36.H. Yin, R. Chen, H. Wang, C. Schwarz, H. Hu, B. Shi and Y. Wang, Co-occurrence of phthalate esters and perfluoroalkyl substances affected bacterial community and pathogenic bacteria growth in rural drinking water distribution systems, *Sci. Total Environ.*, 2023, **856**, 158943.
- 37.H. Park, G. Choo, H. Kim and J. E. Oh, Evaluation of the current contamination status of PFASs and OPFRs in South Korean tap water associated with its origin, *Sci. Total Environ.*, 2018, **634**, 1505-1512.
- 38.K. Y. Kim, O. D. Ekpe, H. J. Lee and J. E. Oh, Perfluoroalkyl substances and pharmaceuticals removal in full-scale drinking water treatment plants, *J. Hazard. Mater.*, 2020, **400**, 123235.
- 39.M. Babayev, S. L. Capozzi, P. Miller, K. R. McLaughlin, S. S. Medina, S. Byrne, G. Zheng and A. Salamova, PFAS in drinking water and serum of the people of a southeast Alaska community: A pilot study, *Environ Pollut*, 2022, **305**, 119246.
- 40.C. S. Skaggs and B. A. Logue, Ultratrace analysis of per- and polyfluoroalkyl substances in drinking water using ice concentration linked with extractive stirrer and

high performance liquid chromatography - tandem mass spectrometry, *J. Chromatogy* $^{\text{View Article Online}}_{59/D5VA00262A}$ *A*, 2021, **1659**, 462493.

- 41.K. Arinaitwe, N. Keltsch, A. Taabu-Munyaho, T. Reemtsma and U. Berger, Perfluoroalkyl substances (PFASs) in the Ugandan waters of Lake Victoria: Spatial distribution, catchment release and public exposure risk via municipal water consumption, *Sci. Total Environ.*, 2021, **783**, 146970.
- 42.Y. Liu, X. Li, X. Wang, X. Qiao, S. Hao, J. Lu, X. Duan, D. D. Dionysiou and B. Zheng, Contamination Profiles of Perfluoroalkyl Substances (PFAS) in Groundwater in the Alluvial-Pluvial Plain of Hutuo River, China, *Water (Basel)*, 2019, **11**, 1-2316.
- 43.M. A. Petre, D. P. Genereux, L. Koropeckyj-Cox, D. R. U. Knappe, S. Duboscq, T. E. Gilmore and Z. R. Hopkins, Per- and Polyfluoroalkyl Substance (PFAS) Transport from Groundwater to Streams near a PFAS Manufacturing Facility in North Carolina, USA, *Environ. Sci. Technol.*, 2021, **55**, 5848-5856.
- 44.A. Wagner, B. Raue, H. J. Brauch, E. Worch and F. T. Lange, Determination of adsorbable organic fluorine from aqueous environmental samples by adsorption to polystyrene-divinylbenzene based activated carbon and combustion ion chromatography, *J. Chromatogr. A*, 2013, **1295**, 82-89.
- 45.L. Gobelius, J. Hedlund, W. Durig, R. Troger, K. Lilja, K. Wiberg and L. Ahrens, Per- and Polyfluoroalkyl Substances in Swedish Groundwater and Surface Water: Implications for Environmental Quality Standards and Drinking Water Guidelines, *Environ. Sci. Technol.*, 2018, **52**, 4340-4349.
- 46.S. Banzhaf, M. Filipovic, J. Lewis, C. J. Sparrenbom and R. Barthel, A review of contamination of surface-, ground-, and drinking water in Sweden by perfluoroalkyl and polyfluoroalkyl substances (PFASs), *Ambio*, 2017, **46**, 335-346.
- 47.M. Filipovic, A. Woldegiorgis, K. Norstrom, M. Bibi, M. Lindberg and A. H. Osteras, Historical usage of aqueous film forming foam: a case study of the widespread distribution of perfluoroalkyl acids from a military airport to groundwater, lakes, soils and fish, *Chemosphere*, 2015, **129**, 39-45.
- 48.E. Hepburn, C. Madden, D. Szabo, T. L. Coggan, B. Clarke and M. Currell, Contamination of groundwater with per- and polyfluoroalkyl substances (PFAS) from legacy landfills in an urban re-development precinct, *Environ Pollut*, 2019, **248**, 101-113.
- 49.D. Szabo, T. L. Coggan, T. C. Robson, M. Currell and B. O. Clarke, Investigating recycled water use as a diffuse source of per- and polyfluoroalkyl substances (PFASs) to groundwater in Melbourne, Australia, *Sci. Total Environ.*, 2018, **644**, 1409-1417.
- 50.X. Song, R. Vestergren, Y. Shi, J. Huang and Y. Cai, Emissions, Transport, and Fate of Emerging Per- and Polyfluoroalkyl Substances from One of the Major Fluoropolymer Manufacturing Facilities in China, *Environ. Sci. Technol.*, 2018, **52**, 9694-9703.
- 51.H.-C. Wang, T.-H. Yeo, S. Nobarany and G. Hsieh, presented in part at the Proceedings of the Third International Symposium of Chinese CHI, 2015.
- 52.Y. Pan, H. Zhang, Q. Cui, N. Sheng, L. W. Y. Yeung, Y. Sun, Y. Guo and J. Dai, Worldwide Distribution of Novel Perfluoroether Carboxylic and Sulfonic Acids in Surface Water, *Environ. Sci. Technol.*, 2018, **52**, 7621-7629.

53.Y. Zhang, R. Dong, F. Ge, M. Hong, Z. Chen, Y. Zhou, J. Wei, C. Gu and Dokong View Article Online Removal of 48 per- and polyfluoroalkyl substances (PFAS) throughout processes in domestic and general industrial wastewater treatment plants: Implications for emerging alternatives risk control, *J. Hazard. Mater.*, 2024, **480**, 136130.

54.K. Y. Kim, M. Ndabambi, S. Choi and J. E. Oh, Legacy and novel perfluoroalkyl

This article is licensed under a Creative Commons Attribution-NonCommercial 3.0 Unported Licence

Open Access Article. Published on 29 2025. Downloaded on 10.11.2025 10:02:00.

- 54.K. Y. Kim, M. Ndabambi, S. Choi and J. E. Oh, Legacy and novel perfluoroalkyl and polyfluoroalkyl substances in industrial wastewater and the receiving river water: Temporal changes in relative abundances of regulated compounds and alternatives, *Water Res.*, 2021, **191**, 116830.
- 55.X. Dauchy, V. Boiteux, C. Bach, A. Colin, J. Hemard, C. Rosin and J. F. Munoz, Mass flows and fate of per- and polyfluoroalkyl substances (PFASs) in the wastewater treatment plant of a fluorochemical manufacturing facility, *Sci. Total Environ.*, 2017, **576**, 549-558.
- 56.S. Huang, M. Sima, Y. Long, C. Messenger and P. R. Jaffe, Anaerobic degradation of perfluoroctanoic acid (PFOA) in biosolids by Acidimicrobium sp. strain A6, *J. Hazard. Mater.*, 2022, **424**, 127699.
- 57.S. Wang, T. Liu, X. Qian, H. Wang, M. Li, X. Wang, S. Wei and H. Chen, Microbial plankton responses to perfluoroalkyl acids and their alternatives in the aquatic environment, *J. Hazard. Mater.*, 2023, **441**, 129980.
- 58.Y. Huang, W. Zhang, M. Bai and X. Huang, One-pot fabrication of magnetic fluorinated carbon nanotubes adsorbent for efficient extraction of perfluoroalkyl carboxylic acids and perfluoroalkyl sulfonic acids in environmental water samples, *Chem. Eng. J.*, 2020, **380**, 122392.
- 59.G. Niarchos, L. Ahrens, D. B. Kleja and F. Fagerlund, Per- and polyfluoroalkyl substance (PFAS) retention by colloidal activated carbon (CAC) using dynamic column experiments, *Environ Pollut*, 2022, **308**, 119667.
- 60.T. A. Bruton and D. L. Sedlak, Treatment of Aqueous Film-Forming Foam by Heat-Activated Persulfate Under Conditions Representative of In Situ Chemical Oxidation, *Environ. Sci. Technol.*, 2017, **51**, 13878-13885.
- 61.Y. Bao, J. Huang, G. Cagnetta and G. Yu, Removal of F-53B as PFOS alternative in chrome plating wastewater by UV/Sulfite reduction, *Water Res.*, 2019, **163**, 114907. 62.J. Cui, P. Gao and Y. Deng, Destruction of Per- and Polyfluoroalkyl Substances (PFAS) with Advanced Reduction Processes (ARPs): A Critical Review, *Environ. Sci. Technol.*, 2020, **54**, 3752-3766.
- 63.M. Pierpaoli, M. Szopinska, B. K. Wilk, M. Sobaszek, A. Luczkiewicz, R. Bogdanowicz and S. Fudala-Ksiazek, Electrochemical oxidation of PFOA and PFOS in landfill leachates at low and highly boron-doped diamond electrodes, *J. Hazard. Mater.*, 2021, **403**, 123606.
- 64.L. P. Wackett, Why Is the Biodegradation of Polyfluorinated Compounds So Rare?, *mSphere*, 2021, **6**, e0072121.
- 65.W. H. Glaze, J.-W. Kang and D. H. Chapin, The Chemistry of Water Treatment Processes Involving Ozone, Hydrogen Peroxide and Ultraviolet Radiation, *Ozone: Sci. Eng.*, 1987, **9**, 335-352.
- 66.L. Yang, Y. Jiao, X. Xu, Y. Pan, C. Su, X. Duan, H. Sun, S. Liu, S. Wang and Z. Shao, Superstructures with Atomic-Level Arranged Perovskite and Oxide Layers for

Advanced Oxidation with an Enhanced Non-Free Radical Pathway, *ACS Sustain*, *Cherry*, *D5VA00262A Eng.*, 2022, **10**, 1899-1909.

- 67.H. J. H. Fenton, LXXIII.—Oxidation of tartaric acid in presence of iron, *J. Chem. Soc., Trans.*, 1894, **65**, 899-910.
- 68.M. H. Zhang, H. Dong, L. Zhao, D. X. Wang and D. Meng, A review on Fenton process for organic wastewater treatment based on optimization perspective, *Sci. Total Environ.*, 2019, **670**, 110-121.
- 69.I. Mesquita, L. C. Matos, F. Duarte, F. J. Maldonado-Hodar, A. Mendes and L. M. Madeira, Treatment of azo dye-containing wastewater by a Fenton-like process in a continuous packed-bed reactor filled with activated carbon, *J. Hazard. Mater.*, 2012, **237-238**, 30-37.
- 70.F. Duarte, F. J. Maldonado-H ó dar and L. M. Madeira, Influence of the characteristics of carbon materials on their behaviour as heterogeneous Fenton catalysts for the elimination of the azo dye Orange II from aqueous solutions, *Appl. Catal. B*, 2011, **103**, 109-115.
- 71.C. Kim, P. Debusmann, M. S. Abdighahroudi, J. Schumacher and H. V. Lutze, Fenton-coagulation process for simultaneous abatement of micropollutants and dissolved organic carbon in treated wastewater, *Water Res.*, 2025, **281**, 123583.
- 72.Z. Ye, E. Brillas, F. Centellas, P. L. Cabot and I. Sires, Expanding the application of photoelectro-Fenton treatment to urban wastewater using the Fe(III)-EDDS complex, *Water Res.*, 2020, **169**, 115219.
- 73.M. J. Chen, S. L. Lo, Y. C. Lee and C. C. Huang, Photocatalytic decomposition of perfluorooctanoic acid by transition-metal modified titanium dioxide, *J. Hazard. Mater.*, 2015, **288**, 168-175.
- 74.X. Dai, Z. Xie, B. Dorian, S. Gray and J. Zhang, Comparative study of PFAS treatment by UV, UV/ozone, and fractionations with air and ozonated air, *Environ. Sci.: Water Res. Technol.*, 2019, **5**, 1897-1907.
- 75.N. Duinslaeger and J. Radjenovic, Electrochemical degradation of per- and polyfluoroalkyl substances (PFAS) using low-cost graphene sponge electrodes, *Water Res.*, 2022, **213**, 118148.
- 76.B. Utset, J. Garcia, J. Casado, X. Domènech and J. Peral, Replacement of H₂O₂ by O₂ in Fenton and photo-Fenton reactions, *Chemosphere*, 2000, **41**, 1187-1192.
- 77.W. Song, M. Cheng, J. Ma, W. Ma, C. Chen and J. Zhao, Decomposition of Hydrogen Peroxide Driven by Photochemical Cycling of Iron Species in Clay, *Environ. Sci. Technol.*, 2006, **40**, 4782-4787.
- 78.M. L. Rodriguez, V. I. Timokhin, S. Contreras, E. Chamarro and S. Esplugas, Rate equation for the degradation of nitrobenzene by 'Fenton-like' reagent, *Adv. Environ. Res.*, 2003, 7, 583-595.
- 79.J. J. Pignatello, E. Oliveros and A. MacKay, Advanced Oxidation Processes for Organic Contaminant Destruction Based on the Fenton Reaction and Related Chemistry,

Open Access Article. Published on 29 2025. Downloaded on 10.11.2025 10:02:00.

No This article is licensed under a Creative Commons Attribution-NonCommercial 3.0 Unported Licence.

Crit. Rev. Environ. Sci. Technol., 2006, 36, 1-84.

View Article Online DOI: 10.1039/D5VA00262A

- 80.Y. C. Lee, S. L. Lo, P. T. Chiueh, Y. H. Liou and M. L. Chen, Microwave-hydrothermal decomposition of perfluorooctanoic acid in water by iron-activated persulfate oxidation, *Water Res.*, 2010, **44**, 886-892.
- 81.S. M. Mitchell, M. Ahmad, A. L. Teel and R. J. Watts, Degradation of Perfluorooctanoic Acid by Reactive Species Generated through Catalyzed H₂O₂ Propagation Reactions, *Environ. Sci. Technol. Lett.*, 2013, **1**, 117-121.
- 82.C. K. O. da Silva-Rackov, W. A. Lawal, P. A. Nfodzo, M. M. G. R. Vianna, C. A. O. do Nascimento and H. Choi, Degradation of PFOA by hydrogen peroxide and persulfate activated by iron-modified diatomite, *Appl. Catal. B*, 2016, **192**, 253-259.
- 83.S. Li, G. Zhang, W. Zhang, H. Zheng, W. Zhu, N. Sun, Y. Zheng and P. Wang, Microwave enhanced Fenton-like process for degradation of perfluorooctanoic acid (PFOA) using Pb-BiFeO₃/rGO as heterogeneous catalyst, *Chem. Eng. J.*, 2017, **326**, 756-764.
- 84.Y. Zhuang, X. Wang, L. Zhang, Z. Kou and B. Shi, Confinement Fenton-like degradation of perfluorooctanoic acid by a three dimensional metal-free catalyst derived from waste, *Appl. Catal. B*, 2020, **275**, 119101.
- 85.X. Wang, Y. Zhuang, J. Zhang, L. Song and B. Shi, Pollutant degradation behaviors in a heterogeneous Fenton system through Fe/S-doped aerogel, *Sci. Total Environ.*, 2020, **714**, 136436.
- 86.J. Zheng and S. Zhang, Subnanoscale spatially confined heterogeneous Fenton reaction enables mineralization of perfluorooctanoic acid, *Water Res.*, 2023, **246**, 120696.
- 87.A. Santos, S. Rodriguez, F. Pardo and A. Romero, Use of Fenton reagent combined with humic acids for the removal of PFOA from contaminated water, *Sci. Total Environ.*, 2016, **563-564**, 657-663.
- 88.Q. Wang, M. Liu, H. Zhao, Y. Chen, F. Xiao, W. Chu and G. Zhao, Efficiently degradation of perfluorooctanoic acid in synergic electrochemical process combining cathodic electro-Fenton and anodic oxidation, *Chem. Eng. J.*, 2019, **378**, 122071.
- 89.Q. Lei, M. Liu, T. Yang, M. Chen, L. Qian, S. Mao, J. Cai and H. Zhao, Controllable Generation of Sulfate and Hydroxyl Radicals to Efficiently Degrade Perfluorooctanoic Acid in Cathode-Dominated Electrochemical Process, *ACS ES&T Water*, 2023, **3**, 3696-3707.
- 90.J. Han, M. Zhao, K. Wu, Y. Hong, T. Huang, X. Gu, Z. Wang, S. Liu and G. Zhu, A bifunctional single-atom catalyst assisted by Fe₂O₃ for efficiently electrocatalytic perfluorooctanoic acid degradation by integrating reductive and oxidative processes, *Chem. Eng. J.*, 2023, **470**, 144270.
- 91.F. Yu, Y. Zhang, Y. Zhang, Y. Gao and Y. Pan, Promotion of the degradation perfluorooctanoic acid by electro-Fenton under the bifunctional electrodes: Focusing active reaction region by Fe/N co-doped graphene modified cathode, *Chem. Eng. J.*, 2023, **457**, 141320.
- 92.Y. Wang, H. Li, J. Li, L. Zhou, C. Feng, G. Liu, J. Wang and C. Hou, Fluorophilic N, S self-doped porous carbon electrodes derived from biomass gelatin for electro-Fenton degradation of GenX, *J. Environ. Chem. Eng.*, 2025, **13**, 115386.

- 93.H. D. Hieu Nhu, D. V. Tri, T. L. Luu, J. Trippel and M. Wagner, Degradation of 2000 per- and poly-fluoroalkyl substances (PFAS) in water using fenton-assisted electrochemical oxidation process, *Sep. Purif. Technol.*, 2025, **362**, 131908.
- 94.H. Tang, Q. Xiang, M. Lei, J. Yan, L. Zhu and J. Zou, Efficient degradation of
- perfluorooctanoic acid by UV-Fenton process, Chem. Eng. J., 2012, 184, 156-162.
- 95.D. Liu, Z. Xiu, F. Liu, G. Wu, D. Adamson, C. Newell, P. Vikesland, A. L. Tsai and P. J. Alvarez, Perfluorooctanoic acid degradation in the presence of Fe(III) under natural sunlight, *J. Hazard. Mater.*, 2013, **262**, 456-463.
- 96.L. H. Zhang, J. H. Cheng, X. You, X. Y. Liang and Y. Y. Hu, Photochemical defluorination of aqueous perfluorooctanoic acid (PFOA) by Fe(0)/GAC microelectrolysis and VUV-Fenton photolysis, *Environ. Sci. Pollut. Res. Int.*, 2016, **23**, 13531-13542.
- 97.B. Gomez-Ruiz, P. Ribao, N. Diban, M. J. Rivero, I. Ortiz and A. Urtiaga, Photocatalytic degradation and mineralization of perfluorooctanoic acid (PFOA) using a composite TiO₂ –rGO catalyst, *J. Hazard. Mater.*, 2018, **344**, 950-957.
- 98.J. Gao, W. Chen, H. Shi, Z. Li, L. Jing, C. Hou, J. Wang and Y. Wang, Co₃O₄@Fe₃O₄/cellulose blend membranes for efficient degradation of perfluorooctanoic acid in the visible light-driven photo-Fenton system, *Surf. Interfaces*, 2022, **34**, 102302.
- 99.P. Su, C. Zhang, Y. Liu, J. Zhang, R. Djellabi, R. Wang, J. Guo, R. Zhang, H. Guo, X. Ding and X. Liu, Boosting PFOA photocatalytic removal from water using highly adsorptive and sunlight-responsive ZIF67/MIL-100(Fe) modified C₃N₄, *J. Environ. Chem. Eng.*, 2023, **11**, 110765.
- 100.Y. Zhang, X. Wang, Y. Xu, L. Huang, W. Wang, C. Gu, M. Zhang and Z. Chen, Photochemical degradation of perfluorooctanoic acid under UV irradiation in the presence of Fe (III)-saturated montmorillonite, *Sci. Total Environ.*, 2023, **876**, 162760.
- 101.C. L. Quiroz-Vela, H. Z ú ñiga-Ben í tez and G. A. Peñuela, Application of photochemical treatments in the removal of perfluorooctanoic acid (PFOA) from aqueous solutions, *J. Environ. Chem. Eng.*, 2024, **12**, 112259.
- 102.L. Wang, L. Sun, Z. Yu, Y. Hou, Z. Peng, F. Yang, Y. Chen and J. Huang, Synergetic decomposition performance and mechanism of perfluorooctanoic acid in dielectric barrier discharge plasma system with Fe₃O₄@SiO₂-BiOBr magnetic photocatalyst, *Mol. Catal.*, 2017, **441**, 179-189.
- 103.J. S. Yang, W. W. Lai and A. Y. Lin, New insight into PFOS transformation pathways and the associated competitive inhibition with other perfluoroalkyl acids via photoelectrochemical processes using GOTiO₂ film photoelectrodes, *Water Res.*, 2021, **207**, 117805.
- 104.Y. Wang, M. Zhao, C. Hou, W. Chen, S. Li, R. Ren and Z. Li, Efficient degradation of perfluorooctanoic acid by solar photo-electro-Fenton like system fabricated by MOFs/carbon nanofibers composite membrane, *Chem. Eng. J.*, 2021, **414**, 128940.
- 105.Y. Wang, S. Li, Y. Shao, L. Jing, R. Ren, L. Ma, X. Wang, Z. Li, J. Wang and C. Hou, Energy-efficient mineralization of perfluorooctanoic acid: Biomass energy driven

solar photo-electro-fenton catalysis and mechanism study, *Chem. Eng. J.*, 2022, 443°/D5VA00262A 136514.

- 106.C. Hou, F. Chen, D. Cheng, S. Zou, J. Wang, M. Shen and Y. Wang, MOFs-derived Cu/Carbon membrane as bi-functional catalyst: Improving catalytic activity in detection and degradation of PFOA via regulation of reactive Cu species, *Chem. Eng. J.*, 2024, **481**, 148467.
- 107.Y. Wang, Y. Chen, Q. Meng, J. Li, L. Jing, H. Li, L. Zhou, Z. Tian, J. Wang and C. Hou, Efficient photo-electro-Fenton catalysis of perfluorooctanoic acid with MOFs based 2D CoFe nanosheets: Oxygen vacancy-mediated adsorption and mineralization ability, *Chem. Eng. J.*, 2024, **483**, 149385.
- 108.H. Hori, E. Hayakawa, H. Einaga, S. Kutsuna, K. Koike, T. Ibusuki, H. Kiatagawa and R. Arakawa, Decomposition of Environmentally Persistent Perfluorooctanoic Acid in Water by Photochemical Approaches, *Environ. Sci. Technol.*, 2004, **38**, 6118-6124. 109.H. Moriwaki, Y. Takagi, M. Tanaka, K. Tsuruho, K. Okitsu and Y. Maeda, Sonochemical Decomposition of Perfluorooctane Sulfonate and Perfluorooctanoic Acid, *Environ. Sci. Technol.*, 2005, **39**, 3388-3392.
- 110.Y. Hui, Mechanisms of Fenton-like reactions for reduction of refractory
- compounds., 2001, Ph.D. Dissertation, Washington State University, Pullman, WA.
- 111.P. Scotland, K. M. Wyss, Y. Cheng, L. Eddy, J. L. Beckham, J. Sharp, Y. Chung, C. H. Choi, T. Si, B. Wang, J. A. Donoso, B. Deng, Y.-Y. Shen, S. G. Zetterholm, C. Griggs, Y. Han, M. Tomson, M. S. Wong, B. I. Yakobson, Y. Zhao and J. M. Tour, Mineralization of captured perfluorooctanoic acid and perfluorooctane sulfonic acid at zero net cost using flash Joule heating, *Nat. Water*, 2025, **3**, 486-496.
- 112.B. Gomez-Ruiz, S. Gómez-Lavín, N. Diban, V. Boiteux, A. Colin, X. Dauchy and
- A. Urtiaga, Efficient electrochemical degradation of poly- and perfluoroalkyl substances (PFASs) from the effluents of an industrial wastewater treatment plant, *Chem. Eng. J.*, 2017, **322**, 196-204.
- 113.M. H. Lin, D. M. Bulman, C. K. Remucal and B. P. Chaplin, Chlorinated Byproduct Formation during the Electrochemical Advanced Oxidation Process at Magneli Phase Ti₄O₇ Electrodes, *Environ. Sci. Technol.*, 2020, **54**, 12673-12683.
- 114.Q. Zhuo, S. Deng, B. Yang, J. Huang, B. Wang, T. Zhang and G. Yu, Degradation of perfluorinated compounds on a boron-doped diamond electrode, *Electrochim. Acta*, 2012, 77, 17-22.
- 115.J. Xu, Y. Liu, D. Li, L. Li, Y. Zhang, S. Chen, Q. Wu, P. Wang, C. Zhang and J. Sun, Insights into the electrooxidation of florfenicol by a highly active La-doped Ti₄O₇ anode, *Sep. Purif. Technol.*, 2022, **291**, 120904.
- 116.J. Ge, X. Zou, S. Almassi, L. Ji, B. P. Chaplin and A. J. Bard, Electrochemical Production of Si without Generation of CO₂ Based on the Use of a Dimensionally Stable Anode in Molten CaCl₂, *Angew Chem Int Ed Engl*, 2019, **58**, 16223-16228.
- 117.Z. Wang, F. Xiao, X. Shen, D. Zhang, W. Chu, H. Zhao and G. Zhao, Electronic Control of Traditional Iron-Carbon Electrodes to Regulate the Oxygen Reduction Route to Scale Up Water Purification, *Environ. Sci. Technol.*, 2022, **56**, 13740-13750.

This article is licensed under a Creative Commons Attribution-NonCommercial 3.0 Unported Licence Open Access Article. Published on 29 2025. Downloaded on 10.11.2025 10:02:00.

View Article Online

118.X. Tan, J. Zhong, C. Fu, H. Dang, Y. Han, P. Král, J. Guo, Z. Yuan, H. Peng, C. Yuan, H. Peng, C.

Zhang and A. K. Whittaker, Amphiphilic Perfluoropolyether Copolymers for the Effective Removal of Polyfluoroalkyl Substances from Aqueous Environments, Macromolecules, 2021, 54, 3447-3457.

- 119.G. Pliego, J. A. Zazo, P. Garcia-Muñoz, M. Munoz, J. A. Casas and J. J. Rodriguez, Trends in the Intensification of the Fenton Process for Wastewater Treatment: An Overview, Crit. Rev. Environ. Sci. Technol., 2015, 45, 2611-2692.
- 120.J. Xiao, S. Guo, D. Wang and Q. An, Fenton-Like Reaction: Recent Advances and New Trends, *Chemistry*, 2024, **30**, e202304337.
- 121.A. Babuponnusami and K. Muthukumar, A review on Fenton and improvements to the Fenton process for wastewater treatment, J. Environ. Chem. Eng., 2014, 2, 557-572.
- 122.M. Umar, H. A. Aziz and M. S. Yusoff, Trends in the use of Fenton, electro-Fenton and photo-Fenton for the treatment of landfill leachate, Waste Manag, 2010, 30, 2113-2121.
- 123.A. Mirzaei, Z. Chen, F. Haghighat and L. Yerushalmi, Removal of pharmaceuticals from water by homo/heterogonous Fenton-type processes - A review, *Chemosphere*, 2017, **174**, 665-688.
- 124.R. G. Zepp, B. C. Faust and J. Hoigne, Hydroxyl radical formation in aqueous reactions (pH 3-8) of iron(II) with hydrogen peroxide: the photo-Fenton reaction, Environ. Sci. Technol., 1992, 26, 313-319.
- 125.M. Roccamante, I. Salmerón, A. Ruiz, I. Oller and S. Malato, New approaches to solar Advanced Oxidation Processes for elimination of priority substances based on electrooxidation and ozonation at pilot plant scale, Catal. Today, 2020, 355, 844-850. 126.M. E. Demir, G. Chehade, I. Dincer, B. Yuzer and H. Selcuk, Synergistic effects of advanced oxidization reactions in a combination of TiO₂ photocatalysis for hydrogen production and wastewater treatment applications, Int. J. Hydrogen Energy, 2019, 44, 23856-23867.

Data availability:No primary research

This article is licensed under a Creative Commons Attribution-NonCommercial 3.0 Unported Licence.

Open Access Article. Published on 29 2025. Downloaded on 10.11.2025 10:02:00.

View Article Online DOI: 10.1039/D5VA00262A

No primary research results, software or code have been included and no new data were generated or analysed as part of this review.